

Parameter Sensitivity in Hydrologic Modeling

Implementation by

David R. Maidment, Ph.D., and

Tanya Nicole Hoogerwerf

Technical Report

The University of Texas at Austin

May 2002

Abstract

Parameter Sensitivity in Hydrologic Modeling

David R. Maidment, Ph.D. and Tanya Nicole Hoogerwerf

The University of Texas at Austin, May 2002

The computation of discharge from a watershed depends on the lag time between rainfall and runoff, while in turn the lag time depends on watershed parameters, such as length of the longest flow path, watershed slope, and the SCS curve number describing the effects of land use and soils. This research explores the variation in lag time and discharge resulting from traditional and automated methods of calculating hydrologic parameters. Four levels of extracting hydrologic parameters are explored: (1) measurement from paper maps, (2) on-screen extraction from raster maps, (3) using GIS and two different resolutions of grid-based digital elevation models (DEMs), and (4) using a triangulated irregular network (TIN). Results show that variations in watershed area and curve number most directly impact the computed discharge, while variations in slope and flow path length are relatively insignificant.

Table of Contents

| | |
|---|------|
| List of Tables..... | vi |
| List of Figures | viii |
| Chapter 1: Introduction | 1 |
| 1.1 Background of GIS use in Water Resources Applications | 2 |
| 1.2 Project History..... | 2 |
| 1.3 Objectives..... | 3 |
| 1.4 Organization | 5 |
| Chapter 2: Literature Review | 6 |
| 2.1 Introduction | 6 |
| 2.2 Summary of Current Hydrologic Practices of TxDOT | 6 |
| 2.3 Extracting Watershed Parameters from Digital Models..... | 8 |
| 2.3.1 Digital Elevation Models | 9 |
| 2.3.2 Triangulated Irregular Networks | 11 |
| 2.4 Lumped Versus Distributed Models | 14 |
| 2.5 Scale Dependency of Hydrologic Parameters | 15 |
| 2.6 Modeling Urban Areas and Future Conditions | 24 |
| Chapter 3: Methodology..... | 26 |
| 3.1 Introduction | 26 |
| 3.2 Case I: Traditional Methods..... | 27 |
| 3.2.1 The Planimeter | 28 |
| 3.2.2 The Map Wheel | 33 |
| 3.2.3 Parameter Extraction | 34 |
| 3.3 Case II: On-Screen Digitizing of Raster Graphic Maps..... | 34 |
| 3.3.1 Digitizing in ArcView GIS 3.2 | 37 |
| 3.3.2 Parameter Extraction | 39 |

| | | |
|------------|---|----|
| 3.4 | Case III: Automated Methods using a DEM | 40 |
| 3.4.1 | Overview of Automated Methods using a DEM..... | 41 |
| 3.4.2 | ArcView GIS 3.2..... | 45 |
| 3.4.2.1 | CRWR-PrePro | 46 |
| 3.4.2.2 | Parameter Extraction using ArcGIS and CRWR- PrePro | 49 |
| 3.4.3 | Watershed Modeling System (WMS) | 51 |
| 3.4.3.1 | TOPAZ | 54 |
| 3.4.3.2 | Parameter Extraction | 55 |
| 3.5 | Case IV: Automated Methods using a TIN | 57 |
| 3.5.1 | TIN Development and Processing..... | 58 |
| 3.5.2 | TIN Parameter Extraction | 60 |
| Chapter 4: | Application | 61 |
| 4.1 | Site Selection..... | 61 |
| 4.2 | Case I: Traditional Methods | 64 |
| 4.3 | Case II: Automated Methods by Digitizing | 67 |
| 4.4 | Case III: Automated Methods Using a DEM | 70 |
| 4.4.1 | ArcView GIS 3.2 and CRWR-PrePro | 71 |
| 4.4.1.1 | 10 Meter DEM | 75 |
| 4.4.1.2 | 30 Meter DEM | 76 |
| 4.4.2 | Automated Methods Using WMS | 78 |
| 4.4.2.1 | 10 Meter DEM | 78 |
| 4.4.2.2 | 30 Meter DEM | 81 |
| 4.5 | Case IV: Automated Methods Using a TIN | 84 |
| Chapter 5: | Results | 89 |
| 5.1. | Case Study Parameter Results Summary | 89 |
| 5.2 | Elasticity Analysis..... | 95 |
| 5.2.1 | Step 1: Sensitivity of SCS Lag Time to Parameter Variations . | 98 |
| 5.2.1.1 | Longest Flow Path..... | 99 |

| | | |
|--------------|---|-----|
| 5.2.1.2 | Slope..... | 102 |
| 5.2.1.3 | Curve Number | 103 |
| 5.2.1.4 | Step 1 Results | 105 |
| 5.2.2 | Step 2: Sensitivity of Flow to Variations in Lag Time | 106 |
| 5.2.2.1 | HEC-1 Model | 108 |
| 5.2.2.2 | Lag Time Variation | 112 |
| 5.2.2.3 | Drainage Area Variation | 115 |
| 5.2.2.4 | Step 2 Results | 118 |
| 5.2.3 | Results from Elasticity Analysis | 119 |
| Chapter 6: | Conclusions and Recommendations | 124 |
| 6.1 | Errors Sources Among Parameter Extraction Methods | 125 |
| 6.1.1 | Parameter Extraction using Paper Maps | 125 |
| 6.1.2 | On-Screen Digitizing of Raster Graphic Maps | 126 |
| 6.1.3 | Parameter Extraction Using Automated Methods..... | 127 |
| 6.1.4 | Parameter Extraction Using TINs | 128 |
| 6.2 | Errors Among Extracted Hydrologic Parameters..... | 129 |
| 6.2.1 | Drainage Area | 129 |
| 6.2.2 | Slope..... | 129 |
| 6.2.3 | Longest Flow Path..... | 130 |
| 6.2.4 | Perimeter | 130 |
| 6.2.5 | Curve Number | 130 |
| 6.3 | Significance of Errors..... | 131 |
| 6.4 | Additional Sources of Error | 134 |
| 6.5 | Recommendations | 135 |
| Appendix A: | Online Internet Resources | 137 |
| Appendix B: | Unmodified HEC-1 Model | 138 |
| Appendix C: | Modified HEC-1 Model in HEC-HMS..... | 141 |
| Bibliography | | 150 |

List of Tables

| | |
|--|-----|
| Table 4.1: Hand Delineation Results..... | 66 |
| Table 4.2: On-Screen Digitizing Results..... | 70 |
| Table 4.3: 10 Meter DEM Watershed Data..... | 75 |
| Table 4.4: 10 Meter DEM in ArcView Results..... | 76 |
| Table 4.5: 30 Meter DEM Watershed Data..... | 77 |
| Table 4.6: 30 Meter DEM in ArcView Results..... | 78 |
| Table 4.7: 10 Meter DEM in WMS Results..... | 81 |
| Table 4.8: 30Meter DEM in WMS Results..... | 83 |
| Table 4.9: TIN Results | 88 |
| Table 5.1: Area 1 Results | 90 |
| Table 5.2: Area 2 Results | 91 |
| Table 5.3: Area 3 Results | 91 |
| Table 5.4: Curve Number Values..... | 95 |
| Table 5.5: Parameter Base Values..... | 99 |
| Table 5.6: Longest Flow Path Calculations | 100 |
| Table 5.7: Slope Calculations..... | 102 |
| Table 5.8: Curve Number Measurements | 104 |
| Table 5.9: Curve Number Calculations..... | 104 |
| Table 5.10: Results from Analytical Calculations | 106 |
| Table 5.11: HEC-1 Modifications | 110 |
| Table 5.12: TxDOT IDF (Intensity-Duration-Frequency) Curves..... | 112 |
| Table 5.13: HEC-1 Lag Input..... | 113 |

| | |
|---|-----|
| Table 5.14: Discharge Variations Due to Lag Variations | 114 |
| Table 5.15: Discharge Elasticity Due to Parameter Variation | 115 |
| Table 5.16: HEC-1 Area Input | 116 |
| Table 5.17: Area Variation..... | 117 |
| Table 5.18: Discharge Elasticity due to Area Variations | 118 |
| Table 5.19: Parameter Coefficients of Variation (CV) | 122 |
| Table 5.20: Discharge Variations for Area 3 | 122 |
| Table 6.1: Elasticity Analysis..... | 132 |

List of Figures

| | |
|---|----|
| Figure 1.1: Lag Time Results (Anderson, 2000)..... | 4 |
| Figure 2.1: DEM Grid Cells..... | 9 |
| Figure 2.2: 30 Meter DEM..... | 10 |
| Figure 2.3: TIN Up-Close | 11 |
| Figure 2.4: Channel Representation with a TIN | 12 |
| Figure 2.5: Frequency Distribution of Subcatchment Length (Garbrecht et al., 1999b)..... | 20 |
| Figure 2.6: Frequency Distribution of Subcatchment Slope (Garbrecht et. al., 1999b)..... | 23 |
| Figure 3.1: Watershed Parameters | 27 |
| Figure 3.2: Planimeter | 29 |
| Figure 3.3: Tracing Arm Movement (Kunkle, 2001)..... | 30 |
| Figure 3.4: Area Calculation (Kunkle, 2001)..... | 31 |
| Figure 3.5: Final Area Calculation (Kunkle, 2001) | 33 |
| Figure 3.6: Map Wheel..... | 34 |
| Figure 3.7: USGS Digital Raster Graphic (DRG)..... | 36 |
| Figure 3.8: On-Screen Digitizing from a Raster Graphic Map | 37 |
| Figure 3.9: New Theme Creation in ArcView | 38 |
| Figure 3.10: Map-Based Model in ArcView..... | 40 |
| Figure 3.11: 8-Direction Pour Point Model (Anderson, 2000) | 42 |
| Figure 3.12: The D- ∞ Model (Tarboton, 1997) | 43 |
| Figure 3.13: 30 Meter Delineated DEM..... | 45 |

| | |
|---|----|
| Figure 3.14: The CRWR-PrePro Menu Bar | 47 |
| Figure 3.15: WMS Drainage Toolbar | 52 |
| Figure 3.16: WMS Module | 53 |
| Figure 3.17: TOPAZ Grids..... | 55 |
| Figure 3.18: Display Options in WMS..... | 56 |
| Figure 3.19: WMS Calculators..... | 57 |
| Figure 3.20: WMS TIN Module..... | 58 |
| Figure 3.21: Vertex Options in WMS | 59 |
| Figure 4.1: Location of Travis County, Texas | 62 |
| Figure 4.2: Location of Buttermilk and Little Walnut in Travis County | 63 |
| Figure 4.3: Area 1, Area 2, and Area 3 | 64 |
| Figure 4.4: Hand Delineation of Area 2..... | 65 |
| Figure 4.5: Area 1 Digitized..... | 68 |
| Figure 4.6: Area 2 Digitized..... | 69 |
| Figure 4.7: Area 3 Digitized..... | 69 |
| Figure 4.8: Land Use/Land Cover (LULC) Data | 73 |
| Figure 4.9: STATSGO Data..... | 74 |
| Figure 4.10: Delineated DEM Study Area..... | 77 |
| Figure 4.11: Area 1 Delineated in WMS..... | 79 |
| Figure 4.12: Area 2 Delineated with WMS..... | 80 |
| Figure 4.13: Area 3 Delineated with WMS..... | 80 |
| Figure 4.14: Area 1 Delineated with WMS..... | 82 |
| Figure 4.15: Area 2 Delineated with WMS..... | 82 |

| | |
|---|-----|
| Figure 4.16: Area 3 Delineated with WMS..... | 83 |
| Figure 4.17: TIN Development in WMS | 85 |
| Figure 4.18: Points, Breaklines, and Bounding Polygon in WMS..... | 86 |
| Figure 4.19: Interpolated TIN for Area 2..... | 87 |
| Figure 4.20: Area 2 TIN Delineated..... | 88 |
| Figure 5.1: Three Study Areas | 89 |
| Figure 5.2: Coefficients of Variation | 94 |
| Figure 5.3: Concept of Elasticity..... | 96 |
| Figure 5.4: Discharge Sensitivity Calculation..... | 97 |
| Figure 5.5: Step 1 in Calculating the Discharge Sensitivity | 98 |
| Figure 5.6: Analytical Calculation of Gradients | 101 |
| Figure 5.7: Slope Gradient Calculation..... | 103 |
| Figure 5.8: Curve Number Gradient Calculation | 105 |
| Figure 5.9: Step 2 in Calculating the Discharge Sensitivity | 107 |
| Figure 5.10: HEC-1 Study Area..... | 108 |
| Figure 5.11: Unmodified HEC-1 model (displayed in HEC-HMS)..... | 109 |
| Figure 5.12: Modified HEC-1 Model (displayed in HEC-HMS)..... | 111 |
| Figure 5.13: Discharge Results for Lag Variations..... | 114 |
| Figure 5.14: Discharge Results for Drainage Area Variations..... | 117 |
| Figure 5.15: Final Discharge Sensitivity Calculation | 119 |
| Figure 5.16: Elasticity Diagram | 120 |
| Figure 5.17: Elasticity Results | 121 |

Chapter 1: Introduction

Hydrology, as defined by the 2001 Texas Department of Transportation (TxDOT) Hydraulic Design Manual, “deals with estimating flood magnitudes as the result of precipitation.” Estimating the magnitude of an extreme flood event is essential in the design of highway drainage facilities such as culverts, bridges, storm drain systems, and detention storage facilities. The time-dependent determination of the quantity of water expected to be conveyed by each structure is used as a guide when designing the structure so that peak flows associated with an extreme flooding event do not cause flooding in areas adjacent to the structure and the road. With proper design of these facilities, damages resulting from an extreme flood event are minimized.

The principal factors affecting flood magnitudes in a watershed include runoff (influenced by precipitation and abstractions), watershed area information (slope, longest flow path, area), land use, and soil type. Detention storage systems, flow diversions, channelization, and impervious cover from urban development also influence the magnitude of an extreme flood event. Currently, TxDOT relies heavily on manual techniques to locate drainage divides and to estimate hydrologic parameters such as flow path length, watershed area, slope, and abstractions. These parameters are necessary in determining the peak discharge at an area outlet, although many runoff estimation techniques assume the size of the contributing watershed and the watershed slope as the principal variables.

1.1 BACKGROUND OF GIS USE IN WATER RESOURCES APPLICATIONS

Recently, the use of automated methods in water resources engineering applications has proven to be a viable alternative to more traditional hand calculation methods for many engineering agencies. The Texas Department of Transportation (TxDOT) is one of many agencies interested in using automated methods to aid in the hydrologic parameter development required for highway drainage facility design.

As a large portion of the cost associated with highway projects is attributed to the design and construction of drainage facilities, research has been dedicated to exploring a more economical and time efficient means of design. Geographic Information Systems (GIS) are a means of simplifying this process in that a GIS is capable of computing spatially derived hydrologic parameters such as watershed area, SCS curve number (for runoff and lag time computation), gridded precipitation, flow length, and slope for each watershed in a relatively short time.

1.2 PROJECT HISTORY

This implementation project follows an investigation conducted by Anderson (2000) for the Texas Department of Transportation (TxDOT). Anderson implemented GIS-based tools developed by CRWR at two sites in Texas: Castleman Creek (McClennan County, TX) and Pecan Bayou (Brown County, TX). The methodology used in Anderson's investigation utilized tools for hydrologic analysis and parameter extraction (CRWR-PrePro), terrain data

development and floodplain delineation (CRWR-FloodMap and HEC-GeoRAS), and lumped parameter hydrologic modeling and steady flow hydraulic analysis (HEC-HMS and HEC-RAS). Anderson's investigation was a first attempt for TxDOT at automating this entire process and for representing the spatial variability of the watershed characteristics, integrating hydrologic and hydraulic modeling processes with GIS, and displaying an accurate floodplain map of the project site.

1.3 OBJECTIVES

The initial scope of the author's project was to implement a study in a different area of Texas and apply the same methodology as Anderson (2000). However, after Anderson's study was completed TxDOT noted that the watershed lag time values calculated using CRWR-PrePro for input into HEC-HMS for the Castleman Creek (in McLennan County, Texas) watershed were over four times greater than the values calculated previously for a TxDOT hydrologic model of the area. At this point it became evident that some assumptions used in Anderson's automated hydrologic study need to be further investigated. Figure 1.1 gives an example of the large differences calculated by Anderson (2000) using automated methods and TxDOT using traditional, paper map-based methods.

| SubBasin | | | HMS | | HEC-1 | |
|----------|----------|-------------------|-----------|-----------|-----------|-----------|
| Location | HMS Code | HEC-1 Code | Lag (min) | Lag (hrs) | Lag (min) | Lag (hrs) |
| NW | 14 | Automated Methods | | 4.17 | 51.60 | 0.86 |
| NE | 15 | | | 4.53 | 53.40 | 0.89 |
| SW | 19 | CRWR | 144.458 | 2.41 | 144.00 | 2.40 |
| SE | 17,18 | | 136.8 | 2.28 | 136.80 | 2.28 |
| Bridge | 1 | Combo3 | 48.806 | 0.81 | n/a | n/a |

Figure 1.1: Lag Time Results (Anderson, 2000)

Discussions with the TxDOT project supervisor, David Stolpa, in March 2001 pertaining to the use of methods for hydrologic modeling led to other uncertainties and doubts about the automated process. Questions arose regarding scale effects of digital elevation models; as well as mechanical processes behind calculating slope, area, and longest flow path for a watershed. This uncertainty in the parameter values led TxDOT to question how variations in hydrologic parameters would ultimately affect watershed lag time values and discharge.

Following these conversations, the scope of the research project was redefined to explore the variation in lag time and discharge resulting from paper map and automated methods of calculating hydrologic parameters. In order to evaluate parameter uncertainty, four levels of extracting hydrologic parameters are explored: (1) measurement from paper maps; (2) on-screen extraction from raster maps; (3) using GIS and two different resolutions of grid-based digital elevation models (DEMs); and (4) using a triangulated irregular network (TIN).

This report attempts to quantify the errors associated from parameter variation in a two-step process. The first step is to quantify the error in lag time

(using the SCS lag equation) based on hydrologic parameter variation. Secondly, a HEC-1 model supplied by TxDOT is modified to quantify the error of discharge based on lag time and drainage area variations.

Although the drainage areas under investigation are urbanized, the scope of this project does not fully take into account small-scale man-made structures such as street gutters, inlets, and drainage ditches and culverts that control surface drainage patterns.

1.4 ORGANIZATION

This implementation project is divided into five principal parts. Chapter 2 explores previous work that has been conducted in the issue of scale dependency of some hydrologic parameters. Chapter 3 provides a general overview of the steps taken in the four case studies, while Chapter 4 gives a step-by-step account of the hydrologic parameter computation process for each of the four case studies. Chapter 5 analyzes the results using the concept of elasticity to determine the overall effect of parameter variation on the discharge. The final chapter, Chapter 6, discusses the findings from this implementation project.

Chapter 2: Literature Review

2.1 INTRODUCTION

From 1996 to 1999, the Center for Research in Water Resources (CRWR) at the University of Texas at Austin developed hydrologic modeling tools for the purpose of floodplain delineation at highway river crossings for TxDOT (Olivera et al., 1999).

From 1999 to 2000, TxDOT funded CRWR to implement these tools and to investigate the possibility of combining existing GIS tools, lumped parameter hydrologic and one-dimensional hydraulic models, and the visual display capabilities of GIS to overcome the historical limitations of floodplain mapping. Anderson (2000) implemented these tools at two existing TxDOT drainage structures. Apart from evaluating the feasibility of implementing the tools developed at CRWR, Anderson (2000) set out to determine if existing digital data are sufficient to produce an accurate representation of the floodplain.

Since the work of Anderson (2000), many issues have arisen regarding the work of GIS in water resources. This chapter reviews some of these problems and work that has been conducted in this area.

2.2 SUMMARY OF CURRENT HYDROLOGIC PRACTICES OF TxDOT

Currently TxDOT relies heavily on manual methods of watershed parameter extraction. Measurements are taken by hand from paper maps and then watershed parameters are entered into a hydrologic model.

Hydrologic modeling practices used by TxDOT are outlined in the 2001 TxDOT Hydraulic Design Manual. Methods used by TxDOT primarily include unit hydrographs, the Rational Method, statistical analysis of stream flow data, and regional regression equations.

The NRCS (National Resource Conservation Service) dimensionless unit hydrograph along with the NRCS Runoff Curve Number Method (also known as the SCS curve number method) is the primary unit hydrograph technique used by TxDOT. The unit hydrograph, a method for estimating storm runoff, was first proposed by L. K. Sherman in 1932. The unit hydrograph is defined as the watershed response to a unit depth of excess rainfall uniformly distributed over the entire watershed and applied at a constant rate for a given period of time (Chow et al., 1988).

Unit hydrograph techniques consider the time distribution of rainfall, the initial rainfall losses, and an infiltration rate that decreases during the course of the storm. Variables include the drainage area, time of concentration, curve number (if the SCS curve number method is used), rainfall distribution, and total design rainfall. Equations to calculate the time of concentration can also consider watershed parameters such as watershed length and slope. Popular unit hydrograph application programs used by TxDOT have included the TR20 (and its TR55 variant) and HEC-1. TxDOT is now moving towards the use of HEC-HMS. (Stolpa, 2002)

The Rational Method is very simple, and is best suited for small urban and rural watersheds. The statistical analysis of stream gauge data method is applied

when long records (greater than 25 years) are available. Statistical analysis provides peak discharge estimates using annual peak stream flow data. Regional regression equations based on the hydrologic parameters area and slope, are commonly used for calculating flows at ungauged sites. These equations were developed by the USGS in 1993 to estimate the magnitude and frequency of floods at ungauged sites in six separate regions in Texas (Jennings et al., 1993).

2.3 EXTRACTING WATERSHED PARAMETERS FROM DIGITAL MODELS

Over the last twenty years, digital representations of topographic information have become increasingly available in the form of digital terrain models (DTMs). Using computers and extracting watershed data from digital terrain models is faster, and provides more reproducible measurements than traditional manual techniques using topographic maps (Garbrecht et al., 1999a).

GIS uses a DTM to describe the spatially distributed attributes of the terrain that are classified as topologic and topographic data. The topography of an area describes its elevation and land surface shape, while also important are the spatial distribution of terrain attributes other than elevation such as the land cover, soil type, and connectivity of the features. A DTM may be used to represent both topographic and/or physiographic features in the format of raster or grid data, triangulated irregular network (TIN) data or vector (point, line, and polygon) data (Olivera et al., 2000).

Using automated methods a surface may be analyzed so that drainage basin boundaries are defined, stream networks created, and drainage basin data

computed in a relatively quick time. Once the drainage basin data have been computed, geometric modeling parameters can be extracted automatically and entered into a hydrologic model (Nelson et al., 1997).

2.3.1 Digital Elevation Models

Digital terrain models are commonly found as grids, referred to in this document as digital elevation models or DEMs (in other documents DEM data includes TIN data). DEMs are composed of identical square cells arranged in rows and columns, each with a unique value to represent the terrain elevation at that point, as shown in Figure 2.1.

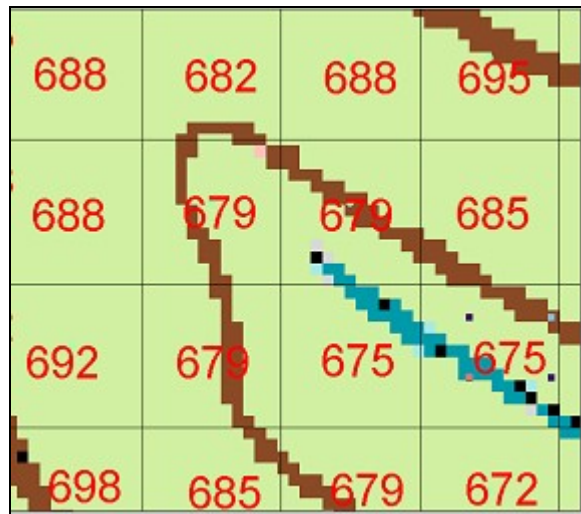


Figure 2.1: DEM Grid Cells

DEMs are provided at 1 km grid cell size for the entire world and 30 meter cell sizes for the entire United States. Figure 2.2 shows an example of a 30 meter DEM terrain representation in Austin, Texas.



Figure 2.2: 30 Meter DEM

DEMs are used in water resources engineering to identify drainage related features such as ridges, valley bottoms, channel networks, and surface drainage patterns. DEMs are also useful in quantifying subcatchment and channel size, length, and slope. The accuracy of this topographic information is a function of the quality and resolution of the DEM, in addition to the DEM processing algorithms used to extract this information (Garbrecht et al., 1999).

One solution to reduce the errors associated with DEMs, as described by Garbrecht et al. (1999a), is to use a high resolution DEM produced by more

advanced methods or to customize a DEM. Another factor affecting accuracy is whether the data are integer or floating points. When data are integers, less memory is required than when data are floating points; however floating point data are more accurate (Olivera et al., 1999). For this reason quality and resolution must be considered when selecting a DEM for hydrologic modeling so that both are consistent with the scale of the model and the objectives of the study being made (Garbrecht et al., 1999a).

2.3.2 Triangulated Irregular Networks

Another form of digital data is the triangulated irregular network or TIN. TINs, however, are currently not as widely used as grid DEMs, but may be used to serve the same purpose. TINs consist of a set of representative irregularly distributed points connected by straight lines to produce triangles, as shown in Figure 2.3.

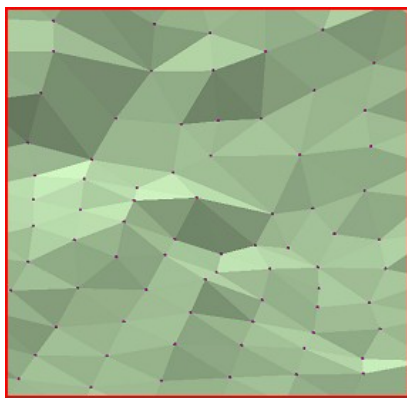


Figure 2.3: TIN Up-Close

Figure 2.4 shows the ability of a TIN to conform to complex terrain and identify channel features.

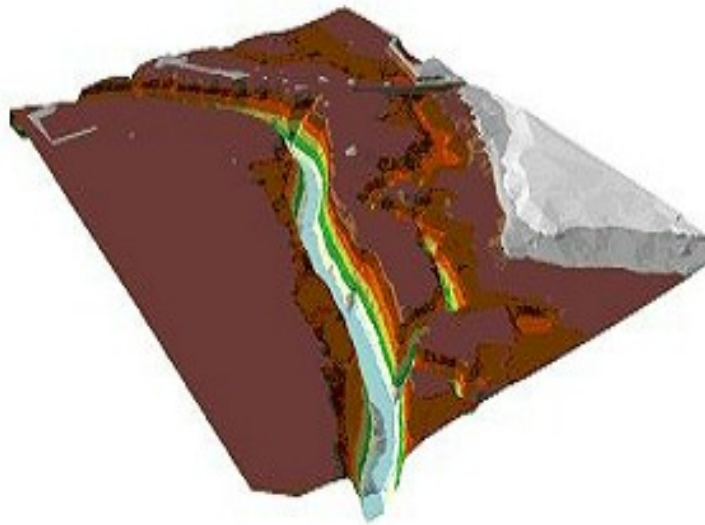


Figure 2.4: Channel Representation with a TIN

Delauney triangulation, based on the concept of maximizing the minimum angle of all triangles produced by connector lines to their nearest neighbor points, is most often used to generate TINs. Breaklines are used to control the smoothness and continuity of the surface such as streamlines or roads by forcing triangles to conform to these lines. For this reason, TINs are generally used for surface representation of stream channels in hydraulic modeling since complex land surface details may accurately be represented (Lee et al., 1980).

TINs have the advantage compared to grid-based elevation models in that they require less memory than grids. In addition, linear features are more accurately represented with TINs than with DEMs. When using grids to model channels and other linear features, edges must be always oriented along the horizontal, vertical, or diagonal directions. TINs eliminate this data redundancy and are thus better suited for modeling streams and other linear features. TINs can be constructed so that triangle edges conform to features and are not restricted to lie in the horizontal, vertical, and diagonal directions. The TIN data structure is also often more efficient because the terrain model can be adapted readily to the surface being modeled. In areas where the terrain is flat, only few a points need to be utilized (Nelson et al., 1999).

Grid-based watershed modeling is advantageous over TIN-based watershed delineation in that grids have a simpler data structure than TINS, grid-based data is very abundant, and grid-based models are reproducible. Other disadvantages of TINs result when inserting breaklines. Inserting breaklines may result in small or long thin triangles which, in turn, will cause difficulties in numerical round off or tolerance problems. TINs have the major disadvantage in that large TINs are difficult to work with, and editing pits and flat triangles can be a very time consuming process, especially when areas are large. Lastly, determining an appropriate resolution for a TIN can be a difficult task (Nelson et al., 1999a).

TIN-based watershed delineation is based on the process of tracing a flow across triangle surfaces. Because each triangle has a flat surface, the mathematics

behind determining the path of maximum downward gradient is straightforward as described by Jones et al. (1990). Watershed boundaries are delineated with TINS by identifying outlet locations. Once outlets have been selected, flow paths are traced along the path of steepest descent and by combining together triangles whose flow paths pass through a common outlet point.

2.4 LUMPED VERSUS DISTRIBUTED MODELS

Creating an accurate hydrologic model of an area is a difficult task. As most hydrologic systems are spatially variable, distributed models may be required to fully describe the system. Distributed models require that calculations be made on a point-to-point basis within the model, and that flow be calculated as a function of time and space throughout the system. Lumped models on the other hand provide a unique representative value for the entire subcatchment. In a lumped model, flow is calculated as a function of time alone (Nelson et al., 1997).

Olivera et al. (1999) discuss how there have been attempts to account for spatially distributed terrain attributes based on lumped models, as the boundary between lumped models and distributed models is not clearly defined. For example, models such as HEC-1, developed by the US Army Corps of Engineers, are neither purely lumped nor purely distributed. HEC-1 may be used to partition the hydrologic system into subsystems and to apply lumped models to each of the subsystems. HEC-1 then routes the responses from each subbasin to the watershed outlet.

Nelson et al. (1997) suggest that although distributed models are the focus of current research, lumped models are still more common and preferred because regulatory agencies have not accepted distributed models due to the effort involved in calibrating and verifying them. Models known as data reduction (DR) models are one way of converting distributed properties of an area, such as slope and subcatchment length, into lumped parameters by reducing distributed properties into a representative value for each subcatchment (Garbrecht et al., 1999a). GIS is a tool that allows the user to jump from strictly lumped models to more spatially distributed models, in that a GIS may be used to generate input files for lumped models based on a distributed interpretation of the terrain (Nelson et al., 1997).

If the rainfall-runoff response of a watershed is linear, a unit hydrograph can be used to relate rainfall to runoff. Most lumped models are based on either synthetic or derived unit hydrographs. Once a unit hydrograph is determined for a watershed, then one can determine the flood hydrograph resulting from any measured or design rainfall. For both traditional and automated processes, the unit hydrograph method is commonly used to model rainfall-runoff processes. Since the systems are linear, the overall response time can be calculated as the sum of the sub-area responses (Nelson et al., 1997).

2.5 SCALE DEPENDENCY OF HYDROLOGIC PARAMETERS

Although using DEMs provides for quick analysis, there are several disadvantages to using DEMs, which include the effect of grid size on some

certain computed topographic parameters (such as longest flow path), and the inability to adjust the grid size to the dimensions of topographic land surface features (Garbrecht et al., 1999).

Miller et al. (1999) explored the effects of spatial resolution and accuracy of DEMs on hydrologic characterization using GIS. The study analyzed the area, slope, drainage density, and surface variation for watersheds ranging in size from 0.0016 km² to 146 km², using 2.5, 10, 30, and 40 meter DEMs. Miller et al. (1999) noted an overall reduction in slope with increasing cell size. In Miller's study, both the mean and standard deviation of watershed slopes are highest for IFSAR DEMs (highest resolution DEMs). A reduction in slope standard deviation implies that much of the natural surface has been simplified to a more continuous smooth surface (Miller et al., 1999).

Another observation drawn by Miller et al. (1999) is that the high resolution DEMs create more tortuous flow paths, more complex routing, and longer drainage networks. Total drainage lengths were found to be considerably different among four DEMs of different cell sizes on smaller watersheds as described by the drainage density (length/area). Mean drainage density is higher for watersheds and channels created with high resolution DEMs than for other surfaces (0.0104 m for the 2.5 m IFSAR DEM as compared to 0.0085 m for the 40 m DEM).

Miller et al. (1999) found that the high resolution IFSAR DEM provided significantly different results at small scales when compared to other surfaces, while the differences among DEMs at larger scales were reduced. The final

conclusion from this study was that the suitability of various digital elevation data is primarily a function of the research objectives and scale of application (Miller et al., 1999).

In a study conducted by Garbrecht et al. (1994), the accuracy of drainage features extracted from DEMs as a function of DEM resolution is evaluated. The horizontal resolution of a DEM with an original grid spacing of 30 meters is decreased by cell aggregation. Selected drainage features for several hypothetical channel network configurations were extracted for a range of DEM resolutions using TOPAZ software.

The study by Garbrecht et al. (1994) concluded that the dependency of physical characteristics on grid resolution “was introduced by the inability of a DEM to accurately reproduce drainage features that are at the same scale as the spatial resolution of the DEM.” In other words, the number of channels, the size of the drainage area, and the channel network pattern from a low resolution DEM may depart considerably from the one obtained by a high resolution DEM. For sinuous channels, the use of a low resolution DEM results in shorter channel lengths. For networks with a high drainage density, the use of a low resolution DEM leads to channel and drainage area capturing, This being the point at which the DEM resolution can no longer resolve the separation between channels or drainage boundaries. If small drainage features are important, then resolution must be selected relative to the size of these features (Garbrecht et al., 1994).

Garbrecht et al. (1999b) discuss the extraction of drainage properties from DEMs. This study compares methods of extracting length and slope values using

both automated and traditional methods from 177 subcatchments located in the USDA-ARS Walnut Gulch Experimental Watershed in Tombstone, Arizona.

For the manual method in Garbrecht's study, length is measured subjectively as the distance between the upslope subcatchment drainage boundary and downslope channel. Slope is calculated as a lumped parameter by converting variable slope into a straight-line profile (Gray's method) while maintaining the horizontal distance and area under the profile. For the automated methods, DEMs were processed using the TOPAZ software, producing 183 subcatchments. Length and slope values were extracted using data reduction (DR) models. (Garbrecht et al., 1999b)

Subcatchment length is important in hydrologic modeling applications because it is used to estimate runoff travel distance or flow routing distance. Garbrecht et al. (1999b) describe two methods for calculating this length using data reduction (DR) models. One method is the *average travel distance*, and the other is the *average flow path length*, or the distance of overland flow within a subcatchment.

The *average travel distance* traveled by surface runoff is calculated as the average distance from every point in the subcatchment to the first downstream channel that the flow reaches at this point, or the arithmetic mean of all travel distances within a subcatchment. For subcatchments that are rectangular in shape the average travel distance is about half the subcatchment length, and twice the average travel distance corresponds to length from the drainage divide at the upstream boundary to the downstream channel, as can be seen in Equation 2.1.

$$L_t = \frac{\sum_{i=1}^{n_s} D_i k_i}{\sum_{i=1}^{n_s} k_i} \quad \text{Equation 2.1}$$

L_t is the average travel distance, n_s is the total number of cells in the subcatchment, D_i is the travel distance of cell i to the adjacent channel, and k_i is a weighting factor with a value of 1 for travel distances originating at subcatchment cells, and $\frac{1}{2}$ for travel distances originating at channel cells. The weighting factor accounts for the fact that channel cells contain a channel and the cell area is evenly split between the right and left subcatchments adjacent to the channel. No adjustments are needed for subcatchment cells, so their weighting factor is 1 (Garbrecht et al., 1999b).

The second method, the *average flow path length*, shown in Equation 2.2, is different in that not all points in the subcatchment are considered in the length calculations. The flow path in this method is considered as the distance from a divide to the first adjacent downstream channel. Only the cells in the drainage divide are considered in this calculation. Drainage divides are not only located at the upstream boundary of the subcatchment, but also within the subcatchment as defined by local ridges in the topography. For this reason the flow path length is generally shorter than the average travel distance method to the drainage divide. (Garbrecht et al., 1999b)

$$L_f = \frac{1}{n_i} \sum_{i=1}^{n_i} l_i^f \quad \text{Equation 2.2}$$

Under this method L_f is the average flow path length, n_i is the number of flow paths in the subcatchment, i is the flow path counter, and l^f the length of individual flow paths. Figure 2.5 shows the results by Garbrecht et al. (1999b) for the 177 subcatchments, using manual and automated methods of length extraction.

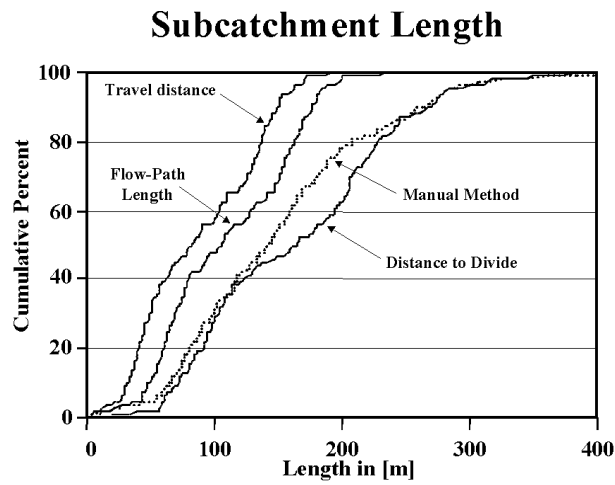


Figure 2.5: Frequency Distribution of Subcatchment Length (Garbrecht et al., 1999b)

Figure 2.5 is an example of parameter value variations, in this case subcatchment length, that occur using different methods of parameter extraction (automated and manual) and different models for data reduction. The distance to divide length is twice the average travel distance for rectangular-shaped subcatchments and 1.33 times the average travel distance for triangular-shaped subcatchments. The distance to divide and the manual method closely resemble each other since they represent the same length from the watershed boundary to

the downstream channel. The travel distance consistently gives the smallest length value since this method accounts for all the cells in the watershed (Garbrecht et al., 1999b).

Moglen et al. (2001) show that DEMs at a 30 meter resolution are not sufficiently dense for analyzing flat areas; thus a higher resolution grid must be used regardless of the quality of the 30 meter grid. Garbrecht et al. (1999a) note the reason that the lower resolution grid will not work is due to the fact that as some DEMs (with the exception of NED DEMs, as NED is in floating point meters) are reported in meters or feet, the computed slope can only take on a limited number of values. For example, a 30 meter DEM in meters could have a slope value of zero, or a multiple of 0.033 (for a 1 meter change in elevation). These increments may be suitable to model terrain in mountainous terrain with large slopes, but insufficient to provide accurate values in flat areas (Garbrecht et al.; 1999a).

Subcatchment slope, similar to subcatchment length, is an important variable for runoff calculations. Garbrecht et al. (1999b) present four DR methods of slope calculation. These are the average terrain slope, the average travel distance slope, the average flow path slope, and the global slope.

Equation 2.3 shows the calculation for average terrain slope is the average of the local slope value at every point in the subcatchment.

$$S_t = \frac{1}{n_s} \sum_{i=1}^{n_s} s_i^t \quad \text{Equation 2.3}$$

For the average terrain slope, S_t is the average terrain slope, n_s is the number of subcatchment cells, and s_i^t is the terrain slope at cell i (Garbrecht et al., 1999b).

The average travel distance slope, Equation 2.4, is the average of the slope from each point in the subcatchment to the next adjacent downstream channel.

$$S_c = \frac{1}{n_s} \sum_{i=1}^{n_s} s_i^c \quad \text{Equation 2.4}$$

S_c is the average travel distance slope, n_s is the number of cells in the subcatchment, and s_i^c is the slope of the travel distance that starts at cell i . The travel distance slope of cell i is the mean of all the slopes along the travel distance between subcatchment i and the adjacent channel (Garbrecht et al., 1999b).

The average flow path slope, Equation 2.5, is the average slope of all the flow paths in the subcatchment, as defined as the route followed by the runoff starting at the divide and ending at the first adjacent downstream channel (Garbrecht et al., 1999b).

$$S_f = \frac{1}{n_f} \sum_{i=1}^{n_f} s_i^f \quad \text{Equation 2.5}$$

S_f is the average flow path slope, n_f is the number of flow paths in the subcatchment, and s_i^f is the flow path slope of the flow path starting at cell i . The

flow path slope, s_i^f , is the mean of all slopes along the flow path between divide cell i and the adjacent channel (Garbrecht et al., 1999b).

The global slope, Equation 2.6, is calculated as the average elevation of the subcatchment minus the average elevation of the receiving channel divided by the average travel distance (Garbrecht et al., 1999b).

$$S_g = \frac{E_s - E_c}{L_t} \quad \text{Equation 2.6}$$

S_g is the global slope for the subcatchment, E_s is the mean elevation of the subcatchment, and E_c is the mean elevation of the adjacent channel and L_t is the average travel distance of the subcatchment (Garbrecht et al., 1999b). Figure 2.6 shows the results from Garbrecht's study in terms of slope.

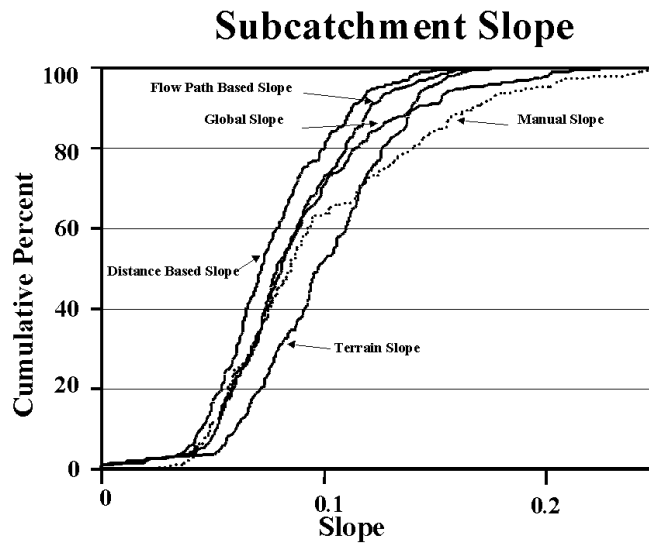


Figure 2.6: Frequency Distribution of Subcatchment Slope (Garbrecht et. al., 1999b)

Figure 2.6 further demonstrates parameter variations among methods of parameter extraction. The average travel distance-based slope method produces the smallest slope because it accounts for the flatter slopes in the lower part of the subcatchment area, thus emphasizing areas that are more subject to higher discharges. The terrain slope method results in the steepest slope values as this method equally emphasizes each maximum local slope value at each cell. The average flow path slope method is steeper than the average travel distance-based slope method because there are fewer divides in the lower part of the catchment. The global slope and manual methods resemble each other in that the models used to calculate these slope values are similar (Garbrecht et al., 1999b).

Garbrecht et al. (1999b) conclude that each method is equally valid, and the user should select a method that is most appropriate for the user's application. For instance, if the user is most interested in calculating runoff, the average travel distance based slope method and the average flow path slope method are better suited for this calculation than the terrain slope method (Garbrecht et al., 1999b).

2.6 MODELING URBAN AREAS AND FUTURE CONDITIONS

Although digital data in the form of DEMs is readily available and easy to work with, it does not accurately describe terrain in urban areas. Barrett (2000) suggests in larger areas, where it is not feasible to digitize these drainage systems, to delineate the watershed under undeveloped conditions. The errors associated from water entering and leaving the watershed should cancel out, at least with larger areas.

In some cases the digital data in the form of DEMs must be edited to reduce the error that occurs from building and road features that are captured in the DEM. Barrett (2000) used a 30 foot grid created from a TIN to help resolve the difference in elevation of roads and bridges from the surrounding terrain, as these features act as dams when performing flow accumulation. The initial grid was also edited manually to improve the stream representation by creating openings in the dams, roads and bridges.

Chapter 3: Methodology

3.1 INTRODUCTION

Case studies were conducted as a means to compare traditional methods of parameter calculation to automated methods of parameter calculation. Case studies were conducted on each of the four levels of current model development. The first case study uses purely traditional methods on paper maps. The second level involves using a computer and ArcView GIS 3.2 to digitize the watershed boundaries and channels from scanned USGS quadrangle maps. The third level involves using ArcView GIS 3.2 (with CRWR-PrePro) and WMS (Watershed Modeling System) to compute hydrologic parameters from two different resolution DEMs, a 10 meter DEM and a 30 meter DEM. The purpose of using two different resolution DEMs is to quantify cell scale effects on channel length, watershed slope, and watershed area. The final method uses a triangulated irregular network (TIN) and the TIN processing capabilities of WMS.

Figure 3.1 illustrates the watershed parameters that are the focus of this investigation. The longest flow path (LFP) is the longest length a drop of water will travel in the watershed. The area of the watershed encompasses all the water that will flow to the watershed outlet, and the slope of the watershed is the difference in a representative watershed elevation divided by a representative watershed length. Chapter 2 outlines several methods used to calculate slope, depending on the application. The soil type and land use are used to derive a

curve number, which along with longest flow path and slope, is used to calculate the lag time of the watershed.

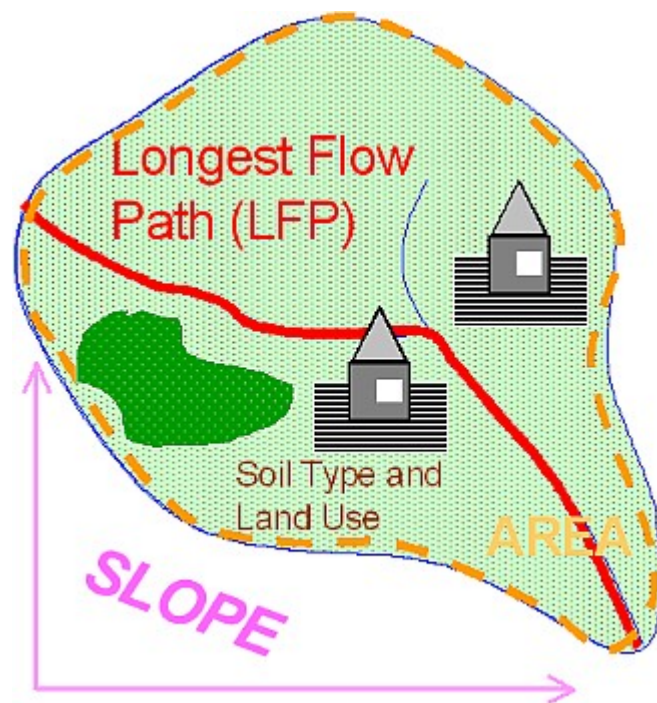


Figure 3.1: Watershed Parameters

3.2 CASE I: TRADITIONAL METHODS

Traditional hydrologic modeling involves calculating watershed parameters based on a paper map. Two instruments, a planimeter and a map wheel, aid in this process.

Traditional methods of computing terrain-based hydrologic data involve delineating the watershed by hand using map contours as guidelines. This is a very time consuming process, as drainage divides may be hard to locate. Pencil

lines are drawn perpendicular to contour lines to indicate drainage divides. Once the perimeter of the watershed has been established, a planimeter is used to measure its area. Perimeter and length of the longest flow path are measured using a map wheel. Slope is calculated by taking the difference in elevation between map contours or from field survey data.

3.2.1 The Planimeter

A planimeter is an instrument used to trace around the perimeter of an object to determine its area. Planimeters are useful tools in determining surface areas from maps and aerial photos. A planimeter mechanically integrates an area, and records this area as a tracing point moves along the boundary of the figure to be measured. This number can be converted to an area by multiplying the planimeter reading by a constant called the *planimeter constant*. This constant varies from planimeter to planimeter.

A planimeter is composed of a graduated drum and disk, vernier, tracing arm and point, and anchor arm and point (anchored to table). An elbow connects the tracing arm and anchor arm, and bends and slides freely. Parallel to the elbow, which slides and bends freely, is a wheel with a scale (consisting of a disk, drum and vernier) that records how far the wheel has turned. Figure 3.2 is a picture of the planimeter used in this study (Kunkle, 2001).



Figure 3.2: Planimeter

Calculating the planimeter constant involves plotting out a square and a circle of known areas, placing the anchor base outside of the area to be measured, and inserting the anchor arm into the drum assembly. Once the planimeter reading is set to zero (or the initial reading is recorded), the perimeter is traced in a clockwise motion and the final readings from the disk, drum, and vernier recorded. The disk reads whole numbers, the drum tenths and hundredths of a unit, and the vernier thousandths of a unit. Three readings of each of the two areas should be taken. Finally, the values derived from areas of the square and circle are averaged.

The planimeter reading from the average of circle and square value calculations is used to solve for the constant $C = N/A$. The value N is the planimeter reading, A is the known area of the object and C is the planimeter constant. Once the planimeter constant is determined, new areas may be

measured using the formula $A = C \cdot N$. For large areas, individual polygons should be solved separately (Knill, 2000).

Kunkle (2001) describes the basic fundamentals behind this mathematical operation. In Figure 3.3, the blue arm (AB) is the anchor arm. It is anchored to the table at *Point A*, located outside the object to be measured. *Point B* is the location of the measuring wheel (drum, disk and vernier). The green arm (BC) is the tracing arm, and C is the tracing point. The movement of the anchor arm is restricted to a circle. As the tracing arm moves in a clockwise direction from C to C' , the area dw is measured.

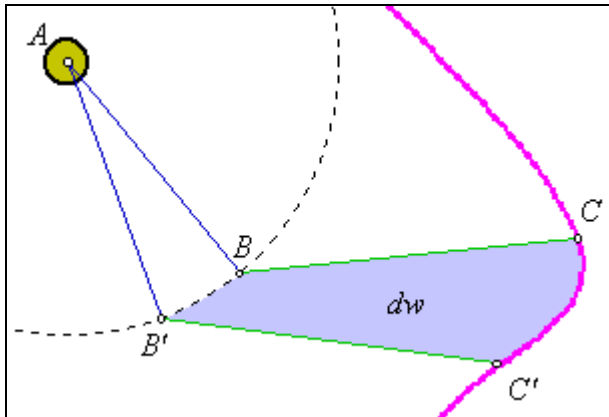


Figure 3.3: Tracing Arm Movement (Kunkle, 2001)

In Figure 3.4, point E divides the area dw into a trapezoid and a triangle to separate the components of the sliding and turning motion of the measurement wheel. Area BCE represents the area covered while the tracing arm is pivoting. During this pivoting motion $d\theta$ is the rotation of the arm. Area $EC'B'B$ is the area covered as the tracing arm slides, and dm is the change in the scale reading while

the arm is sliding. Both $d\theta$ and dm are arbitrarily small, and reflect the rotation of the scale in a plane perpendicular to the tracing arm.

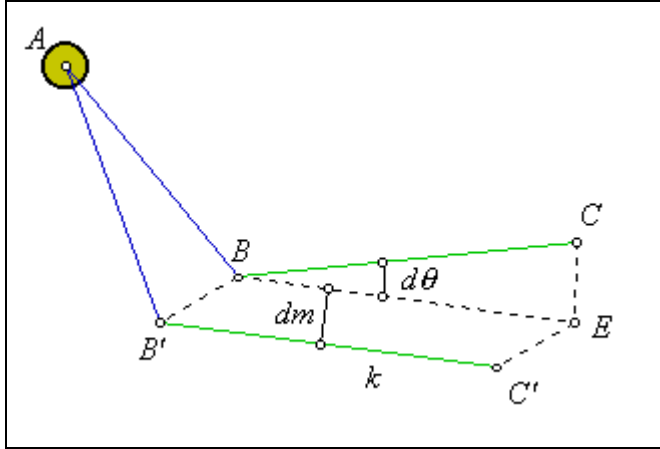


Figure 3.4: Area Calculation (Kunkle, 2001)

The area of the pentagon $BCEC'B'$ can be expressed as the sum of area BCE and area $EC'B'B$ as shown in Equation 3.1. The area of BCE is that of a triangle, while area $EC'B'B$ is that of a rectangle. As mentioned earlier, k is the length of the tracing arm.

$$\begin{aligned}
 dw &= \text{area}(BCEC'B') \\
 dw &= \text{area}(BCE) + \text{area}(EC'B'B) \\
 dw &= \frac{1}{2} k^2 d\theta + k dm
 \end{aligned}
 \tag{Equation 3.1}$$

The region traced by the tracing arm is determined by integrating Equation 3.1. The formula for W , as shown in Equation 3.2, describes the area of the entire region $EC'B'B$.

$$\begin{aligned}
W &= \oint dw \\
W &= \frac{1}{2} k^2 \oint d\theta + k \oint dm
\end{aligned}$$

Equation 3.2

Since the planimeter begins and ends in the same position, the net change in the angle $d\theta$ is zero. The net change in the scale reading is due only to the change in the scale reading. Integration of dm over the entire circuit is M , the final reading in the scale as also shown in Equation 3.3.

$$\begin{aligned}
\oint d\theta &= 0 \\
\Rightarrow W &= k \oint dm \\
W &= kM
\end{aligned}$$

Equation 3.3

In Figure 3.5, Kunkle (2001) shows how the final area is determined. When the arm is sliding backwards, the area covered is subtracted from the total area. The result is only the area crossed by the tracing arm, k .

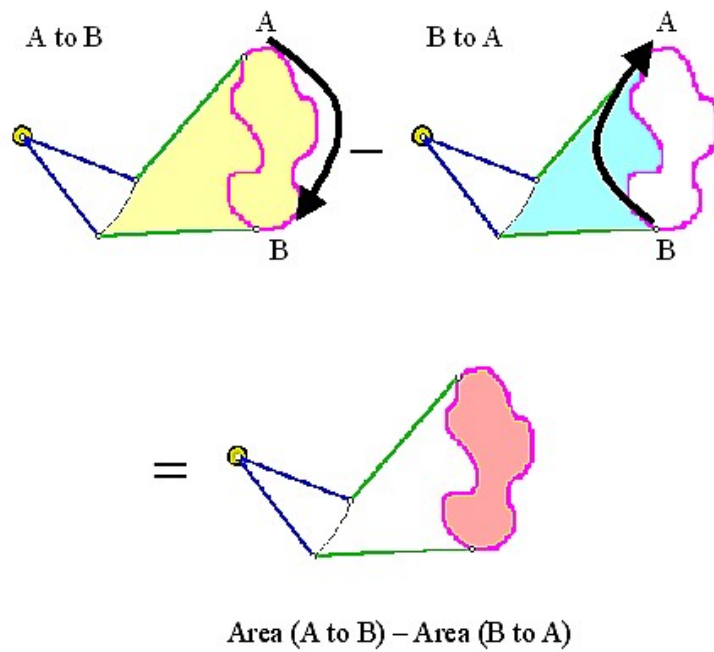


Figure 3.5: Final Area Calculation (Kunkle, 2001)

3.2.2 The Map Wheel

The map wheel, shown in Figure 3.6, is a simple device that measures length. A map wheel is comprised of a wheel connected to a scale that measures the distance the wheel has traced. This measure is then multiplied by a factor to correct for the map scale.



Figure 3.6: Map Wheel

3.2.3 Parameter Extraction

Using traditional methods, hydrologic parameters are extracted from paper maps. Slope is manually calculated based on the difference in contour line elevations from the upper point of the longest flow path and from the outlet. The difference in elevation is divided by the length of the longest flow path. Perimeter and longest flow path length are determined by using the map wheel, and area is calculated using the planimeter.

3.3 CASE II: ON-SCREEN DIGITIZING OF RASTER GRAPHIC MAPS

The process of on-screen digitizing of raster graphic maps is the next closest method to the traditional, paper map based methods of using a map wheel and a planimeter. The methodology is analogous; with the exception that the

process of digitization involves using a computer-aided mouse to draw drainage divides on a scanned map and to trace along lines to determine their length.

Geospatial input to watershed models can be described with vector data. Points or nodes can be used to represent outlet points, arcs (polylines) can be used to represent streams, and enclosed polygons used to represent the watershed. This is usually done by digitizing the streams and an approximate boundary for a watershed with an image of the site in the background. In this study a digital raster graphic, or DRG, is used as the basis for digitizing as shown in Figure 3.7. This is a scanned image of a USGS topographic map produced at a 1:24,000 scale, obtained by the USGS (Appendix A). DRGs are frequently used to edit and revise other digital data. Once the USGS map is scanned, the digital image is georeferenced to the true ground coordinates and projected into the Universal Transverse Mercator (UTM) for projection consistency (USGS, 1999).

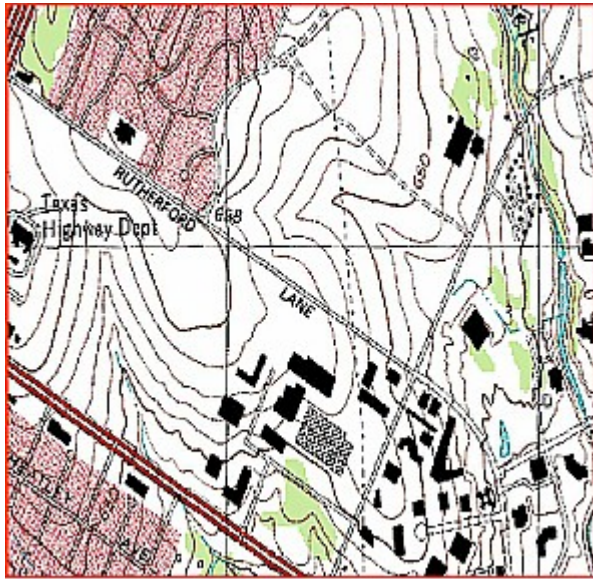


Figure 3.7: USGS Digital Raster Graphic (DRG)

Figure 3.8 shows watershed delineation using raster maps. The arrows point in the direction of steepest slope, while the lines divide the drainage boundaries. Arcs may also be used to define canals, railroads, streets, or other features that tend to act like streams during a rainfall/runoff event (Nelson et al., 1997).

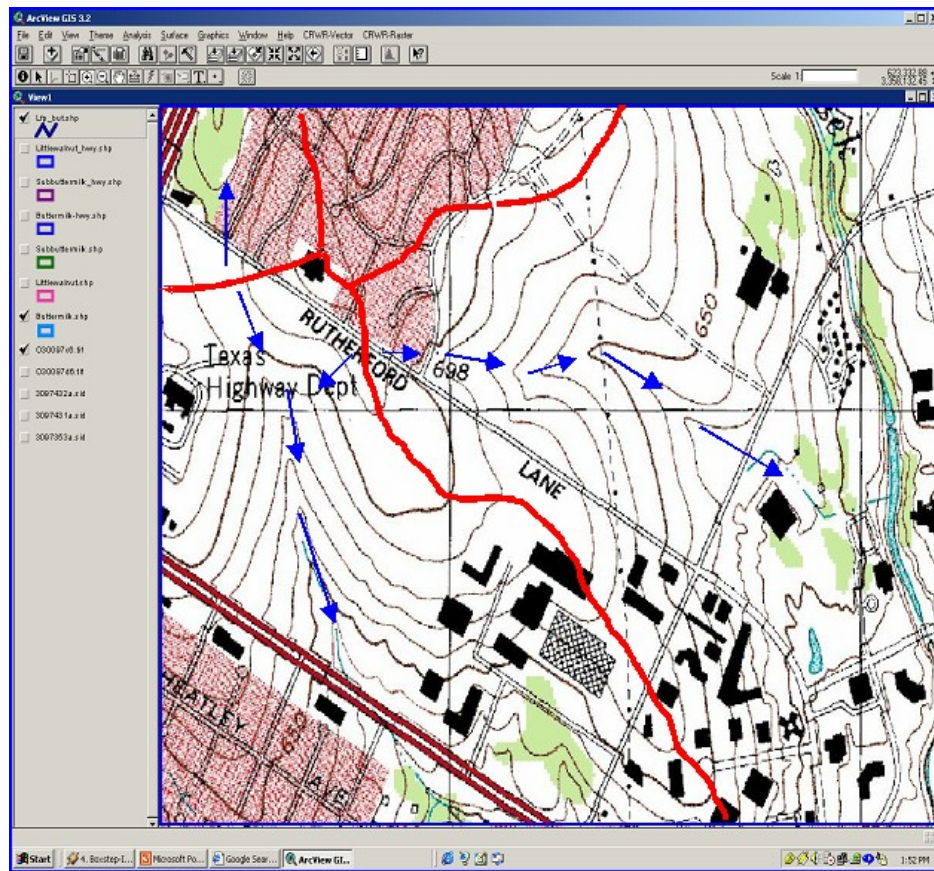


Figure 3.8: On-Screen Digitizing from a Raster Graphic Map

3.3.1 Digitizing in ArcView GIS 3.2

The first step in digitizing is to create a new theme as selected from the ArcView menu, as shown in Figure 3.9.



Figure 3.9: New Theme Creation in ArcView

A polyline is used to represent the longest flow path. Once the polyline is drawn (or polygon for area), ArcWorkstation is used to convert the new themes to coverages. After the polylines and polygons are converted to coverages, they are processed using the ArcWorkstation commands *build* and *clean*. Following this process the coverages are opened once again in ArcView GIS 3.2 and converted back to shapefiles.

3.3.2 Parameter Extraction

Figure 3.10 shows an example of a map-based model along with its length, area, and perimeter attributes. Information provided in the attribute tables for each shapefile give the length, area, and perimeter for each shape. Slope, determined using the same method as with paper maps, is calculated by subtracting the contour value at the outlet from the contour value at the start of the longest flow path. The difference in elevation is then divided by the length of the longest flow path.

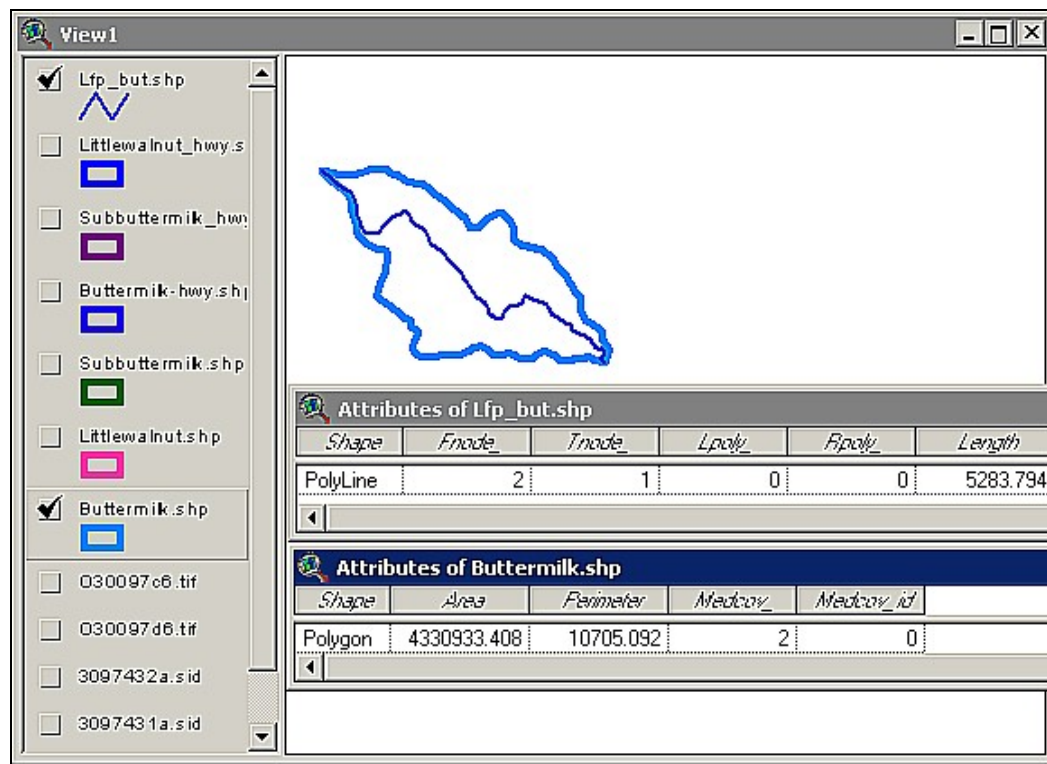


Figure 3.10: Map-Based Model in ArcView

3.4 CASE III: AUTOMATED METHODS USING A DEM

In Case III, hydrologic parameters are extracted from a grid-based digital elevation model (DEM) using both 10 meter and 30 meter DEM data. Two different processes are used to extract hydrologic parameters from elevation data. The first method involves using ArcView GIS 3.2 and CRWR-PrePro, while the second method extracts hydrologic parameters using the Watershed Modeling System (WMS). Both methods involve the same fundamental steps. These include 1) a raster-based terrain analysis, 2) raster-based sub-basin and stream network delineation, and 3) vectorization of the sub-basins and stream segments.

3.4.1 Overview of Automated Methods using a DEM

Topographic, topologic, and hydrologic information from digital spatial data can be extracted using a DEM and automated methods. This section describes the fundamental steps that must be taken to process a DEM and accurately extract information.

Errors in DEMs are usually classified as sinks (pits) or peaks. Removing the pits is a standard operation when working with grid-based DEMs. A peak is less detrimental to the calculation of flow direction and is usually ignored. A DEM free of sinks is termed a depressionless DEM, and is the ideal input to calculate flow direction for watershed delineation.

The 8-Direction Pour Point Model as shown below in Figure 3.11 represents the direction water flows based on the neighboring cell with the lowest elevation. This method is the most widely used raster DEM processing method.

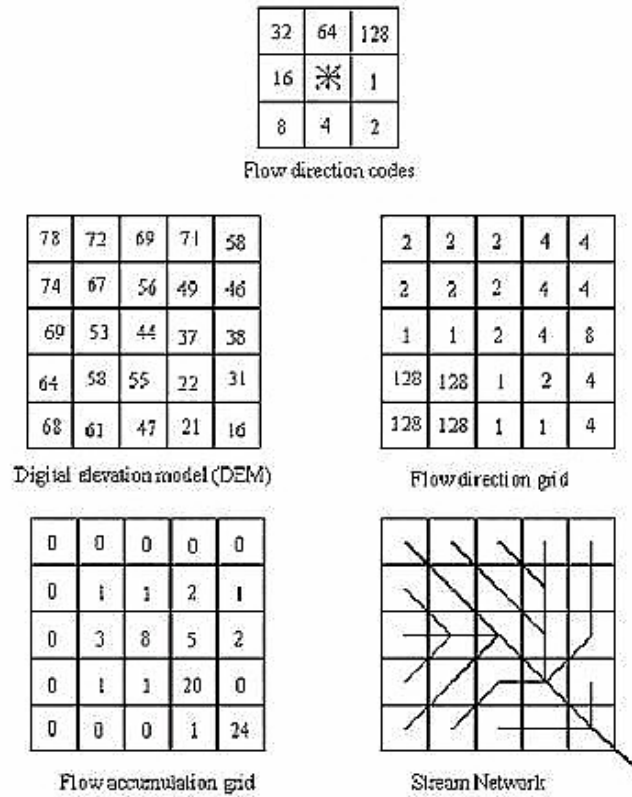


Figure 3.11: 8-Direction Pour Point Model (Anderson, 2000)

Most basin delineation techniques for grids are based around the 8-Direction Pour Point Model concept. However, the 8-Direction Pour Point Model has been criticized because it permits only one flow direction leaving a cell. Garbrecht et al. (1999a) note that this is satisfactory if being used for large drainage areas with well-defined channels, but the model may be less appropriate for overland flow analysis on hill slopes. A second method for determining flow direction is the $D-\infty$ Model developed by Tarboton (1997). Figure 3.12 below depicts this model.

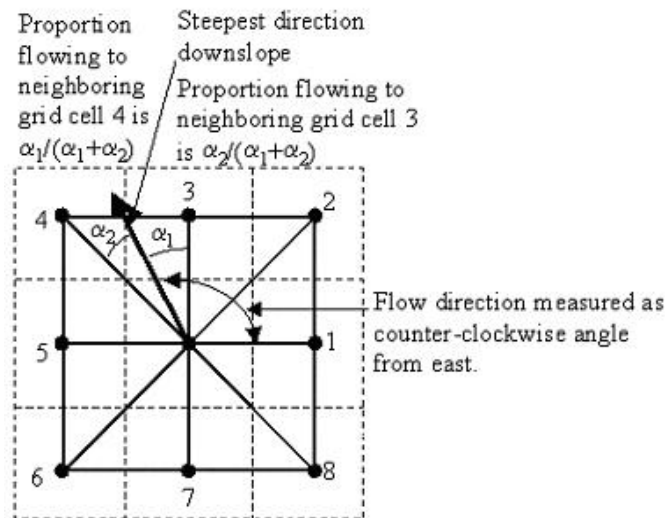


Figure 3.12: The D- ∞ Model (Tarboton, 1997)

The D- ∞ Model assigns a flow direction based on steepest slope on a triangular facet (Tarboton, 1997). The automated methods covered in this report do not use the D- ∞ approach, and so this method of watershed delineation is not further investigated.

Before computing filling pits and computing flow direction, the user may want to “burn-in” streams. This process raises the land surface cells off the stream cells by an arbitrary elevation so that streams delineated from the DEM match those produced in the National Hydrography Dataset (NHD) produced by the USGS. This step is not necessary for high resolution DEMs (Olivera et al., 1999).

Once flow direction has been calculated, a flow accumulation grid is computed. This is done by counting the number of contributing cells to each cell

in the grid. Based on the flow accumulation grid, a raster-based stream network can be developed based on a user-defined cell threshold (Olivera et al., 2000).

Threshold, a term used to describe the number of cells that drain to a point, also defines the number of cells that constitute the beginning of a stream. The selected threshold creates a drainage (stream) network based on all the cells with a catchment area greater than the threshold. The choice of threshold is complicated. Two methods for determining a threshold are the *constant area threshold method* and the *slope-dependent critical support area method*.

The *constant threshold area method* represents the change in sediment transport from sheet flow to concentrated flow, rather than a spatial transition in longitudinal slope profiles. Using the *slope-dependent critical support area method* the drainage density is greater in steeper portions of the catchment, as found in natural landscapes (Tarboton et al., 1991). The *constant threshold area method* is considered more practical in application than the *slope-dependent critical support area method*, and is the only method considered in this report. In this study, both CRWR-PrePro and WMS use the *constant threshold area method*. (Garbrecht et al., 1999)

Once the DEM has been processed by filling pits, flow direction and flow accumulation grids have been computed and a threshold chosen, the user may add streams and watershed outlets to the model. The final step for DEM processing is to vectorize the streams and watersheds. While a grid is convenient for the development of hydrologic data, it is inefficient for data storage. This is because with a grid there is a one-to-many relationship for most basin parameters. A more

convenient and efficient way to store both stream and basin data is through vectors and polygons (Nelson et al., 1997).

Figure 3.13 below shows an example of a watershed delineated from a grid-based digital elevation model (DEM).

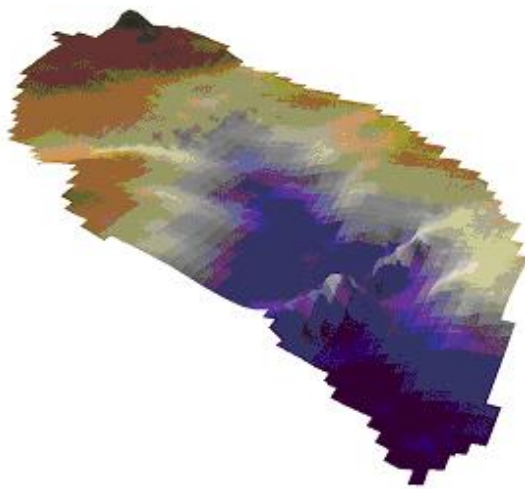


Figure 3.13: 30 Meter Delineated DEM

The following paragraphs describe this process using both ArcView GIS 3.2 (with CRWR-PrePro) and WMS.

3.4.2 ArcView GIS 3.2

The Environmental Systems Research Institute, Inc. (ESRI) developed ArcView GIS 3.2. This has now been replaced by ESRI's ArcGIS software package. ArcView GIS 3.2 is still very widely used in the professional world, and is examined in this study for the reason that the Texas Department of

Transportation (TxDOT) has this software package, and also that the preprocessor under investigation, CRWR-PrePro, operates only with ArcView GIS 3.2.

3.4.2.1 CRWR-PrePro

CRWR-PrePro was developed by several investigators at CRWR. It is the combination of several pieces of work developed by different researchers over a period of time. The first person to work on CRWR-PrePro was Ferdi Hellwager (1997). That same year, the *Watershed Delineator* ArcView extension was developed by Dean Djokic and Zichuan Ye of ESRI. This work was followed by the *Flood Flow Calculator* ArcView GIS 3.2 extension in 1997 by CRWR to estimate flood peak flows according to regional regression equations using the spatial data extraction capabilities of GIS. Combining these three ArcView extensions led to development of a hydrologic modeling tool that prepares an input file for the HEC-HMS basin component (Olivera et al., 1999). CRWR-PrePro, shown in Figure 3.14, is the predecessor to the more commonly used HEC-GeoHMS, as described in the forward of the HEC-HMS User's Manual USACOE-HEC, (2000).

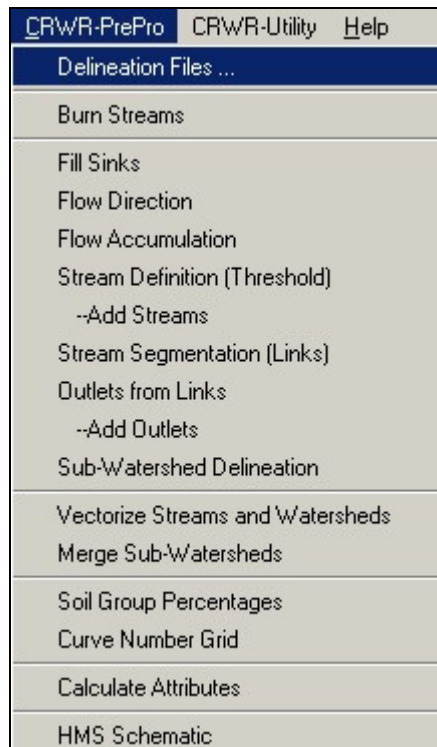


Figure 3.14: The CRWR-PrePro Menu Bar

CRWR-PrePro conducts a raster-based terrain analysis that includes burning-in streams, filling sinks, and calculating the flow direction (using the 8-Direction Point Pour Method as described earlier) and flow accumulation grids.

Following a raster-based terrain analysis (*Fill Sinks*, *Flow Direction*, and *Flow Accumulation* commands), a raster-based sub-basin and reach network analysis creates stream definition grids based on threshold (*Stream Definition*), stream segmentation grids (*Stream Segmentation*), an outlet grid (*Outlets from Links*), and delineated watershed grid (*Sub-Watershed Delineation*). Finally sub-basins and reach segments are vectorized (*Vectorize Streams and Watersheds*).

CRWR-PrePro calculates losses using the SCS curve number method or the initial plus constant loss method. To calculate curve number, soils data must be obtained. This may be done easily free of charge by downloading the data from the USDA-NRCS website (Appendix A). Attribute tables that relate to the soils data include the *mapunit.dbf* and *comp.dbf* tables, which should be added to the working directory in ArcView. The tables are modified and the CRWR-PrePro function *Soil Group Percentages* may be executed. This creates a table called *muidjoin.dbf*. Next Land Use/Land Cover (LULC) data must be obtained. Similar to the soils data, these data may be downloaded free of charge from the USGS website (Appendix A). By combining the LULC data and the soils data, a curve number grid (CN) may be generated using the *Curve Number Grid* command in CRWR-PrePro. An additional table that may be obtained off the CRWR-PrePro webpage, *rcn.txt*, is used as a look-up table to link curve number values to land use and soils data. Table *wshpar.txt* is necessary when the initial plus constant loss method is used (fields in table include *Initial_Loss*, *Const_LossRate*, and *Wsh_Velocity*). The final CN for each sub-basin is calculated as the average of the curve number values within the sub-basin polygon (Olivera et al., 1999).

Once the data are in vector format, hydrologic parameters of sub-basins and reaches such as reach length, reach routing method (Muskingum or lag), and either number of sub-reaches into which the reach is subdivided (for Muskingum routing), or the flow time (for pure lag) are computed. The other reach parameters such as flow velocity and Muskingum X cannot be computed from

spatial data and must be supplied by the user. The attributes are generated using the CRWR-PrePro command *Calculate Attributes* (Olivera et al., 1999).

3.4.2.2 Parameter Extraction using ArcGIS and CRWR-PrePro

CRWR-PrePro uses the SCS unit hydrograph method for sub-basin routing, and lag time may be calculated either with the SCS lagtime formula or length over velocity. The SCS equation is most frequently used owing to the fact that all the parameters for this equation can easily be extracted using GIS. The SCS Lag Time Equation (1972) is shown below in Equation 3.4. In Equation 3.4 $TLAG$ is the lag time in hours, L is the length of the longest flow path in feet, S is the slope of the longest flow path, and CN is the average curve number in the sub-basin.

$$TLAG = \frac{L^{0.8} [(1000 / CN) - 9]^{0.7}}{31.67 * S^{0.5}} \quad \text{Equation 3.4}$$

In the case of the length over velocity equation, flow velocities must be known for each cell in the subwatershed, and generally this is not readily known. As shown in Equation 3.5, $TLAG$ is the lag time in hours, L the length of the longest flow path in feet, and v (m/s) is the representative velocity in the longest flow path. As CRWR-PrePro only operates in metric units, all English units are converted into metric units.

$$TLAG = 0.6 * \frac{0.3048 * L}{60 * v} \quad \text{Equation 3.5}$$

Once the watershed of interest has been clipped, the user is prompted to select a time step. The time step is the interval that determines the resolution of model results during a run in HEC-HMS. Gauge data is linearly interpolated to the time interval, which may be chosen to range from 1 minute to 24 hours (USACOE-HEC, 2000). The Muskingum and lag methods are used for flow routing in the reaches, depending on the travel time. If the longest flow path (LFP) divided by the reach velocity is less than the time step the pure lag equation is used; otherwise Muskingum routing is used. It is apparent that time step selection and velocity have a very large effect on the outcome and should be modified accordingly (Olivera et al., 1999).

In addition to the fact that losses may only be calculated using the SCS curve number or the initial plus constant loss rate method, and lag time with only the SCS lagtime formula or length over velocity, another constraint of CRWR-PrePro is the slope calculation. CRWR-PrePro calculates slope based on the DEM cell elevations at 1% and 99% of the longest flow path divided by their distance along the longest flow path, and allows the user no flexibility in calculating watershed slope unless the user changes the Avenue code.

The user may want to calculate the slope at 10% and 85% of the longest flow path, not 1% and 99% percent of this flow path. In this way the high slope of the shallow concentrated flow is not included in the calculations for lag time. CRWR-PrePro calculates the longest flow path of a sub-basin in the set of cells

for which the sum of the downstream flow length to the outlet plus the upstream flow length to the drainage divide is maximum (Olivera et al., 1999).

Preparation of the HMS basin file (an ascii file readable by HEC-HMS) is the final step of CRWR-PrePro. In order to do thi, transfer and parameter tables (*wshpar.txt* and *streamp.txt* as mentioned above) are needed and are posted on the CRWR-PrePro webpage (Appendix A). All units must be in SI (Système International d'unités) (Olivera et al., 1999). In this study only the parameters curve number, slope, and longest flow path were extracted from the delineated watershed, and thus the HEC-HMS ascii file was not created.

3.4.3 Watershed Modeling System (WMS)

WMS was developed by the Environmental Modeling Research Laboratory (EMRL) at Brigham Young University for use in hydrologic computation and modeling. WMS is a set of modeling codes along with grid and mesh generation utilities, and post-processing and visualization tools in both two and three dimensions (Nelson et al., 1997). WMS is different from using ArcView GIS 3.2 in conjunction with CRWR-PrePro in that it may be used to run different hydrologic modeling programs in addition to computing hydrologic parameters. Similar to a GIS, WMS automates watershed delineation and parameter calculation from digital elevation terrain data, importing GIS data, and extracting watershed information from the GIS database.

As shown in Figure 3.15, the WMS drainage menu is similar to the CRWR-PrePro menu. Like CRWR-PrePro, the WMS drainage menu bar contains

basic DEM processing algorithms to compute flow direction and flow accumulation, although in WMS this is done with a program called TOPAZ. The drainage menu in WMS also gives the user the ability to vectorize data (*Basins->Polygons*), and compute the basin data (*Compute Basin Data*).

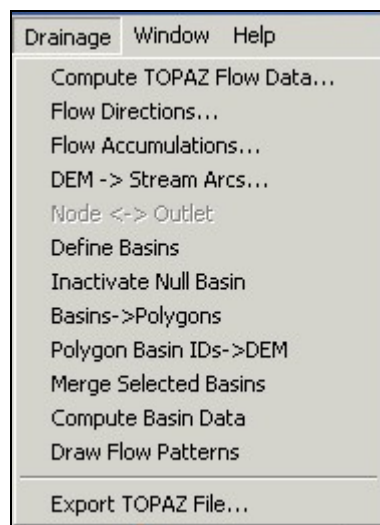


Figure 3.15: WMS Drainage Toolbar

Figure 3.16 shows the editing tools that are included in the DEM module. Among these tools are a *draw flow path* tool, in which a flow path will be traced across the DEM from point to point according to the flow direction grid. Additional tools include point, vertex, arc and polygon selection and creation tools, a measuring tool, and an upstream arc selection tool.

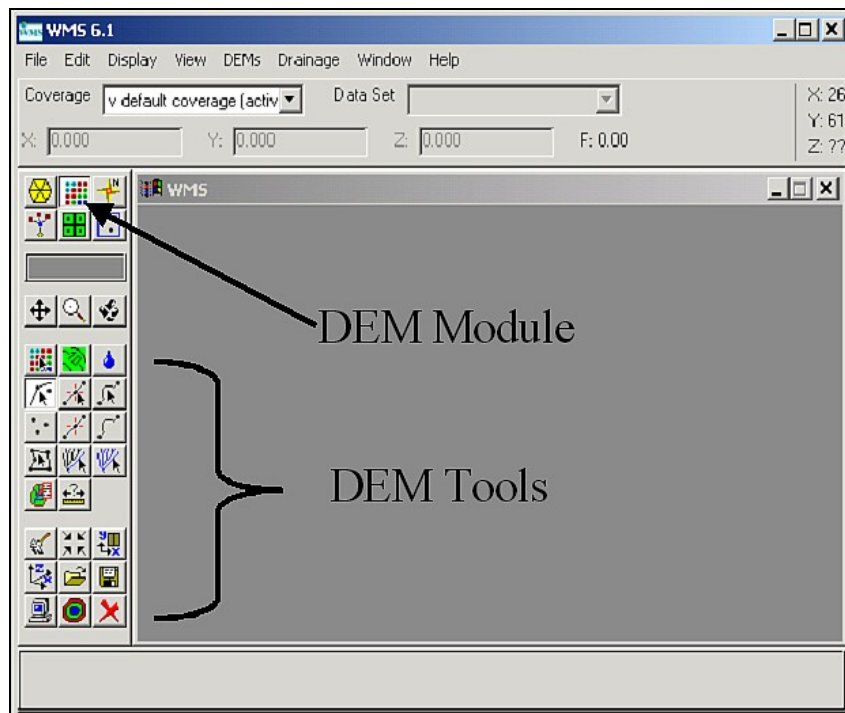


Figure 3.16: WMS Module

Additional modules available in WMS include a map module (which allows the import of GIS vector-based data to be used in WMS for watershed definition and hydrologic attribute mapping), hydrologic modeling with HEC-1, NFF (National Flood Frequency), TR-20, TR-55, Rational Method, and HSPF (Hydrologic Simulation Program Fortran), and hydrologic/hydraulic calculators. Unlike a GIS system, WMS can run hydrologic modeling programs without having to export or import data.

3.4.3.1 TOPAZ

The Watershed Modeling System (WMS) can be used to automatically delineate watersheds and sub-basin boundaries from digital elevation models (DEMs). WMS uses TOPAZ to delineate grid elevation data. However, flow directions and accumulations may also be computed by ArcInfo, ArcView, or GRASS and imported into WMS in grid ascii format. In this study, TOPAZ is run to determine the flow direction and flow accumulation grids for WMS. TOPAZ (Topographic Parameterization) is an automated digital landscape analysis tool for topographic evaluation, drainage identification, watershed segmentation, and sub-catchment parameterization, and is similar to CRWR-PrePro, which also uses the 8-Direction Point Pour Model.

TOPAZ, shown in Figure 3.17, creates three grids: a new elevation grid (*relief.dat*), a flow direction grid (*flowec.dat*) and a flow accumulation grid (*uparea.dat*).

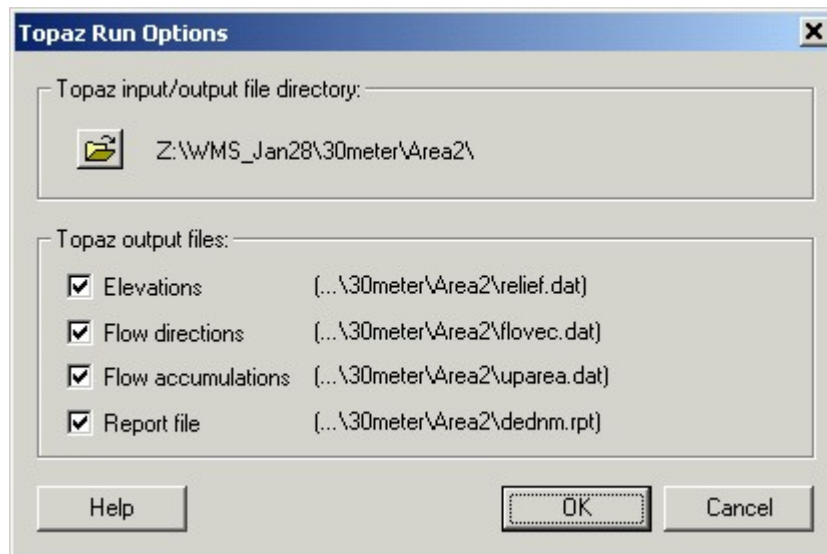


Figure 3.17: TOPAZ Grids

3.4.3.2 *Parameter Extraction*

Once a watershed has been delineated in WMS and all its hydrologic data has been defined using the *Compute Basin Data* command, a hydrologic model may be run. Hydrologic parameters were extracted using the *Display Options* tool, shown in Figure 3.18, so that the parameters of interest as calculated by WMS are displayed on the map.

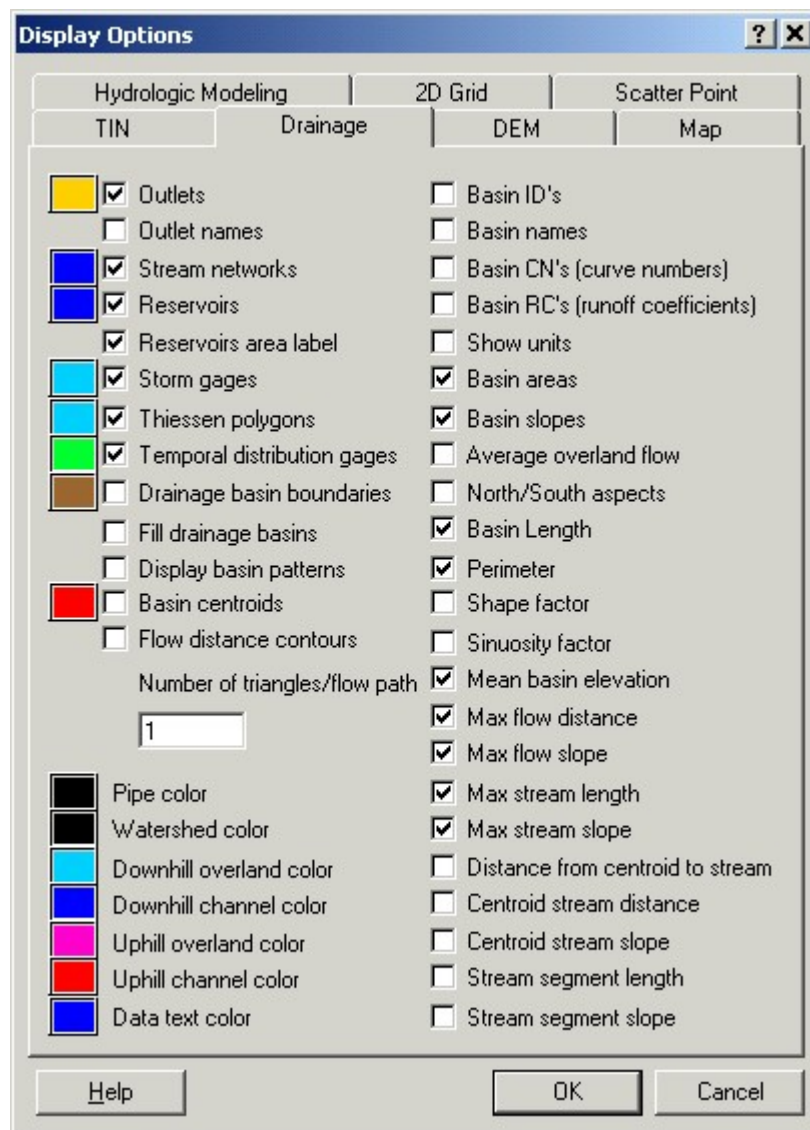


Figure 3.18: Display Options in WMS

Because WMS has tools to automatically calculate parameters such as the Green-Ampt parameters, time of concentration and other modeling parameters in a single application, it can be used to model watersheds more efficiently than traditional methods (Nelson et al., 1999a). Figure 3.19 shows a very handy tool in

WMS to compute time of travel, using user-defined equations or a variety of predefined equations which include the Tulsa District Lag Time Equation, the Denver Lag Time Equation, and SCS Lag Time Equation.

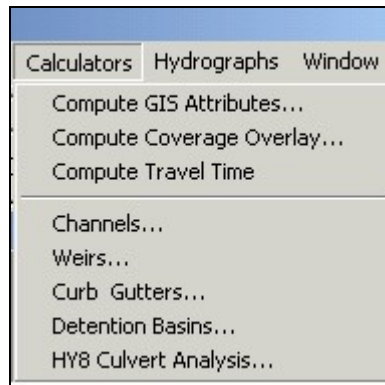


Figure 3.19: WMS Calculators

3.5 CASE IV: AUTOMATED METHODS USING A TIN

In addition to working with DEM terrain data, WMS also has the capability to work with TIN (triangulated irregular network) data. Similar to grid-based DEMs, TINs have also been used to characterize watersheds. TINs may be created in many ways, such as from gridded data, raw survey data, and digitizing contour data. Working with TINs is useful in that TINs provide a more precise description of the landscape than grids; however TINs are not as widely available and used as grids. TINs consist of a set of vertex points, connected by triangles, that represent scattered X, Y, and Z locations. (Nelson et al., 1999b)

For TINs to be used efficiently for basin delineation and hydrologic modeling, they need to be constructed from readily available data such as USGS

DEMs (Nelson et al., 1999b). According to Nelson et al. (1999b), TINs should be constructed around streams, canals, streets, and other linear features so that the TIN conforms to these features.

3.5.1 TIN Development and Processing

Figure 3.20 allows the user to create and edit TINs.

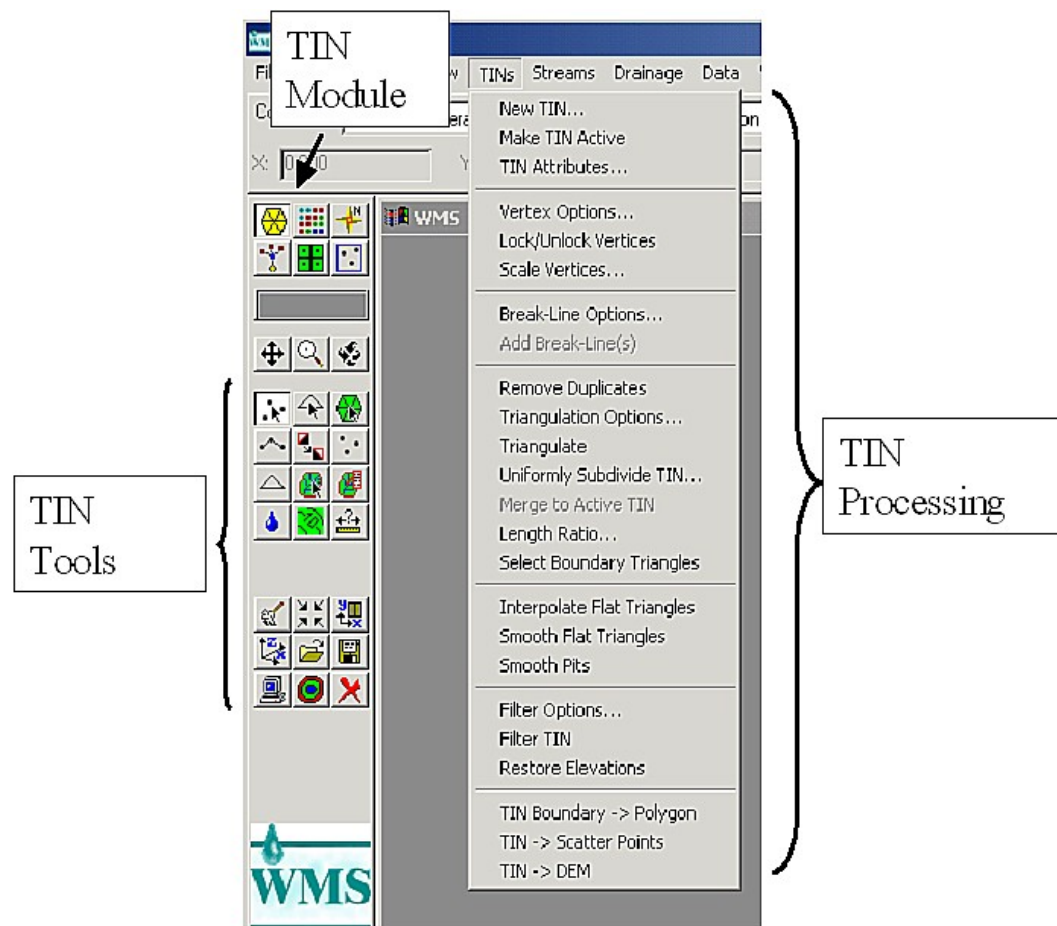


Figure 3.20: WMS TIN Module

The TIN is first created using *Vertex Options* under the *TINs* menu bar. By selecting an elevation, and a location on the background map (such as a digital raster graphic, or DRG), a point is added to the map at the specified elevation as shown in Figure 3.21. Alternatively elevation data can be imported from a LIDAR or aerial land survey.

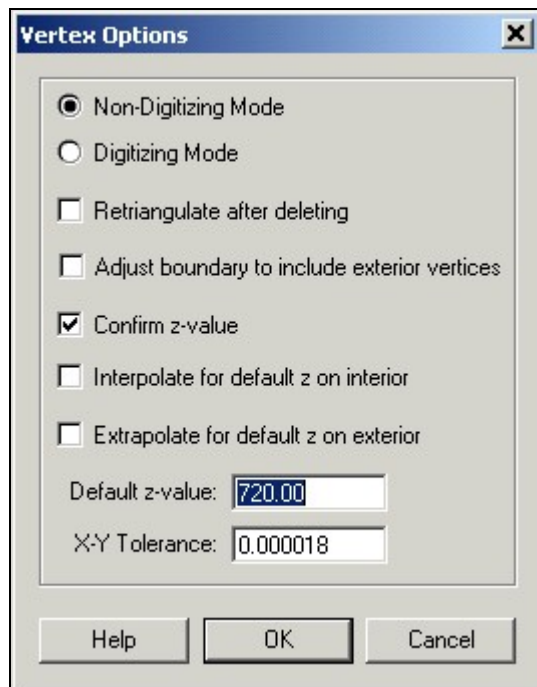


Figure 3.21: Vertex Options in WMS

Once the user is satisfied with the amount of points, TIN breaklines may be added to the model to reflect streams and other terrain features. When breaklines are added, the triangles created conform to these lines. So that the TIN conforms to the terrain, breaklines must be created where the water drains. This is done by selecting the conceptual (map) model icon and turning off the TIN.

Using the rough boundary and stream network defined in the conceptual model, WMS can create a triangulated irregular network (TIN) using the *adaptive tessellation algorithm*. The adaptive tessellation algorithm generates a mesh of triangular elements. The mesh lies within the model domain, and honors the conceptual model set up of point elevations and channel and watershed boundaries. The boundary defines the TIN extents, and the stream and ridge arcs are forced into the TIN as breaklines to ensure that the triangle edges will be enforced along all streams and ridges. A stream is created from the triangle edges. Following the development of the TIN based on background contour information, a DEM may be used as a background elevation source (Nelson et al., 1999b).

After the TIN has been created, the final step before the TIN can be delineated is to condition the TIN. Conditioning is necessary because there are usually flat triangles and pits in the TIN. WMS comes with tools to condition the TIN. These tools include elevation smoothing, edge swapping, adjusting elevations, and adding or deleting vertices (Nelson et al., 1999b).

3.5.2 TIN Parameter Extraction

Once the basins have been defined, geometric attributes such as stream lengths, stream slopes, basin areas, basin slopes, and maximum drainage distance within a basin, are automatically computed from the TIN model. These attributes may be combined with runoff curve numbers to generate a runoff model.

Chapter 4: Application

This implementation study applies traditional methods in hydrologic modeling and compares those traditional processes to those using GIS for three differently sized watershed areas. Four different case studies were performed: (1) measurement from paper maps; (2) on-screen extraction from raster maps; (3) using GIS and two different resolutions of grid-based digital elevation models (DEMs); and (4) using a triangulated irregular network (TIN).

4.1 SITE SELECTION

The study areas were determined in a meeting Friday, February 9th, 2001 with David Stolpa of TxDOT. During this meeting Mr. Stolpa mentioned that he was interested in comparing analyses for certain area sizes, and these watersheds each met this area size criteria. Buttermilk Creek watershed was chosen initially as this is an area in which TxDOT has conducted an analysis for a highway project.

All three study areas are located in Travis County, Texas, as shown in Figure 4.1.



Figure 4.1: Location of Travis County, Texas

Within Travis County are two watersheds, Buttermilk and Little Walnut, located in northern Austin. A shapefile of these two watersheds, provided by the City of Austin, is shown in Figure 4.2. Little Walnut is the larger watershed, and Buttermilk is the smaller watershed.

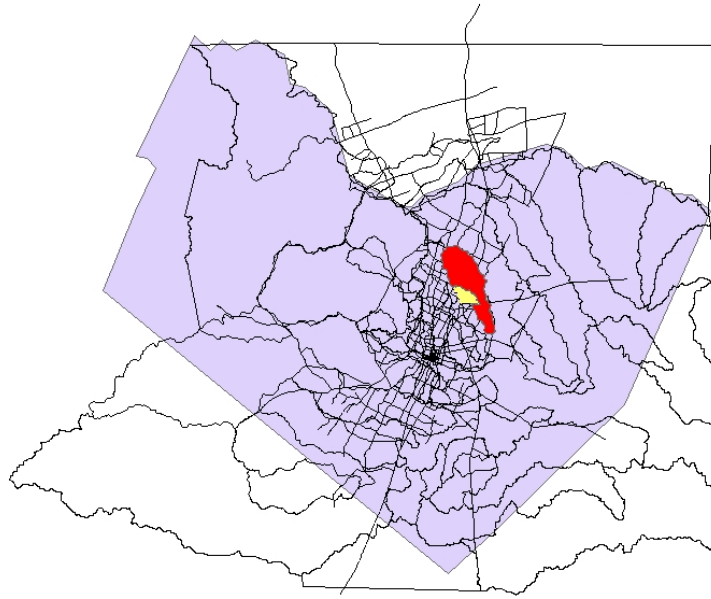


Figure 4.2: Location of Buttermilk and Little Walnut in Travis County

Area 1, the small area, is a subwatershed of Buttermilk Creek. This area is located at the upper end of Buttermilk. Area 2 is Buttermilk watershed, and Area 3 is Little Walnut creek above its confluence with Buttermilk Creek. The stream lines shown are from the National Hydrography Dataset (NHD). Figure 4.3 gives a general idea of the shape and location of the three study areas.

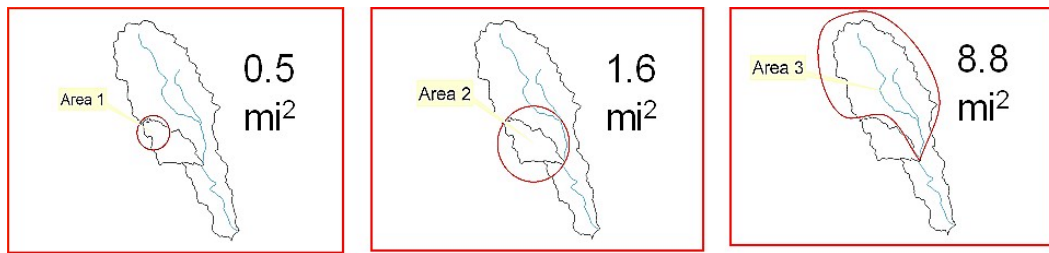


Figure 4.3: Area 1, Area 2, and Area 3

4.2 CASE I: TRADITIONAL METHODS

Two USGS quad maps, Austin East (3097-242) and Pflugerville West (3097-243), were required to cover the study area of Buttermilk and Little Walnut watersheds. Measurements were all done by hand for the three differently sized areas, Area 1, Area 2, and Area 3.

The first watershed to be delineated was Area 2 (Buttermilk). The first step to determine Area 2's boundary was to locate the outlet point from the USGS map. This point marks the confluence of Buttermilk with Little Walnut Creek watershed. Using a pencil, the watershed of Buttermilk was traced on the USGS maps. Secondly, the portion of Area 3 (Little Walnut) above its confluence with Area 2 was delineated. The subwatershed of Buttermilk was delineated last (Area 1). For each area the longest flow path was determined and traced with the pencil. Figure 4.4 shows the outlet point for Area 2 and Area 3.

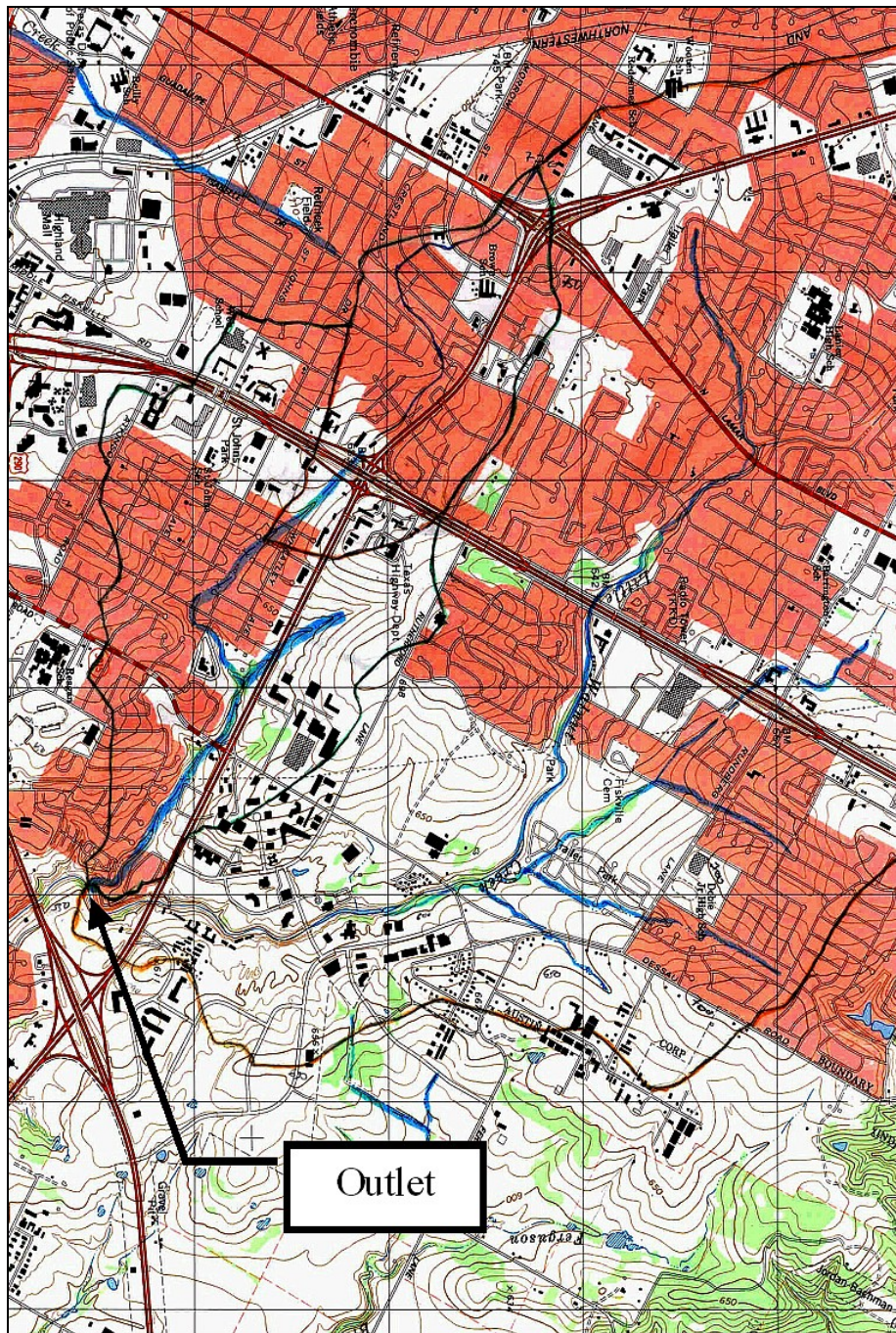


Figure 4.4: Hand Delineation of Area 2

The areas were measured by first determining the planimeter constant. The constant was determined by measuring a square area of 4 in². Three readings were taken that varied by only 0.002 units. These three measurements were averaged, and a constant of 13.730 calculated. Following this procedure, a circle of area 4 in² was measured three times and the average of these readings calculated. For the circle, an average constant of 13.029 was calculated. The final step in determining the overall planimeter constant was by averaging these two constants. In this way, both straight lines and curved lines are taken into account in the calculation of area. The final averaged planimeter constant was 13.380.

The perimeter and longest flow path length were determined using a map wheel. Similar to measurements taken with the planimeter, each area was measured three times, and the average measurement taken. Lastly, slope was calculated by subtracting the elevation of the longest flow path at the outlet of the subbasin from the elevation at the start of the longest flow path, divided by the length of the longest flow path. Table 4.1 outlines the results of each calculation for area, perimeter, longest flow path, and slope as derived by traditional methods.

Table 4.1: Hand Delineation Results

| Watershed | Area (mi²) | Perimeter (mi) | Longest Flow Path (mi) | Slope (%) |
|------------------|----------------------------------|---------------------------|-----------------------------------|------------------|
| Area 1 | 0.55 | 3.31 | 1.69 | 1.27 |
| Area 2 | 1.65 | 6.17 | 3.14 | 1.47 |
| Area 3 | 8.49 | 13.83 | 6.28 | 0.77 |

4.3 CASE II: AUTOMATED METHODS BY DIGITIZING

In Case II watershed boundaries are digitized using ArcView GIS 3.2 from digital raster maps (DRGs) assuming undeveloped conditions. With the DRG placed on the computer screen, new shapefiles are created using the digitizing capabilities of ArcView GIS 3.2 and ArcWorkstation.

A USGS digital raster graphic (DRG) was used as a background in ArcView GIS 3.2. The DRGs used were Austin West (o30097c6.tif and o30097d6.tif), produced by the USGS in 1988.

The first step in digitizing is to create a new theme as selected from the ArcView menu. As discussed in Chapter 3, watersheds are delineated in the same fashion as with the paper maps, except with a computer-aided mouse. For each area a polygon was used to represent area, and a polyline to represent the longest flow path. Once the polyline was drawn (or polygon for area), ArcWorkstation was used to convert the new themes to coverages using the *shapearc* command. After the polylines and polygons were converted to coverages, they were processed using the ArcWorkstation commands *build* and *clean*. Once they were built and cleaned, they were opened once again in ArcView and converted back to shapefiles.

During the process of digitization, it became apparent that some areas were difficult to digitize because the contour lines could not easily be seen in areas with highway overpasses. In an effort to incorporate parameter variations that might be encountered due to highway construction, two delineations were

made for each study area--one incorporating infrastructure and one disregarding the infrastructure.

Figure 4.5 below shows the digitization results for Area 1, both for highways excluded and highways included. The largest difference occurs at the upper end of Area 1, where it is very difficult to distinguish the contour lines.

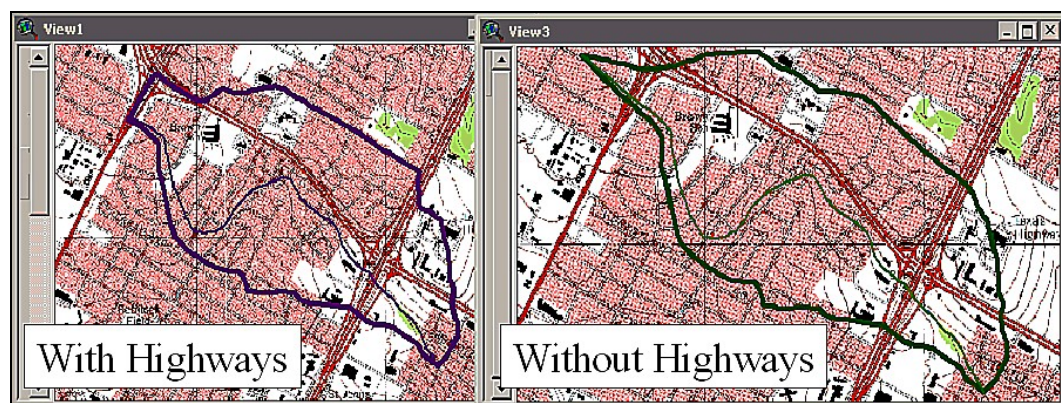


Figure 4.5: Area 1 Digitized

The delineation of Area 2 yielded the following, as shown in Figure 4.6. As Area 2 lies within Area 1, the digitization of the upper end of Area 2 replicates the digitization process for Area 1.

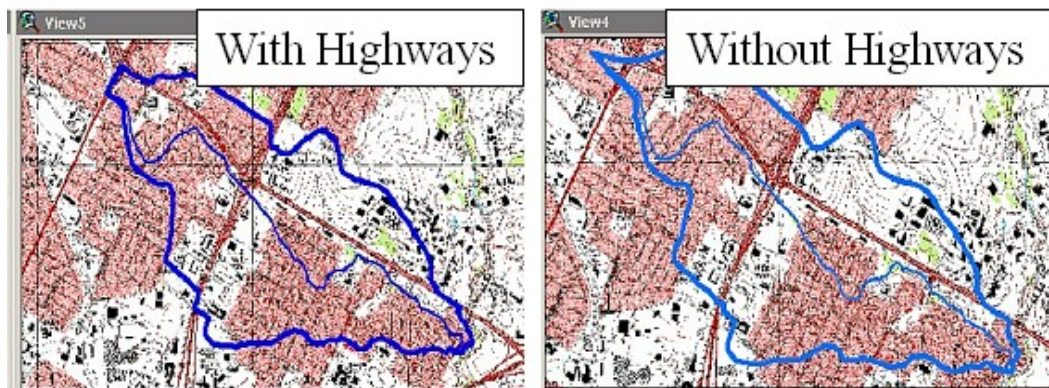


Figure 4.6: Area 2 Digitized

The delineation of Area 3 is shown in Figure 4.7. The differences between *With Highways* as opposed to *Without Highways* are hard to note in this figure due to the large area that Area 3 encompasses.

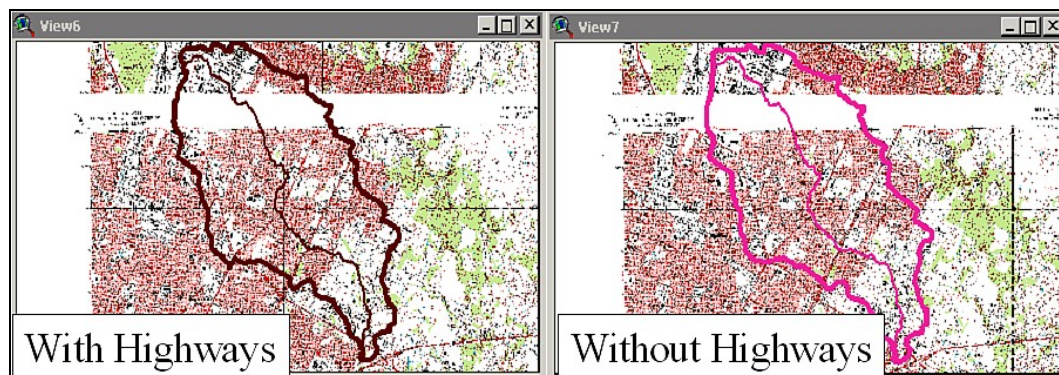


Figure 4.7: Area 3 Digitized

Watershed parameters are calculated using the GIS (for area, perimeter and longest flow path). From the new shapefile the parameters area and perimeter

can be calculated automatically. A longest flow path is also digitized from the DRG and its length calculated by the GIS.

Table 4.2 outlines the results of Area 1, Area 2, and Area 3 from digitization.

Table 4.2: On-Screen Digitizing Results

| Watershed | No Hwy/ Hwy | Area (mi²) | Perimeter (mi) | Longest Flow Path (mi) | Slope (%) |
|------------------|------------------------|----------------------------------|---------------------------|---------------------------------------|------------------|
| Area 1 | No Hwy | 0.55 | 3.42 | 1.79 | 1.27 |
| | Hwy | 0.52 | 3.24 | 1.57 | 1.32 |
| Area 2 | No Hwy | 1.68 | 6.57 | 3.28 | 1.47 |
| | Hwy | 1.65 | 6.50 | 3.09 | 1.44 |
| Area 3 | No Hwy | 8.85 | 14.75 | 6.63 | 0.77 |
| | Hwy | 8.87 | 15.53 | 6.58 | 0.78 |

4.4 CASE III: AUTOMATED METHODS USING A DEM

Case III is divided into two parts. The first part describes using ArcView GIS 3.2 and CRWR-PrePro to delineate the watersheds and extract watershed parameters using two different spatial resolution DEMs. The second part explores using the Watershed Modeling System (WMS) to also delineate the watersheds and extract watershed parameters at the same two spatial resolutions as with ArcView GIS 3.2.

The most widely available grid DEMs in the US are distributed by the USGS and are of 7.5 minute resolution (same coverage as a standard USGS 7.5 minute map series quadrangle), with a grid spacing of 30 x 30 meters. These

USGS digital elevation models are produced from models based on aerial photographs and satellite remote sensing images. The USGS 7.5 minute DEM data are georeferenced using the Universal Transverse Mercator (UTM) coordinate system. For this study, the DEMs used were developed by the USGS and distributed by the Texas Natural Resources Information System (TNRIS). The USGS is also producing a 10 meter DEM; however the regional availability of these elevation models is less than that of the 30 meter DEMs.

4.4.1 ArcView GIS 3.2 and CRWR-PrePro

Case III explores using ArcView GIS 3.2 and CRWR-PrePro to delineate the watersheds using two different spatial resolutions. As mentioned previously, this part of the study entails using two different resolution grid DEMs: a 10 meter DEM and a 30 meter DEM. All data are projected into the TCMS Albers Equal Area georeferencing system. The Texas Geographic Information Council (TGIC) defines a statewide mapping system for use in projected geospatial datasets that cover Texas in order to facilitate overlay and integration of datasets. The Texas Centric Mapping System/ Albers Equal Area or TCMS/AEA is defined below:

Mapping System Name: Texas Centric Mapping System/Albers Equal Area

Mapping System Abbreviation: TCMS/AEA

Projection: Albers Equal Area Conic

Longitude of Origin: 100 degrees West (-100)

Latitude of Origin: 18 degrees North (18)

Lower Standard Parallel: 27 degrees, 30 minutes (27.5)

Upper Standard Parallel: 35 degrees (35.0)

False Easting: 1,500,000 meters

False Northing: 6,000,000 meters

Datum: North American Datum of 1983 (NAD83)

The DEMs were clipped by first converting a box theme (as digitized in ArcView around the study area) to a coverage using the ArcWorkstation command *shapearc box boxcov*. Then the *boxcov* coverage was processed using the ArcWorkstation *build boxcov* command. The cell size was set to that of the DEM (*setcell grid*), and the window to that of the box coverage (*setwindow boxcov grid*). The coverage was turned into a grid (*temp = polygrid [boxcov]*), set to one (*temp2 = temp / temp*) and then clipped (*clpgrd = temp2 * dem30m*).

Once the DEM was clipped, it was projected into the TCMS Albers projection. This was done in ArcWorkstation. Each DEM was processed as outlined under CRWR-PrePro in Chapter 3.

The development of a curve number (CN) grid was necessary to estimate the spatial variability of runoff from a rainfall event. After the DEMs were clipped, the same was done with the USGS Land Use/Land Cover (LULC) coverage and the USDA/NRCS STATSGO soils coverage for the same area. Figure 4.8 shows the Land Use/Land Cover data clipped to the area of interest.

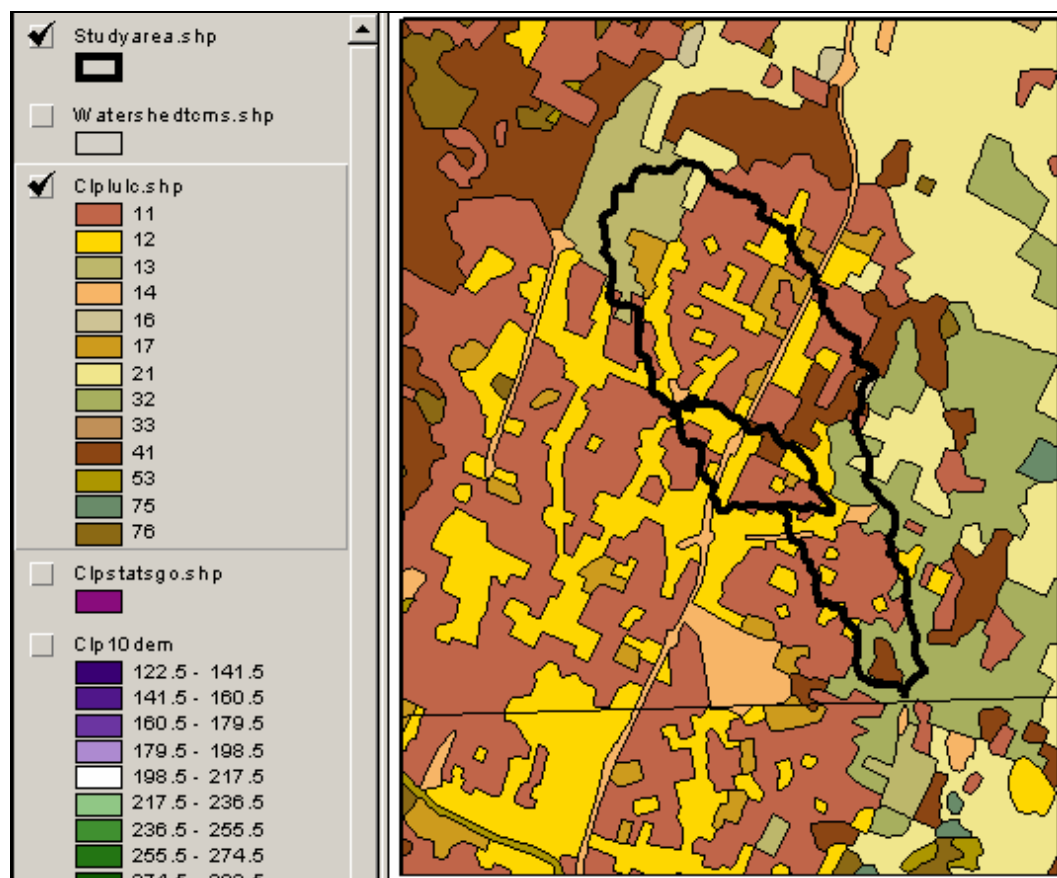


Figure 4.8: Land Use/Land Cover (LULC) Data

Figure 4.9 below shows the USDA/NRCS STATSGO soils data clipped to the study area. Similar to the USGS LULC coverage, the STATSGO coverage is a 1:250,000-scale map product. Both coverages are coarse compared to the resolutions of the 10 and 30 meter DEMs.

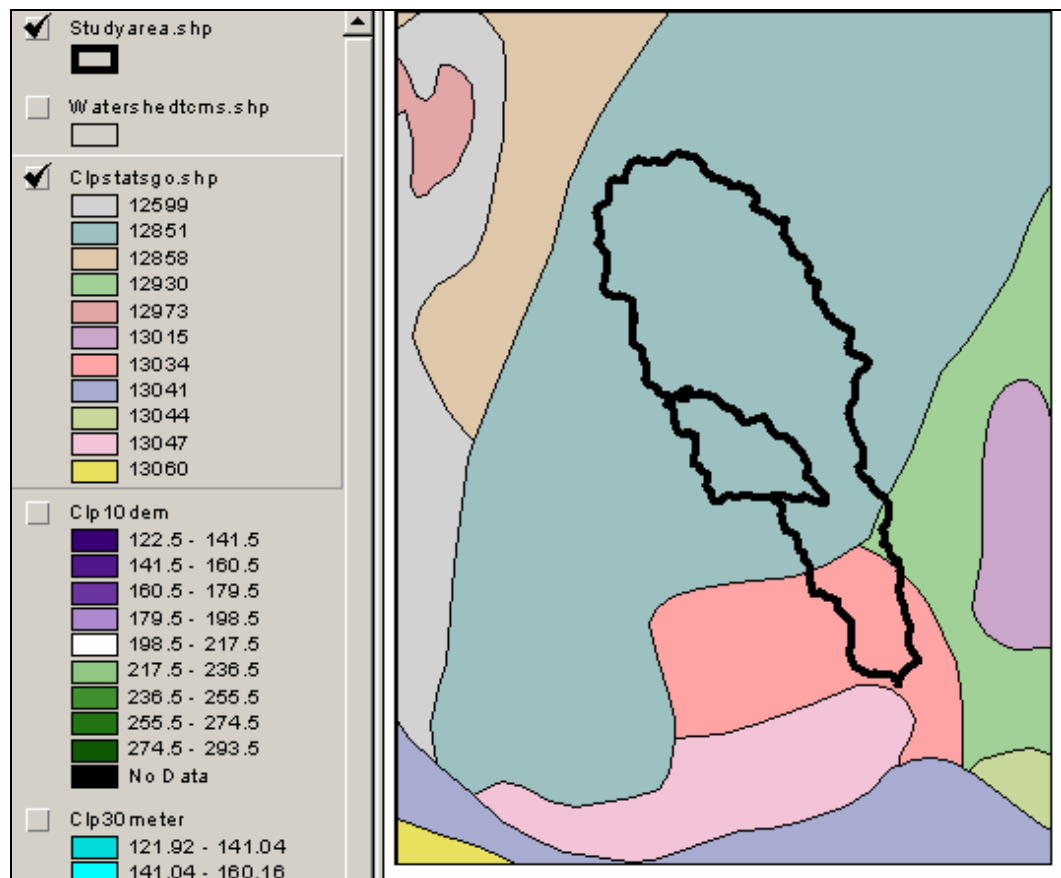


Figure 4.9: STATSGO Data

The DEMs were clipped to a small area, and delineated separately for the three areas. For each area, a threshold was chosen so that the areas of interest would be delineated as separate units.

4.4.1.1 10 Meter DEM

As each 10 meter DEM covers an area of about 66 mi², the DEMs were first merged and clipped so that the study areas were covered completely by the DEM.

For the large watershed an outlet was placed at the confluence with Buttermilk. The steps taken were those described earlier for watershed delineation using CRWR-PrePro. Table 4.3 below outlines these data, and the thresholds chosen for each area.

Table 4.3: 10 Meter DEM Watershed Data

| Watershed | Threshold | Cells in Watershed | Area/Cell |
|------------------|------------------|---------------------------|------------------|
| Area 1 | 4500 | 13895 | 100 |
| Area 2 | 22500 | 43504 | 100 |
| Area 3 | 90000 | 228578 | 100 |

In a study conducted by Garbrecht et al. (1999b) on an agricultural watershed, digital elevation models were applied to the study areas with cells ranging from 5 to 500 meters. In this study the ratio of average subcatchment area to grid cell area was used as an indicator of spatial resolution. An overall catchment-to-grid ratio of 100 was found to be an acceptable threshold of spatial resolution for reasonable model result. For this reason this parameter has been incorporated into the analysis. Table 4.4 below outlines the physical parameters determined from this study using a 10 meter DEM.

Table 4.4: 10 Meter DEM in ArcView Results

| Watershed | Area (mi²) | Perimeter (mi) | Longest Flow Path (mi) | Slope (%) |
|------------------|----------------------------------|---------------------------|-----------------------------------|------------------|
| Area 1 | 0.54 | 4.08 | 1.56 | 1.36 |
| Area 2 | 1.68 | 8.38 | 3.21 | 1.43 |
| Area 3 | 8.83 | 20.04 | 6.96 | 0.74 |

4.4.1.2 30 Meter DEM

The 30 meter DEMs were delineated in a similar fashion to the 10 meter DEMs. The DEMs used for this study are *Pflueastm* (Pflugerville East), *Pflugwestm* (Pflugerville West), *Manorm* (Manor), *Jollyvillm* (Jollyville), *Austinwestm* (*Austin West*), and *Austinestm* (Austin East).

In the same process as done for the 10 meter DEM, LULC and STATSGO data were prepared for the 30 meter DEM. The results for the three areas are shown below. In both cases (10 meter and 30 meter DEM delineations) an outlet was added to delineate the large watershed at the confluence with Buttermilk. Figure 4.10 shows the three areas delineated separately, and the longest flow path for each.

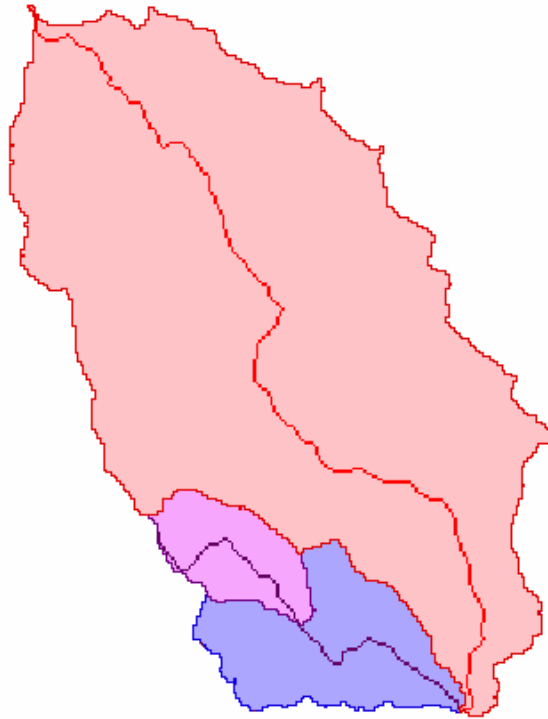


Figure 4.10: Delineated DEM Study Area

For the large watershed an outlet was placed at the confluence with Buttermilk, as with the 10 meter DEM data. The steps taken were those described earlier for watershed delineation using CRWR-PrePro. Table 4.5 outlines these data, and the thresholds chosen for each area.

Table 4.5: 30 Meter DEM Watershed Data

| Watershed | Threshold | Cells in Watershed | Area/Cell |
|------------------|------------------|---------------------------|------------------|
| Area 1 | 500 | 1568 | 899 |
| Area 2 | 2500 | 4835 | 900 |
| Area 3 | 10000 | 25427 | 900 |

The following table, Table 4.6, outlines the DEM derived parameters from this study using a 30 meter DEM.

Table 4.6: 30 Meter DEM in ArcView Results

| Watershed | Area (mi²) | Perimeter (mi) | Longest Flow Path (mi) | Slope (%) |
|------------------|----------------------------------|---------------------------|-----------------------------------|------------------|
| Area 1 | 0.54 | 4.06 | 1.50 | 1.26 |
| Area 2 | 1.68 | 8.16 | 3.06 | 1.39 |
| Area 3 | 8.84 | 19.08 | 6.78 | 0.76 |

4.4.2 Automated Methods Using WMS

The second part of the DEM-based analysis examines using WMS to delineate both the 10 meter and 30 meter DEMs. Results from the WMS analysis are expected to give slightly different results than with ArcView GIS 3.2 and CRWR-PrePro, because different algorithms are used to extract the hydrologic parameters.

4.4.2.1 10 Meter DEM

The 10 meter digital elevation data used for the WMS study are the same as those used for the CRWR-PrePro study. The same grid that was clipped for the CRWR-PrePro study was imported into WMS as a grid ascii file using the *import data* command. Once this was done the DRG for the area was placed in the background to locate the study area. Flow direction and flow accumulation grids

were computed using TOPAZ. Figure 4.11 shows the WMS delineating of Area 1, and its area value as 0.53 mi².

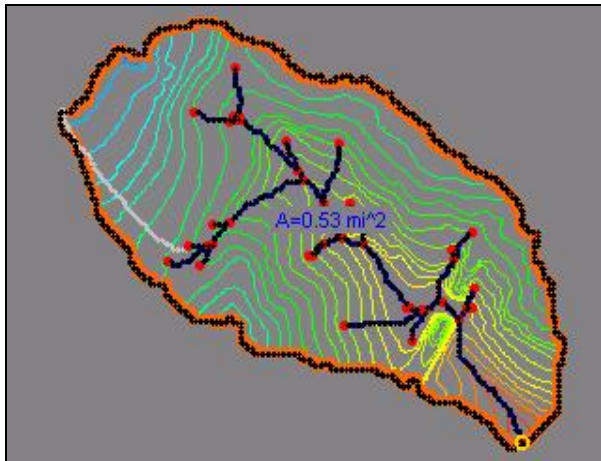


Figure 4.11: Area 1 Delineated in WMS

Figure 4.12 shows the area of Area 2 to be 1.66 mi². The white line is the longest flow path.

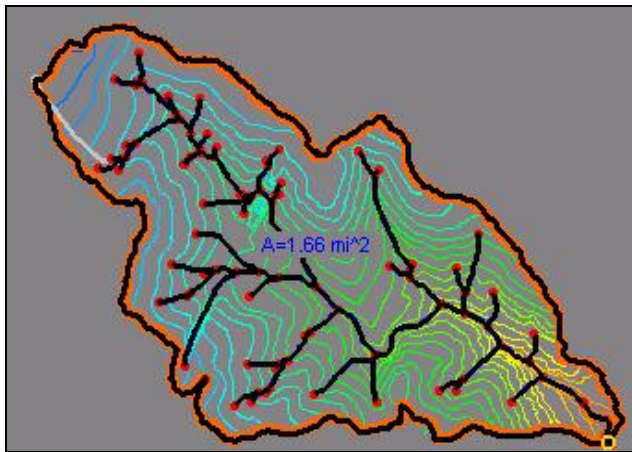


Figure 4.12: Area 2 Delineated with WMS

Figure 4.13 shows the area of Area 3 to be 8.76 mi².

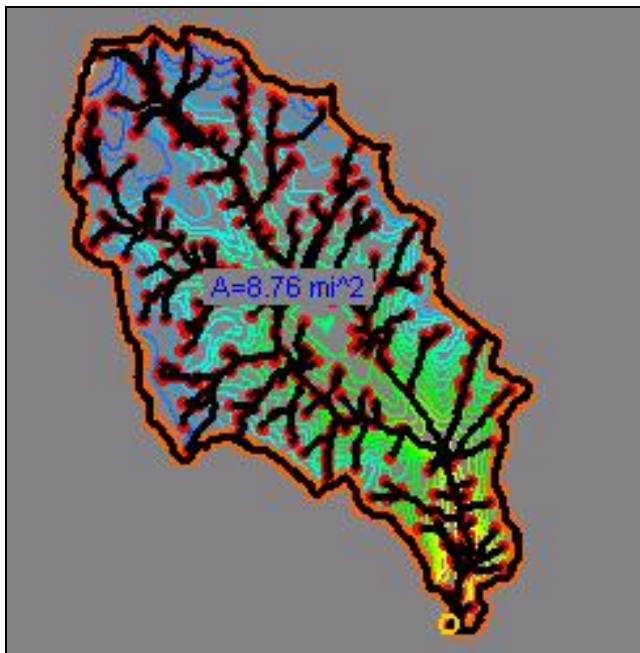


Figure 4.13: Area 3 Delineated with WMS

Table 4.7 shows the results from the study using a 10 meter DEM to extract watershed parameters in WMS.

Table 4.7: 10 Meter DEM in WMS Results

| Watershed | Area (mi²) | Perimeter (mi) | Longest Flow Path (mi) | Slope (%) |
|------------------|----------------------------------|---------------------------|-----------------------------------|----------------------|
| Area 1 | 0.53 | 4.09 | 1.54 | 1.25 |
| Area 2 | 1.66 | 8.53 | 3.15 | 1.41 |
| Area 3 | 8.76 | 19.85 | 6.81 | 0.77 |

4.4.2.2 30 Meter DEM

The 30 meter digital elevation data used for the WMS study are also the same as those used for the CRWR-PrePro study. The same grid that was clipped for the CRWR-PrePro study was imported into WMS as a grid ascii file, using the *import data* command. Once this was done the DRG for the area was placed in the background to locate the study area. TOPAZ computed the flow direction and flow accumulation.

Figure 4.14 shows the area of Area 1 to be 0.53 mi².

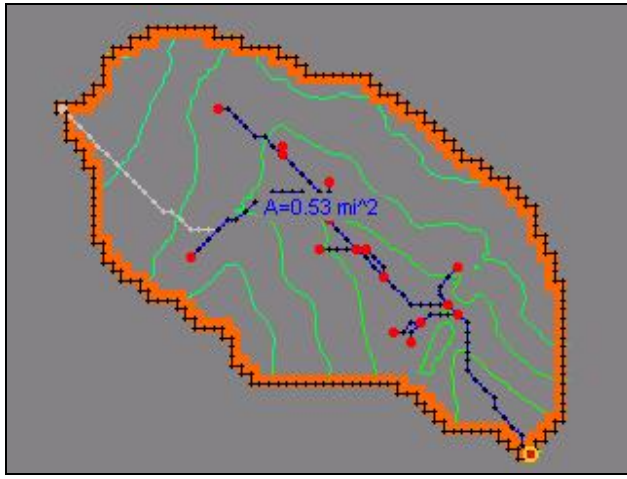


Figure 4.14: Area 1 Delineated with WMS

Figure 4.15 shows the area of Area 2 to be 1.67 mi².

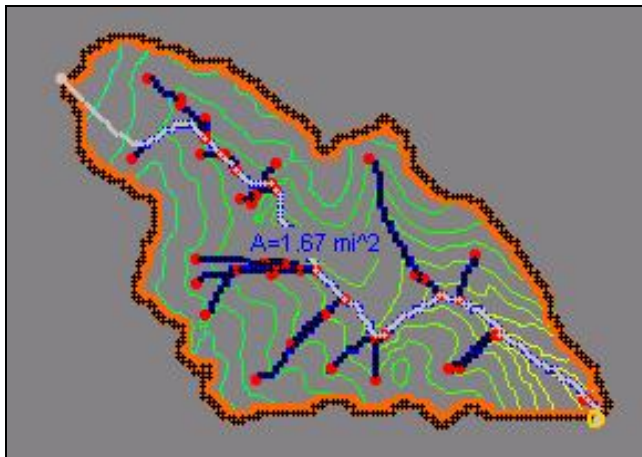


Figure 4.15: Area 2 Delineated with WMS

Figure 4.16 shows the area of Area 3 to be 8.84 mi².

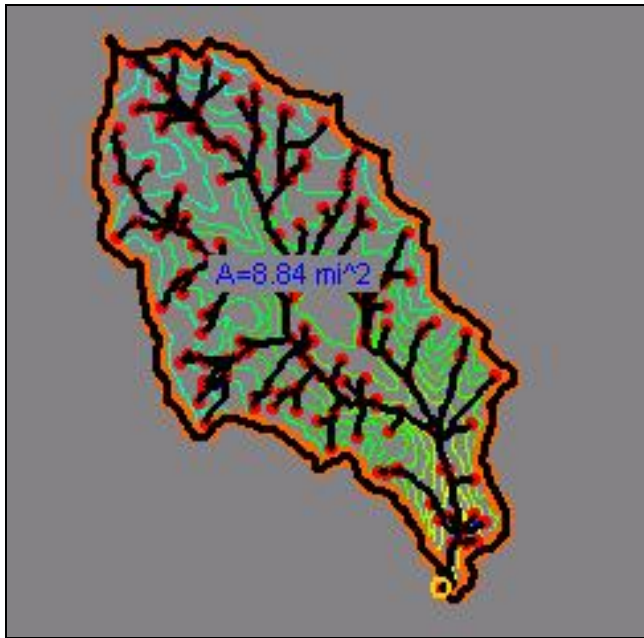


Figure 4.16: Area 3 Delineated with WMS

Table 4.8 shows the results from the study using a 30-meter DEM to extract watershed parameters in WMS.

Table 4.8: 30 Meter DEM in WMS Results

| Watershed | Area (mi²) | Perimeter (mi) | Longest Flow Path (mi) | Slope (%) |
|------------------|----------------------------------|-----------------------|-----------------------------------|------------------|
| Area 1 | 0.53 | 3.76 | 1.38 | 1.36 |
| Area 2 | 1.67 | 7.89 | 2.87 | 1.46 |
| Area 3 | 8.84 | 18.72 | 6.66 | 0.78 |

4.5 CASE IV: AUTOMATED METHODS USING A TIN

In Case IV a TIN is created in WMS for Area 2, and the watersheds are delineated in WMS. The TIN is made using the conceptual model approach and interpolating points from a 30 meter DEM. WMS has the ability to create and delineate TINs. Once the TIN has been delineated, geometric basin attributes may be computed.

The steps to create a TIN using the conceptual model approach involve digitizing points from a DRG (the same DRG as used in Case II). This was done by opening the TIN module in WMS, and selecting *edit vertex points* from *Vertex Options* in the TIN menu. Once the *Vertex Options* box is open, point elevations are entered based on contour lines. Figure 4.17 shows the point elevations entered using DRG contour lines as a reference of elevation.

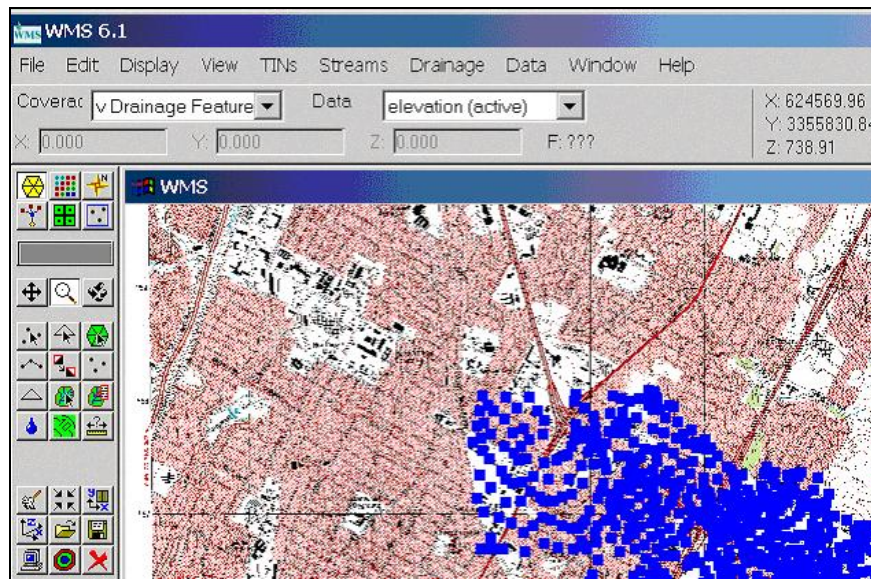


Figure 4.17: TIN Development in WMS

Points were added until the study area was densely populated with point elevations. Breaklines were added to the model to reflect streams and other terrain features as shown on the DRG. In this way, when the triangles are created they are forced to conform to these lines. To add breaklines, the conceptual model icon was selected and the TIN was turned off. A new coverage of type *drainage* was created with attributes typed as *generic* to form the bounding polygon around Area 2. Generic arcs were used to cut around the TIN. Under *Feature Objects*, arcs were converted to polygons.

To create the streams, stream arcs (feature type is *stream*) were generated to make the triangle edges conform to the streamlines as shown in Figure 4.18. The feature objects were then edited to redistribute spacing of points every 75 meters (this number was chosen fairly arbitrarily).

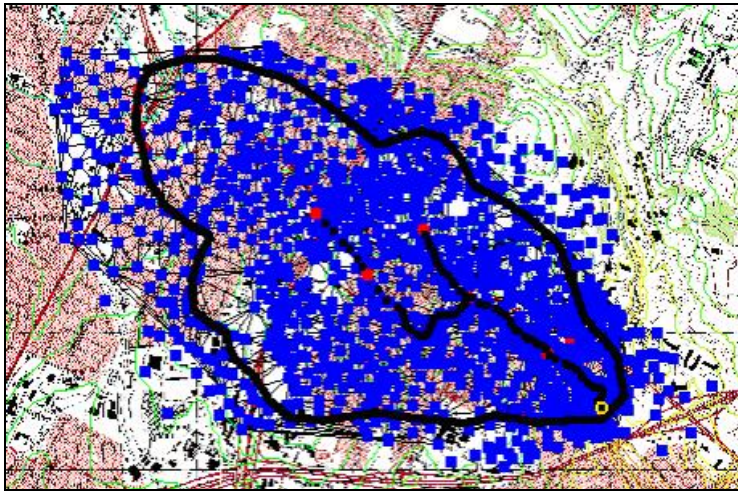


Figure 4.18: Points, Breaklines, and Bounding Polygon in WMS

Once the triangles were turned on again, the polygon marking the boundary around Area 2 was selected, and under *feature objects* the *create TIN* command was selected. The TIN options selected for this study are linear interpolation from DEM with a size bias of 0.5.

Once the TIN was conditioned and free of pits and flat triangles, the TIN was used to delineate the drainage network. Figure 4.19 shows the TIN for Area 2 after it has been interpolated off the 30 meter DEM surface. Once the TIN is ready to be delineated, the user must add an outlet so that the basins may be defined.

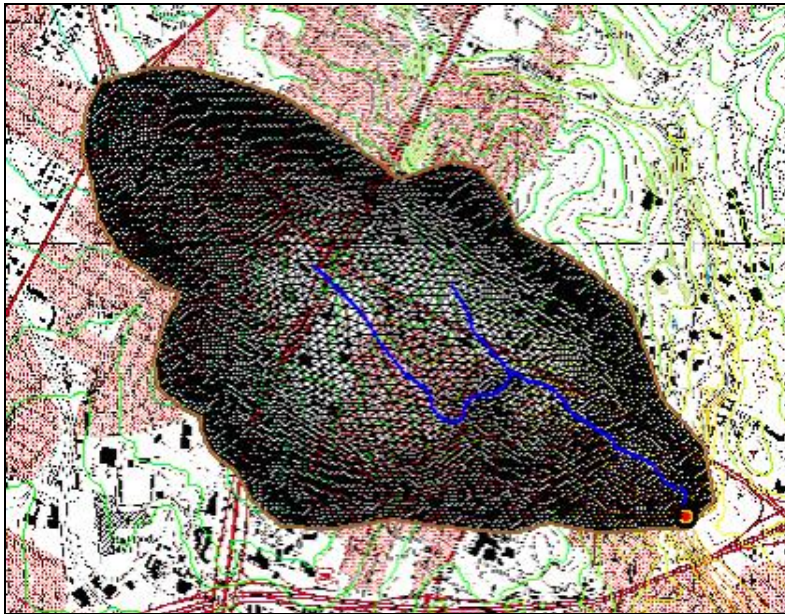


Figure 4.19: Interpolated TIN for Area 2

Once the TIN is delineated, basin data may also be calculated by WMS for input into a hydrologic model as shown in Figure 4.20.

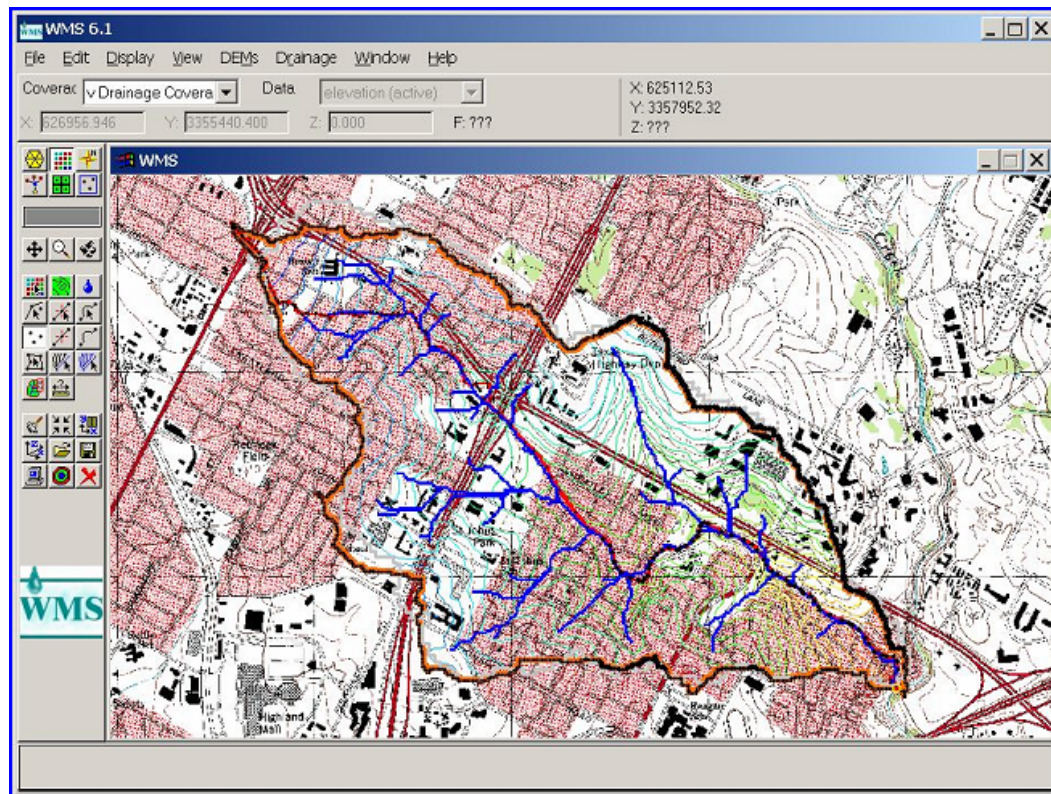


Figure 4.20: Area 2 TIN Delineated

TINs may be modified very easily, and for this reason are useful data sources for urban areas. This study was not replicated for Area 3, because after the time it took to work with Area 2 it was deemed impractical to proceed to the larger area. Table 4.9 shows the results for Area 2.

Table 4.9: TIN Results

| Watershed | Area (mi ²) | Perimeter (mi) | Longest Flow Path (mi) | Slope (%) |
|-----------|-------------------------|----------------|------------------------|-----------|
| Area 2 | 1.68 | 7.4 | 3.14 | 1.53 |

Chapter 5: Results

5.1. CASE STUDY PARAMETER RESULTS SUMMARY

The results from the case study are evaluated for the following parameters: slope, longest flow path, area, perimeter, and curve number. Figure 5.1 shows the three drainage areas used in this study.

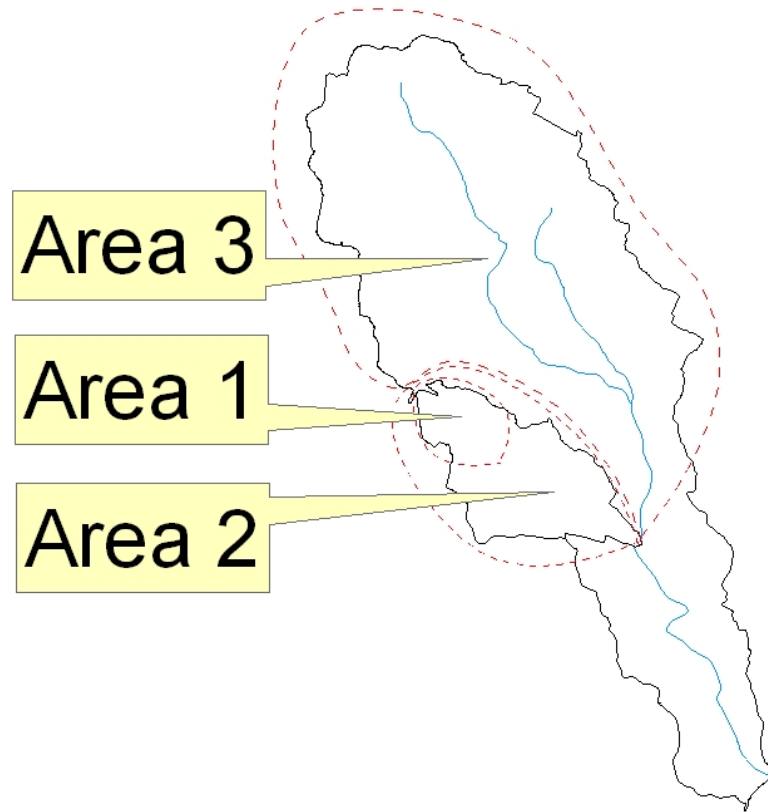


Figure 5.1: Three Study Areas

Methods used to extract the watershed parameters (as discussed in detail in Chapter 4) include (1) measurement from paper maps; (2) on-screen extraction from raster maps; (3) using GIS and two different resolutions of grid-based digital elevation models (DEMs); and (4) using a triangulated irregular network (TIN). Table 5.1, Table 5.2, and Table 5.3 summarize the results found for Area 1, Area 2, and Area 3. It should be noted that perimeter is not a hydrologic parameter. It is evaluated in this study to examine trends in line computation among methods.

Table 5.1: Area 1 Results

| Area 1 | Area 1 Case Number | Area Miles² | Perimeter Miles | LFP Miles | Slope % |
|--------------------------|-------------------------------|-----------------------------------|----------------------------|----------------------|--------------------|
| Hand | Case I | 0.55 | 3.31 | 1.69 | 1.27 |
| Digitized- <i>no hwy</i> | Case II | 0.55 | 3.42 | 1.79 | 1.27 |
| Digitized- <i>hwy</i> | Case II | 0.52 | 3.24 | 1.57 | 1.32 |
| PrePro-30 | Case III | 0.54 | 4.06 | 1.50 | 1.26 |
| PrePro-10 | Case III | 0.54 | 4.08 | 1.56 | 1.36 |
| WMS-30 | Case III | 0.53 | 3.76 | 1.38 | 1.36 |
| WMS-10 | Case III | 0.53 | 4.09 | 1.54 | 1.25 |
| <i>Mean</i> | | <i>0.54</i> | <i>3.71</i> | <i>1.58</i> | <i>1.30</i> |
| <i>Std.Dev.</i> | | <i>0.01</i> | <i>0.38</i> | <i>0.13</i> | <i>0.05</i> |
| <i>CV(%)</i> | | <i>2.07</i> | <i>10.28</i> | <i>8.42</i> | <i>3.65</i> |

Table 5.2: Area 2 Results

| Area 2 | Area 2 Case Number | Area Miles² | Perimeter Miles | LFP Miles | Slope % |
|------------------|-------------------------------|-----------------------------------|----------------------------|----------------------|--------------------|
| Hand | Case I | 1.65 | 6.17 | 3.14 | 1.47 |
| Digitized-no hwy | Case II | 1.68 | 6.57 | 3.28 | 1.47 |
| Digitized-hwy | Case II | 1.65 | 6.50 | 3.09 | 1.44 |
| PrePro-30 | Case III | 1.68 | 8.16 | 3.06 | 1.39 |
| PrePro-10 | Case III | 1.68 | 8.38 | 3.21 | 1.43 |
| WMS-30 | Case III | 1.67 | 7.89 | 2.87 | 1.46 |
| WMS-10 | Case III | 1.66 | 8.53 | 3.15 | 1.41 |
| <i>TIN</i> | <i>Case IV</i> | <i>1.68</i> | <i>7.40</i> | <i>3.14</i> | <i>1.53</i> |
| <i>Mean</i> | | <i>1.67</i> | <i>7.45</i> | <i>3.12</i> | <i>1.45</i> |
| <i>StdDev</i> | | <i>0.01</i> | <i>0.93</i> | <i>0.12</i> | <i>0.04</i> |
| <i>CV(%)</i> | | <i>0.81</i> | <i>12.48</i> | <i>3.90</i> | <i>2.97</i> |

Table 5.3: Area 3 Results

| Area 3 | Area 3 Case Number | Area Miles² | Perimeter Miles | LFP Miles | Slope % |
|------------------|-------------------------------|-----------------------------------|----------------------------|----------------------|--------------------|
| Hand | Case I | 8.49 | 13.83 | 6.28 | 0.77 |
| Digitized-no hwy | Case II | 8.85 | 14.75 | 6.63 | 0.77 |
| Digitized-hwy | Case II | 8.87 | 15.53 | 6.58 | 0.78 |
| PrePro-30 | Case III | 8.84 | 19.08 | 6.78 | 0.76 |
| PrePro-10 | Case III | 8.83 | 20.04 | 6.96 | 0.74 |
| WMS-30 | Case III | 8.84 | 18.72 | 6.66 | 0.78 |
| WMS-10 | Case III | 8.76 | 19.85 | 6.81 | 0.77 |
| <i>Mean</i> | | <i>8.78</i> | <i>17.40</i> | <i>6.67</i> | <i>0.77</i> |
| <i>Std.Dev.</i> | | <i>0.13</i> | <i>2.61</i> | <i>0.22</i> | <i>0.01</i> |
| <i>CV(%)</i> | | <i>1.52</i> | <i>14.99</i> | <i>3.22</i> | <i>1.80</i> |

Table 5.1, Table 5.2, and Table 5.3 without further analysis provide important information regarding variations of hydrologic parameters as a function of area size and method of parameter extraction. Coefficient of variation (CV),

the standard deviation of each parameter divided by its mean, is used in addition to the standard deviation to evaluate each of the watershed parameters. Assuming that errors are normally distributed, in 68% of the cases the observed variation will fall within one standard deviation above or below the mean, or \pm CV expressed as a percent of the mean.

The standard deviation for area and slope is small for all three areas. For both Area 1 and Area 2, the drainage area can be determined within approximately ± 0.01 square miles (2.07% for Area 1 and 0.81% for Area 2), and ± 0.13 square miles (1.52%) for Area 3. For Area 3, using traditional delineation techniques on paper maps produces an area smaller than any of the other techniques (0.29 square miles below the mean). This is most likely attributed to area measurement using the planimeter.

Similar to area, the standard deviation (as well as the CV) for slope is small for all three areas. The standard deviation for slope is highest for Area 1, at a value of 0.05%. The highest coefficient of variation for slope, as calculated for Area 1, is 3.65%.

Longest flow path and perimeter show different results from area and slope, in that there is much more parameter variation among extraction methods. Longest flow path was determined within ± 0.13 miles for Area 1, ± 0.12 miles for Area 2, and ± 0.22 miles for Area 3. Precision in determining the longest flow path increases as the area becomes larger, with a CV for Area 1 of 8.42% and a CV for Area 3 of 3.22%. This is most likely because the flow path for Area 1 is small, and hence there is more error in this measurement. Secondly, for Area 3 a

larger portion of the flow path was already marked with a blue line on paper maps and on the DRG, whereas for Area 1 the blue line was not drawn on the map. It should also be noted that longest flow path using traditional paper map-based methods for Area 3 (6.28 miles) is 0.39 miles below the mean of 6.67 miles, well below the measurements using other methods of longest flow path extraction.

Perimeter measurements become less precise as the drainage area increases (the CV for Area 1 is 10.28%, while the CV for Area 3 is 14.99%). In addition, the perimeter values found using traditional methods and on-screen digitizing of raster graphic maps are smaller than those found using DEMs. Part of the reason for this large variation in perimeter could be due to the subjective nature of traditional paper map-based methods and on-screen digitizing of raster graphic maps, in addition to the more tortuous path created by digital data.

Table 5.3 shows that automated methods using CRWR-PrePro, WMS, and on-screen digitizing produce more consistent results than using manual hand delineation techniques on paper maps to determine area, longest flow path and perimeter for large areas. The values for area, longest flow path, and perimeter determined using traditional paper map-based methods for Area 3 are much smaller than those determined using more automated methods. Figure 5.2 outlines the CV results from Table 5.1, Table 5.2, and Table 5.3.

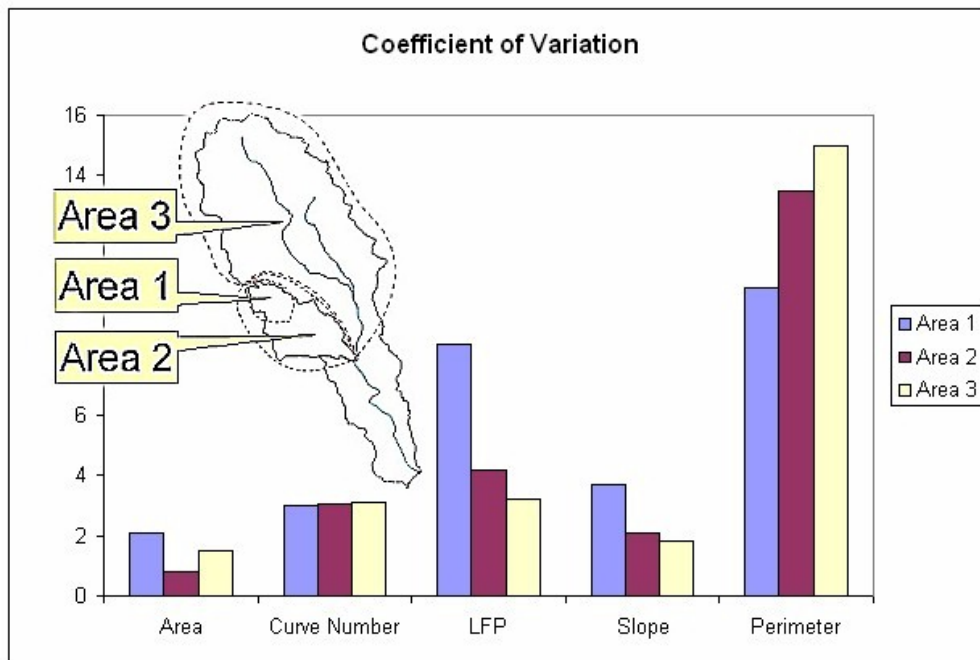


Figure 5.2: Coefficients of Variation

In Figure 5.2, SCS curve number is shown to give the reader an idea of the curve number variation that will be applied to the remainder of the study. For Area 2, a range of curve numbers was evaluated using a curve number selected by TxDOT as a low value (85.8), and a curve number derived by STATSGO soils data along with Land Use/Land Cover data as a high value (91.7). TxDOT did not provide curve number values for Area 1 and Area 3. Instead, a range the same as used in Area 2 was applied, with the curve number derived by STATSGO soils data along with Land Use/Land Cover data as a high value. These values, shown in Table 5.4, were used to reflect reasonable variations of curve number that one might encounter in hydrologic modeling.

Table 5.4: Curve Number Values

| | Area 1 | Area 2 | Area 3 |
|----------|--------|--------|--------|
| CN- 10m | 94.0 | 91.7 | 90.7 |
| CN- 30m | 93.9 | 91.7 | 90.7 |
| CN-HEC-1 | - | 85.82 | - |
| Range | 87-95 | 85-93 | 84-92 |
| Mean | 91 | 89 | 88 |
| StdDev | 2.74 | 2.74 | 2.74 |
| CV (%) | 3.01 | 3.08 | 3.11 |

Figure 5.2 shows that for the areas analyzed, there is a general trend for both longest flow path (LFP) and slope. The trend in variations in slope reflects the trend in variations in longest flow path, as it is calculated from the longest flow path measurement. Both show higher variations with Area 1 and lower variations for Area 3. Another key point shown by Figure 5.2 is that for the small area (Area 1), there is more variation among parameters than for the larger area, Area 3, except in the case of perimeter and curve number.

5.2 ELASTICITY ANALYSIS

In this study “elasticity” is used as a measure of the influence of one variable on another. While gradient describes the relationship between two variables, it is a unit-dependent quantity. Elasticity, on the other hand, is a dimensionless quantity. In simple terms, elasticity is the percent change in output per percent change in input. If the elasticity is greater than one, the parameter is “elastic” in that the dependent variable is more sensitive to the independent

variable. If the elasticity is less than one, the parameter is “inelastic” in that the dependent variable is less sensitive to the independent variable. Figure 5.3 below shows the concept of elasticity graphically:

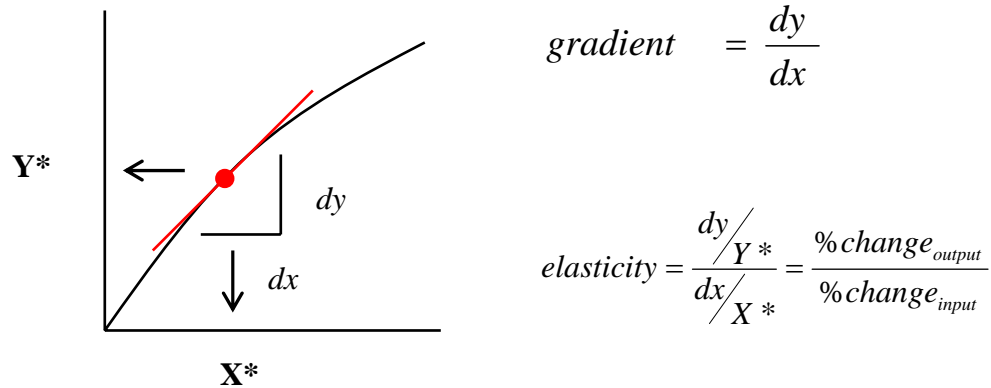


Figure 5.3: Concept of Elasticity

The goal of this analysis is to determine the effect of parameter variations on the lag time, and subsequently the effect of lag time variations due to parameter variations on discharge. This analysis is conducted only for Area 2. The reason for this is that Area 2 is the only study area for which TxDOT has created a hydrologic model. After an analytical calculation of gradients to determine lag time elasticity for each parameter, the hydrologic model created by TxDOT is used to numerically calculate the elasticity of discharge with lag time as shown in Figure 5.4.

% change in parameter... % change in lag... % change in Q



Figure 5.4: Discharge Sensitivity Calculation

Equation 5.1, Step 1 in calculating the discharge sensitivity, describes the calculation of lag time elasticity. The first term in this equation is the gradient. The gradient is multiplied by the average parameter value for Area 2, and divided by the lag time calculated at the average parameter.

$$elasticity_{lag-parameter} = \frac{\partial(lag)}{\partial(parameter)} * \frac{parameter_{avg}}{lag(parameter_{avg})}$$

Equation 5.1

Equation 5.2, Step 2 in calculating the discharge sensitivity, describes the calculation of discharge elasticity based on changes in lag values. Similar to Equation 5.1 the gradient is multiplied by the average lag time value and divided by the discharge calculated at the average lag time.

$$elasticity_{Q-lag} = \frac{\partial(Q)}{\partial(lag)} * \frac{lag_{avg}}{Q(lag_{avg})}$$

Equation 5.2

The final step approximates the overall discharge sensitivity as a result of variation in parameter values. Equation 5.3 outlines this calculation. The results from Equation 5.1 describing the lag time elasticity with respect to each parameter are multiplied by the discharge elasticity with respect to lag time as calculated by Equation 5.2.

$$\begin{aligned} elasticity_{Q-parameter} &= \left[\frac{\partial(Q)}{\partial(lag)} * \frac{lag}{Q(lag)} \right] * \left[\frac{\partial(lag)}{\partial(parameter)} * \frac{parameter}{lag(parameter)} \right] \\ &= \left[\frac{\partial(Q)}{\partial(parameter)} * \frac{parameter}{Q(parameter)} \right] \end{aligned}$$

Equation 5.3

5.2.1 Step 1: Sensitivity of SCS Lag Time to Parameter Variations

Figure 5.5 describes the process analyzed in this section. Variations in parameter values are used to calculate resulting variations in SCS lag times.

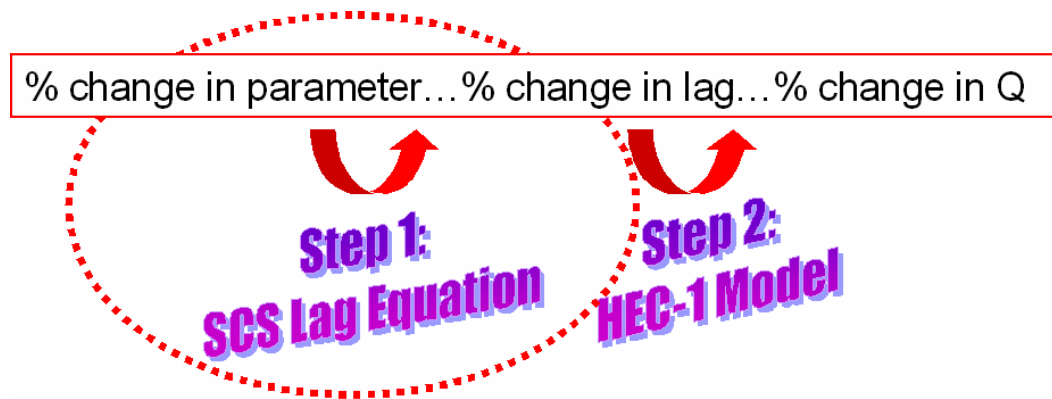


Figure 5.5: Step 1 in Calculating the Discharge Sensitivity

Analytical calculation of the gradient involves plugging in each of the parameters derived from each level of parameter extraction into the SCS lag equation, shown in Equation 5.4, while holding the other parameters constant.

$$t_{lag}(\text{min}) = \frac{L_w^{0.8} \left(\frac{1000}{CN} - 9 \right)^{0.7}}{31.67 \sqrt{s}} \quad \text{Equation 5.4}$$

In Equation 5.4, L_w is longest flow path in units of feet, and slope is expressed as a percentage. Curve number is symbolized by CN , and t_{lag} is the lag time in minutes. Table 5.5 outlines the base values used for these calculations. These numbers are the mean values calculated for Area 2, as shown previously in Table 5.2 and Table 5.4.

Table 5.5: Parameter Base Values

| Parameter | Base Value |
|-----------|------------|
| LFP | 3.12 Miles |
| Slope | 1.45 % |
| CN | 89 |

5.2.1.1 Longest Flow Path

To evaluate changes in SCS lag time that result from changes in the longest flow path, the curve number and average slope were held constant while

longest flow path was allowed to vary. Table 5.6 gives the lag time values calculated for each longest flow path measurement.

Table 5.6: Longest Flow Path Calculations

| | LFP Miles | % Slope (mean) | CN (mean) | SCS Lag, Min |
|---|----------------------|---------------------------|---|-------------------------|
| | | 1.45 | 89.00 | |
| Hand | 3.14 | | | 109.8 |
| Digitized- <i>no hwy</i> | 3.28 | | | 113.7 |
| Digitized- <i>hwy</i> | 3.09 | | | 108.4 |
| PrePro-30 | 3.06 | | | 107.5 |
| PrePro-10 | 3.21 | | | 111.7 |
| WMS-30 | 2.87 | | | 102.2 |
| WMS-10 | 3.15 | | | 110.1 |
| TIN | 3.14 | | | 109.8 |
| <i>MEAN</i> | 3.12 | | <i>MEAN</i> | 109.0 |
| $\Delta X_{\text{max-min}}/X_{\text{mean}}$ | 13.2% | | $\Delta Y_{\text{max-min}}/Y_{\text{mean}}$ | 10.6% |

Subtracting the highest longest flow path measurement from the lowest longest flow path measurement, and then dividing by the mean flow path length determines the longest flow path variation. Figure 5.6 below demonstrates this process for the calculation of longest flow path.

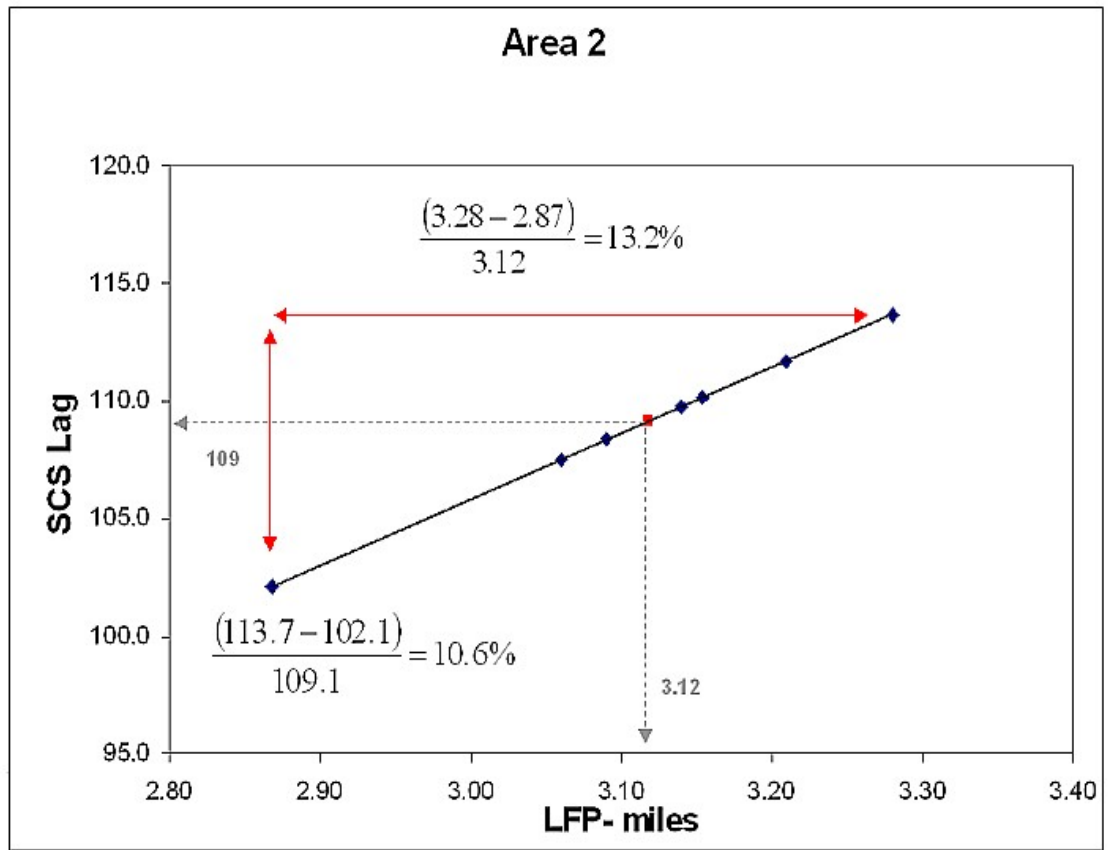


Figure 5.6: Analytical Calculation of Gradients

As the longest flow path varies by 13.2%, the lag varies by 10.6% when evaluated at the base value for longest flow path (3.12 miles). The elasticity is then $10.6 \div 13.2$ or 0.80. As this number is less than one, the relationship between longest flow path and lag time is considered inelastic, signifying that lag time is not sensitive to changes in longest flow path length. These results show that a 1% increase in longest flow path will cause a 0.8% increase in SCS lag time.

5.2.1.2 Slope

The lag time elasticity with respect to slope was calculated by holding the longest flow path and curve number constant and varying the slope. The results from this calculation are shown in Table 5.7.

Table 5.7: Slope Calculations

| | % Slope (mean) | LFP (mean),Miles | CN (mean) | SCS Lag, Min. |
|--|---------------------------|-----------------------------|--|--------------------------|
| | | 3.12 | 89.00 | |
| Hand | 1.47 | | | 107.8 |
| Digitized- <i>no hwy</i> | 1.47 | | | 107.8 |
| Digitized- <i>hwy</i> | 1.44 | | | 108.9 |
| PrePro-30 | 1.39 | | | 110.9 |
| PrePro-10 | 1.43 | | | 109.3 |
| WMS-30 | 1.46 | | | 108.2 |
| WMS-10 | 1.41 | | | 110.1 |
| TIN | 1.53 | | | 105.7 |
| <i>MEAN</i> | <i>1.45</i> | | <i>MEAN</i> | <i>108.6</i> |
| $\Delta X_{\max-\min}/X_{\text{mean}}$ | 9.7% | | $\Delta Y_{\max-\min}/Y_{\text{mean}}$ | -4.8% |

As can be seen from Figure 5.7, there is an inverse relationship between lag time and slope.

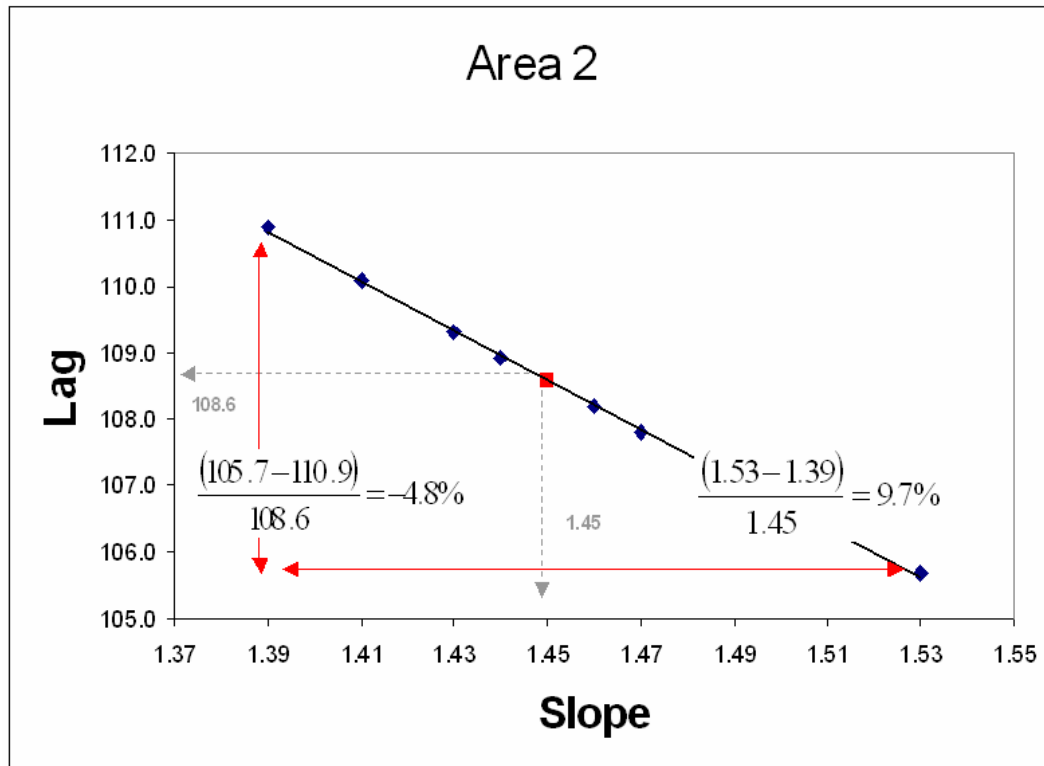


Figure 5.7: Slope Gradient Calculation

The elasticity of lag time with respect to slope is calculated as $-4.8/9.7$, or -0.50 . In other words, a 1 % increase in slope will cause a 0.5% decrease in SCS lag time.

5.2.1.3 Curve Number

The lag time elasticity with respect to curve number was determined for Area 2 by holding slope and longest flow path constant, and varying the curve number. Curve numbers for Area 2 are shown in Table 5.8. These are the same values shown earlier in Table 5.4.

Table 5.8: Curve Number Measurements

| | 10m | 30m | HEC-1 |
|----------|------|------|-------|
| CN range | 91.7 | 91.7 | 85.8 |

Table 5.9 outlines the curve number values. As mentioned earlier, this range is used to reflect a range of curve numbers that could likely result using traditional methods and derived mathematically using digital Land Use/ Land Cover and STATSGO soils data.

Table 5.9: Curve Number Calculations

| | %Slope CN | LFP (mean), Miles | SCS Lag, Min. |
|--|----------------------|--|--------------------------|
| | 1.45 | 3.12 | |
| 85 | | | 126.4 |
| 86 | | | 122.0 |
| 87 | | | 117.6 |
| 88 | | | 113.3 |
| 89 | | | 108.9 |
| 90 | | | 104.6 |
| 91 | | | 100.4 |
| 92 | | | 96.1 |
| 93 | | | 91.9 |
| MEAN | 89 | MEAN | 109.0 |
| $\Delta X_{\max-\min}/X_{\text{mean}}$ | 9.0% | $\Delta Y_{\max-\min}/Y_{\text{mean}}$ | -31.7% |

This curve is plotted in Figure 5.8. The graph shows the inverse relationship between curve number and lag time.

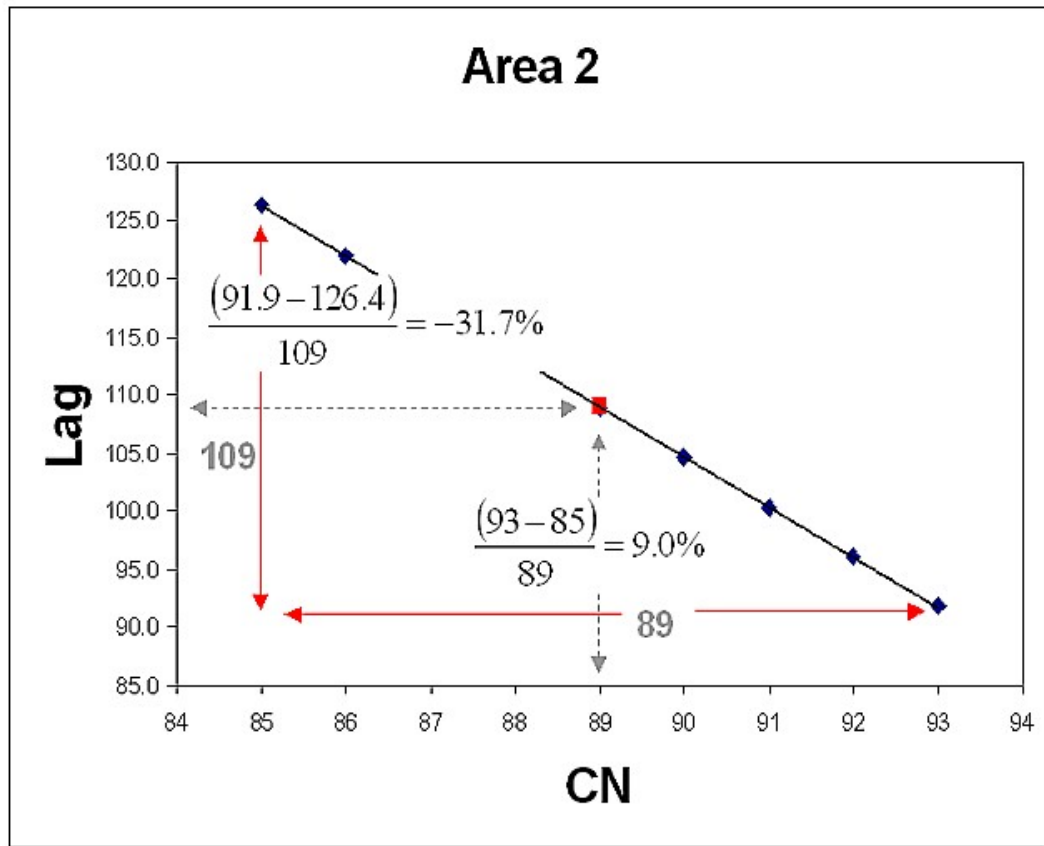


Figure 5.8: Curve Number Gradient Calculation

The elasticity of the lag time to the curve number, $-31.7/9.0$, is -3.52 . These results show that a 1% increase in CN will result in a 3.52% decrease in lag time.

5.2.1.4 Step 1 Results

Table 5.10 summarizes the results from the lag time elasticity study. Results show that the only elastic parameter is curve number. Both the longest flow path and slope are inelastic parameters.

Table 5.10: Results from Analytical Calculations

| Variation- LFP | Variation- Lag | Elasticity Lag-LFP |
|-----------------------------|---------------------------|---------------------------------|
| 13.2% | 10.6% | $10.6/13.2=0.80$ |
| Variation- Slope | Variation- Lag | Elasticity Lag-Slope |
| 9.7% | -4.8% | $-2.8/5.6=-0.50$ |
| Variation- CN | Variation- Lag | Elasticity Lag-CN |
| 9.0% | -31.7% | $-31.7/9.0=-3.52$ |

5.2.2 Step 2: Sensitivity of Flow to Variations in Lag Time

Now that the relationships between physical parameters and SCS lag time have been quantified, the next step is to quantify the relationship between SCS lag time and discharge. Figure 5.9 below shows the process analyzed in this section in which variations in SCS lag time values are used to calculate resulting variations in discharge.

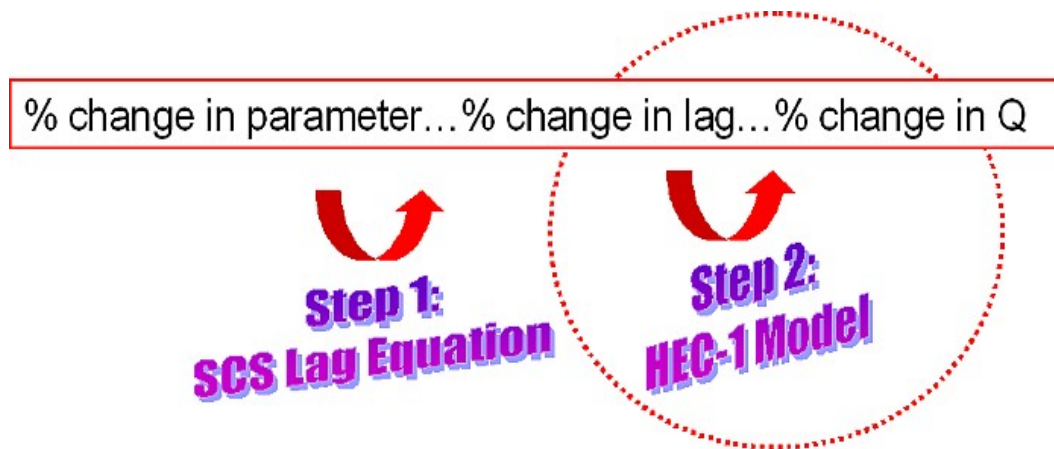


Figure 5.9: Step 2 in Calculating the Discharge Sensitivity

In 1992, a contractor for TxDOT developed a HEC-1 model of Buttermilk watershed (Area 2) as an undeveloped area. This pre-developed HEC-1 model included areas outside of Buttermilk watershed. These areas were edited, and the new, slightly modified HEC-1 model was imported into HEC-HMS.

The U.S. Corps of Engineers' Hydrologic Modeling System (HMS) is a "next generation" software for the precipitation-runoff simulation that will supersede HEC-1. HEC-HMS contains most of the watershed runoff and routing capabilities of HEC-1, in addition to continuous hydrograph simulation over long periods of time, and distributed runoff computation using a grid cell depiction of the watershed (HEC-HMS User's Manual, 2000).

There are two principal parameters that are evaluated in this study with respect to discharge: lag time and drainage area. After modification of the HEC-1 model, lag times are varied in each sub-basin. For each lag time variation,

discharge is calculated. Next, the drainage area of each sub-basin is varied, and discharge calculated once again for each area variation.

5.2.2.1 HEC-1 Model

Figure 5.10 shows the area delineated by TxDOT for the HEC-1 model. The area in blue is included in the HEC-1 model although it does not pertain to Buttermilk (Area 2). For this analysis, the blue area is deleted from the HEC-1 model.

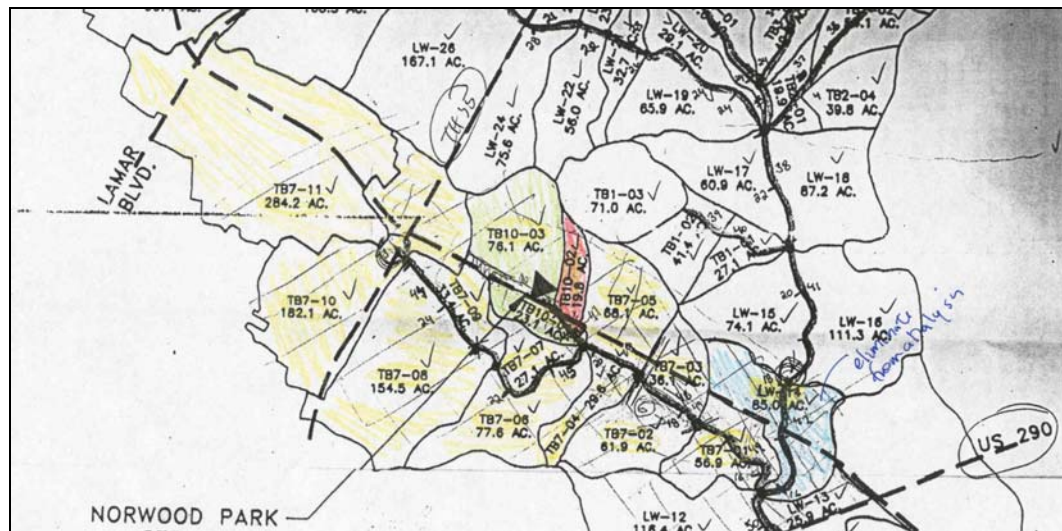


Figure 5.10: HEC-1 Study Area

The corresponding unmodified HEC-HMS diagram (the HEC-1 model was imported into HEC-HMS) is shown below in Figure 5.11.

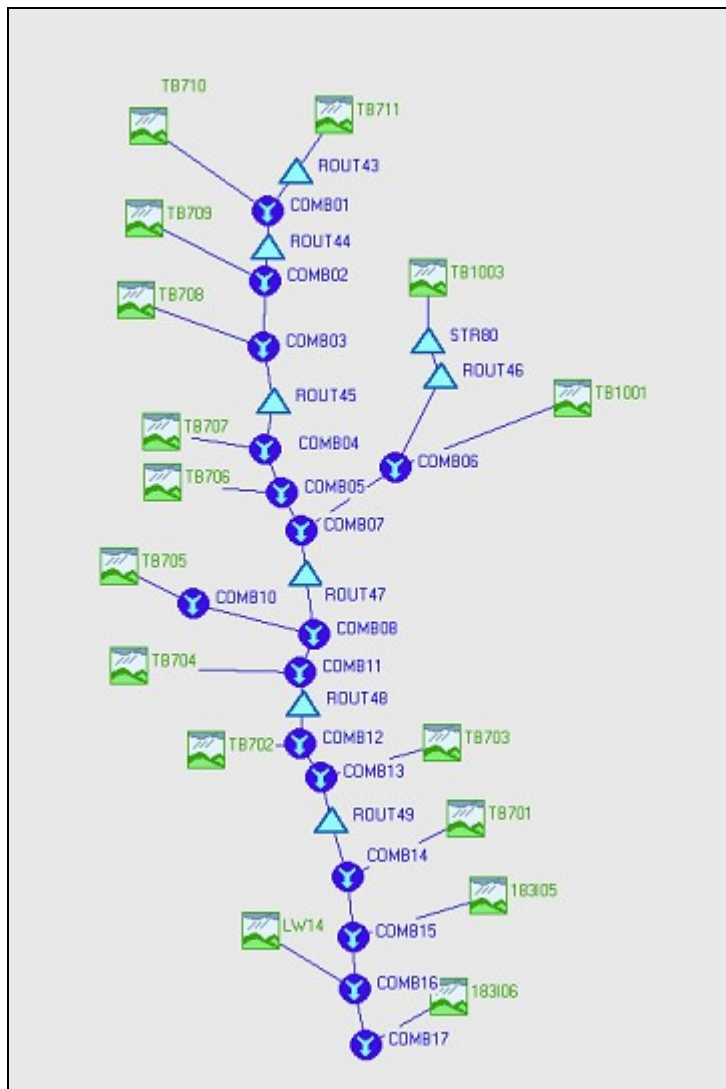


Figure 5.11: Unmodified HEC-1 model (displayed in HEC-HMS)

As mentioned previously, the HEC-1 model had to be modified for this analysis. Table 5.11 below gives the name of each sub-basin along with its drainage area, SCS lag time, and SCS curve number. In the modification process,

the area downstream of COMB14 was deleted. This area includes 183105, LW14 and 183106 as shown in red italicized print.

Table 5.11: HEC-1 Modifications

| Sub-basin | Area mi ² | SCS Lag (min) | SCS Curve Number |
|---------------|----------------------|---------------|------------------|
| Tb711 | 0.444 | 15.30 | 89 |
| Tb710 | 0.285 | 17.88 | 88 |
| Tb709 | 0.052 | 7.74 | 80 |
| Tb708 | 0.241 | 15.72 | 86 |
| Tb707 | 0.042 | 9.36 | 87 |
| Tb706 | 0.121 | 16.02 | 84 |
| Tb1003 | 0.150 | 6.66 | 77 |
| 183101 | 0.011 | - | 85 |
| Tb1001 | 0.025 | 11.1 | 85 |
| 183103 | 0.004 | - | 83 |
| Tb705 | 0.102 | 12.3 | 83 |
| Tb704 | 0.046 | 7.74 | 87 |
| Tb702 | 0.097 | 9.72 | 86 |
| 183104 | 0.004 | - | 85 |
| Tb703 | 0.052 | 8.22 | 85 |
| Tb701 | 0.088 | 8.40 | 86 |
| 183105 | 0.001 | - | 86 |
| <i>Lw14</i> | <i>0.127</i> | <i>7.5</i> | <i>80</i> |
| <i>183106</i> | <i>0.006</i> | <i>-</i> | <i>80</i> |
| Total Area | 1.898 | | |

The new area, after modification, is 1.764 mi². The modified model is shown in Figure 5.12. The weighted curve number after modification is 85.82.

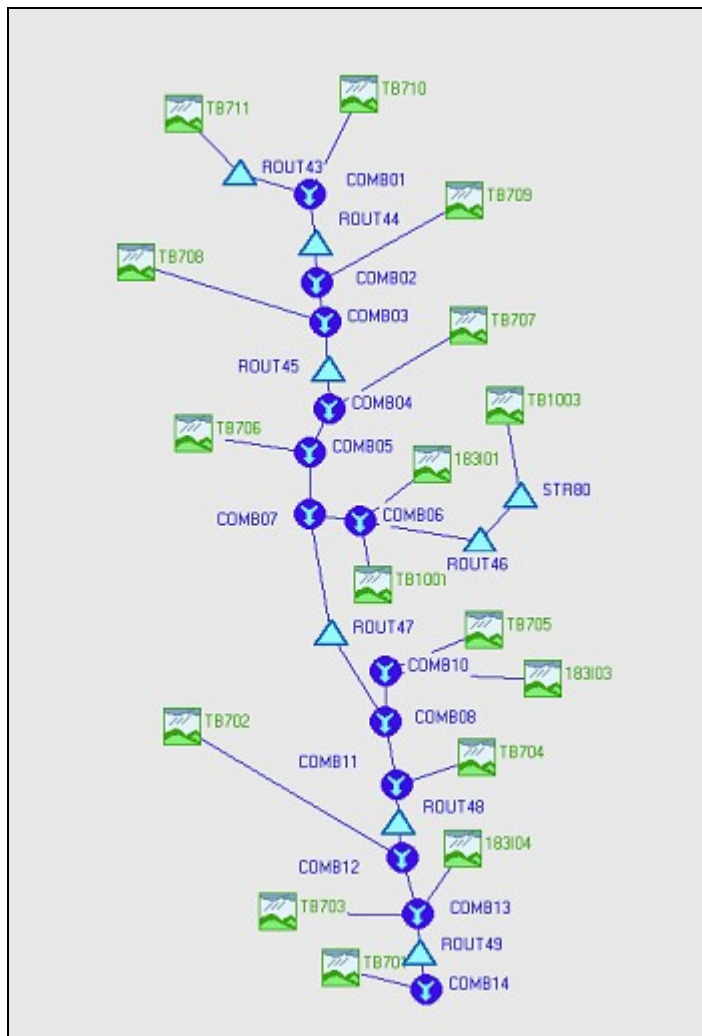


Figure 5.12: Modified HEC-1 Model (displayed in HEC-HMS)

For rainfall-runoff modeling HEC-HMS requires a basin component, a precipitation component, and a control component. The basin and precipitation components are heavily dependent on spatial factors.

The HEC-1 model is imported as the basin component. For the precipitation component, six different return periods are analyzed using the

TxDOT IDF (Intensity-Duration-Frequency) curves and an alternating block cumulative precipitation hyetograph for Travis county and a three-hour design storm. Equation 5.4 and Table 5.12 are used to calculate the cumulative rainfall for a three-hour storm in six-minute increments for each sub-basin. A six-minute increment is chosen because this is the value TxDOT used.

$$I = \frac{a}{(T_d + b)^c} \quad \text{Equation 5.4}$$

Table 5.12: TxDOT IDF (Intensity-Duration-Frequency) Curves

| Return Period | 2 Years | 5 Years | 10 Years | 25 Years | 50 Years | 100 Years |
|--------------------------|----------------|----------------|-----------------|-----------------|-----------------|------------------|
| a | 56 | 69 | 77 | 87 | 91 | 103 |
| b | 8.1 | 8.6 | 8.6 | 8.6 | 8.6 | 8.1 |
| c | 0.796 | 0.780 | 0.775 | 0.766 | 0.751 | 0.752 |

5.2.2.2 Lag Time Variation

The next step was to determine the discharge elasticity from changes in lag time. This was done by proportionally changing the lag time values for each of the sub-basins in the HEC-1 model. Table 5.13 gives the original SCS lag value for each sub-basin, followed by 5%, 10%, and 20% increases in lag time, then 5%, 10%, and 20% decreases in lag time.

Table 5.13: HEC-1 Lag Input

| Subbasin | Lag, min | Lag +5% | Lag +10% | Lag +20% | Lag -5% | Lag -10% | Lag -20% |
|-----------------|-----------------|----------------|-----------------|-----------------|----------------|-----------------|-----------------|
| TB711 | 15.30 | 16.07 | 16.83 | 18.36 | 14.54 | 13.77 | 12.24 |
| TB710 | 17.88 | 18.77 | 19.67 | 21.46 | 16.99 | 16.09 | 14.30 |
| TB709 | 7.74 | 8.13 | 8.51 | 9.29 | 7.35 | 6.97 | 6.19 |
| TB708 | 15.72 | 16.51 | 17.29 | 18.86 | 14.93 | 14.15 | 12.58 |
| TB707 | 9.36 | 9.83 | 10.30 | 11.23 | 8.89 | 8.42 | 7.49 |
| TB706 | 16.02 | 16.82 | 17.62 | 19.22 | 15.22 | 14.42 | 12.82 |
| TB1003 | 6.66 | 6.99 | 7.33 | 7.99 | 6.33 | 5.99 | 5.33 |
| TB1001 | 11.10 | 11.66 | 12.21 | 13.32 | 10.55 | 9.99 | 8.88 |
| TB705 | 12.30 | 12.92 | 13.53 | 14.76 | 11.69 | 11.07 | 9.84 |
| TB704 | 7.74 | 8.13 | 8.51 | 9.29 | 7.35 | 6.97 | 6.19 |
| TB702 | 9.72 | 10.21 | 10.69 | 11.66 | 9.23 | 8.75 | 7.78 |
| TB703 | 8.22 | 8.63 | 9.04 | 9.86 | 7.81 | 7.40 | 6.58 |
| TB701 | 8.40 | 8.82 | 9.24 | 10.08 | 7.98 | 7.56 | 6.72 |

Figure 5.13 shows the discharge values in cubic feet per second (cfs) for each return period. The relationship between discharge (Y-axis) and lag time (X-axis) is given by the linear equations shown in Figure 5.12 for 2, 5, 10, 25, 50, and 100-year events.

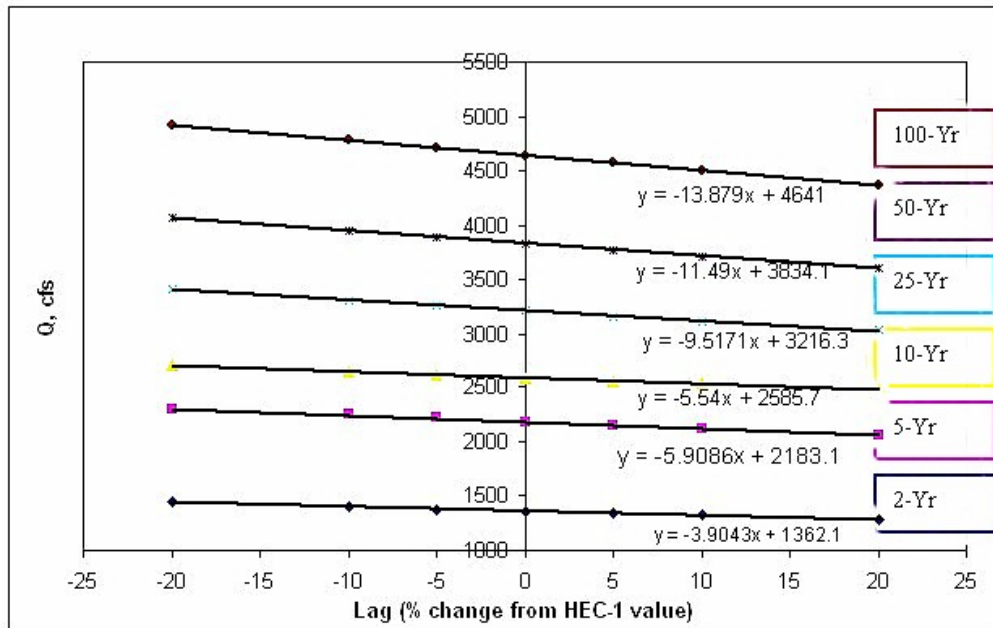


Figure 5.13: Discharge Results for Lag Variations

To determine the percent change in discharge resulting from a percent change in lag time (due to parameter variations), the discharge (Q) for each corresponding lag variation is calculated using the linear equations relating lag time to discharge. Table 5.14 shows the percent changes in discharge for each return period corresponding to each variation in SCS lag time.

Table 5.14: Discharge Variations Due to Lag Variations

| Lag (From LFP Variations) | Q_2 | Q_5 | Q_{10} | Q_{25} | Q_{50} | Q_{100} |
|------------------------------------|-------------------------|-------------------------|----------------------------|----------------------------|----------------------------|-----------------------------|
| 10.6% | -3.04% | -2.87% | -2.27% | -3.14% | -3.18% | -3.17% |
| Lag (From Slope Variations) | Q_2 | Q_5 | Q_{10} | Q_{25} | Q_{50} | Q_{100} |
| -4.8% | 1.38% | 1.30% | 1.03% | 1.42% | 1.44% | 1.44% |
| Lag (From CN Variations) | Q_2 | Q_5 | Q_{10} | Q_{25} | Q_{50} | Q_{100} |
| -31.7% | 9.09% | 8.58% | 6.79% | 9.38% | 9.50% | 9.48% |

For each return period, the elasticity of discharge with respect to SCS lag time is calculated by dividing the percent change in discharge by the percent change in SCS lag time. As shown in Table 5.15, there are slight variations in discharge elasticity for each return period. These variations were averaged to establish a relationship between SCS lag time and discharge. The averaged value is -0.28.

Table 5.15: Discharge Elasticity Due to Parameter Variation

| Elasticity Q ₂ -Lag | Elasticity Q ₅ -Lag | Elasticity Q ₁₀ -Lag | Elasticity Q ₂₅ -Lag | Elasticity Q ₅₀ -Lag | Elasticity Q ₁₀₀ -Lag | Elasticity Q_{avg}-Lag |
|-----------------------------------|-----------------------------------|------------------------------------|------------------------------------|------------------------------------|-------------------------------------|---|
| -0.29 | -0.27 | -0.21 | -0.30 | -0.30 | -0.30 | -0.28 |

Results from this analysis show that a 1% increase in SCS lag time yields a -0.28% decrease in discharge.

5.2.2.3 Drainage Area Variation

The second component involving analysis of the HEC-1 model is to evaluate changes in area, and how these changes affect discharge. Similar to the lag time study, the areas of each sub-basin were increased by 5%, 10%, and 20% and also decreased by 5%, 10%, and 20%. Table 5.16 shows these values.

Table 5.16: HEC-1 Area Input

| Sub-basin | Area Miles² | Area +5% | Area +10% | Area +20% | Area -5% | Area -10% | Area -20% |
|------------------|-----------------------------------|-----------------|------------------|------------------|-----------------|------------------|------------------|
| TB711 | 0.444 | 0.466 | 0.488 | 0.533 | 0.422 | 0.400 | 0.355 |
| TB710 | 0.285 | 0.299 | 0.314 | 0.342 | 0.271 | 0.257 | 0.228 |
| TB709 | 0.052 | 0.055 | 0.057 | 0.062 | 0.049 | 0.047 | 0.042 |
| TB708 | 0.241 | 0.253 | 0.265 | 0.289 | 0.229 | 0.217 | 0.193 |
| TB707 | 0.042 | 0.044 | 0.046 | 0.050 | 0.040 | 0.038 | 0.034 |
| TB706 | 0.121 | 0.127 | 0.133 | 0.145 | 0.115 | 0.109 | 0.097 |
| TB1003 | 0.150 | 0.158 | 0.165 | 0.180 | 0.143 | 0.135 | 0.120 |
| TB1001 | 0.025 | 0.026 | 0.028 | 0.030 | 0.024 | 0.023 | 0.020 |
| 183101 | 0.011 | 0.012 | 0.012 | 0.013 | 0.010 | 0.010 | 0.009 |
| TB705 | 0.102 | 0.107 | 0.112 | 0.122 | 0.097 | 0.092 | 0.082 |
| 183103 | 0.004 | 0.004 | 0.004 | 0.005 | 0.004 | 0.004 | 0.003 |
| TB704 | 0.046 | 0.048 | 0.051 | 0.055 | 0.044 | 0.041 | 0.037 |
| TB702 | 0.097 | 0.102 | 0.107 | 0.116 | 0.092 | 0.087 | 0.078 |
| 183104 | 0.004 | 0.004 | 0.004 | 0.005 | 0.004 | 0.004 | 0.003 |
| TB703 | 0.052 | 0.055 | 0.057 | 0.062 | 0.049 | 0.047 | 0.042 |
| TB701 | 0.088 | 0.092 | 0.097 | 0.106 | 0.084 | 0.079 | 0.070 |

Figure 5.14 shows the discharge values in cubic feet per second (cfs) for each return period. The relationship between discharge (Y-axis) and area (X-axis) is given by the linear equations, also shown in Figure 5.14 below, for 2, 5, 10, 25, 50, and 100-year events.

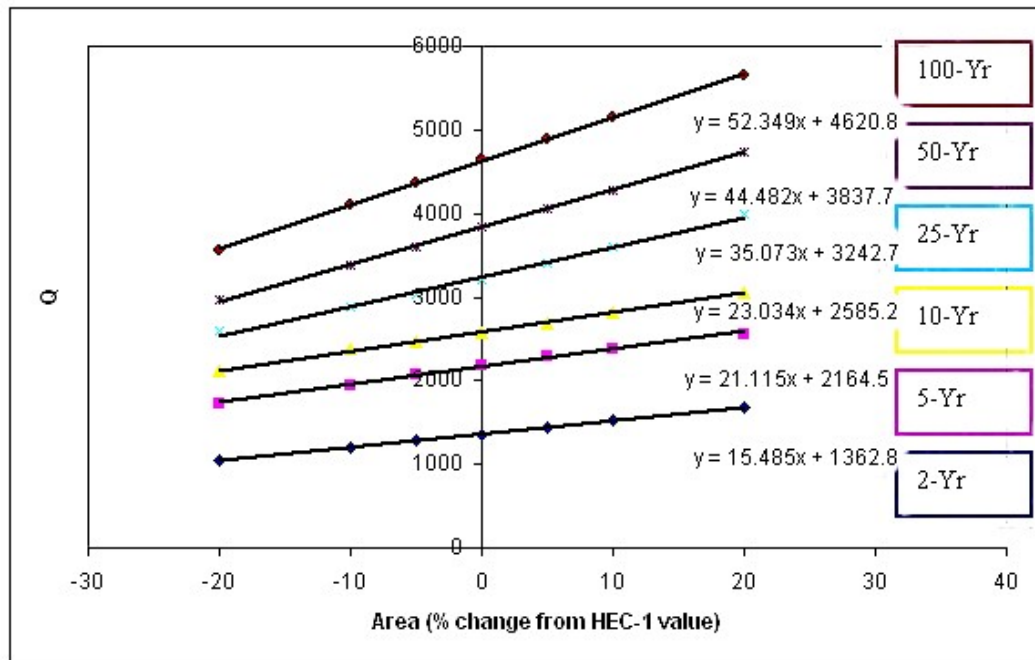


Figure 5.14: Discharge Results for Drainage Area Variations

Table 5.17 gives the variation in area for Area 2 (Buttermilk). The variation in drainage area among methods is 1.80%.

Table 5.17: Area Variation

| | Area, Miles ² |
|--|--------------------------|
| Hand | 1.65 |
| Digitized-no hwy | 1.68 |
| Digitized-hwy | 1.65 |
| PrePro-30 | 1.68 |
| PrePro-10 | 1.68 |
| WMS-30 | 1.67 |
| WMS-10 | 1.66 |
| TIN | 1.68 |
| MEAN | 1.67 |
| $\Delta X_{\max-\min}/X_{\text{mean}}$ | 1.8% |

The same steps were taken to determine the effect of drainage area on discharge as were taken to determine the effects of lag time on discharge. For each return period, the percent variation in discharge was calculated based on the percent variation in drainage area (1.80%). There were slight variations in percent discharge for each return period. Discharge elasticity for each return period was calculated by dividing each discharge variation by 1.80% (the variation in drainage area). There were slight differences in elasticity for each return period. These numbers were averaged to provide an approximate discharge elasticity, as shown in Table 5.18.

Table 5.18: Discharge Elasticity due to Area Variations

| Q₂ | Q₅ | Q₁₀ | Q₂₅ | Q₅₀ | Q₁₀₀ | Elasticity Q_{avg}-Area |
|------------------------------------|------------------------------------|-------------------------------------|-------------------------------------|-------------------------------------|--------------------------------------|--|
| 2.05% | 1.74% | 1.60% | 1.96% | 2.09% | 1.99% | |
| Elasticity Q ₂ -Area | Elasticity Q ₅ -Area | Elasticity Q ₁₀ -Area | Elasticity Q ₂₅ -Area | Elasticity Q ₅₀ -Area | Elasticity Q ₁₀₀ -Area | |
| 1.14 | 0.97 | 0.89 | 1.09 | 1.16 | 1.11 | 1.91/1.80=1.06 |

The resulting elasticity of discharge with respect to area is 1.06. Hence, a 1% increase in area yields approximately a 1% increase in discharge, as one would expect.

5.2.2.4 Step 2 Results

Results from the numerical calculations of gradient show that there is a constant, inversely proportional, relationship between lag time and discharge.

This elasticity value, -0.28, shows the relatively inelastic effect of lag time changes on discharge, e.g., a 1% increase in lag time results in a 0.28% decrease in discharge. Area, as one would expect, is purely elastic and directly proportional to discharge. In this case a 1% increase in area would result in a 1% increase in discharge.

5.2.3 Results from Elasticity Analysis

The effect of parameter variation on discharge is determined by multiplying elasticity results from Step 1 (sensitivity of SCS lag time to parameter variations) by Step 2 (sensitivity of flow to variations in discharge). The overall picture is shown once again in Figure 5.15.

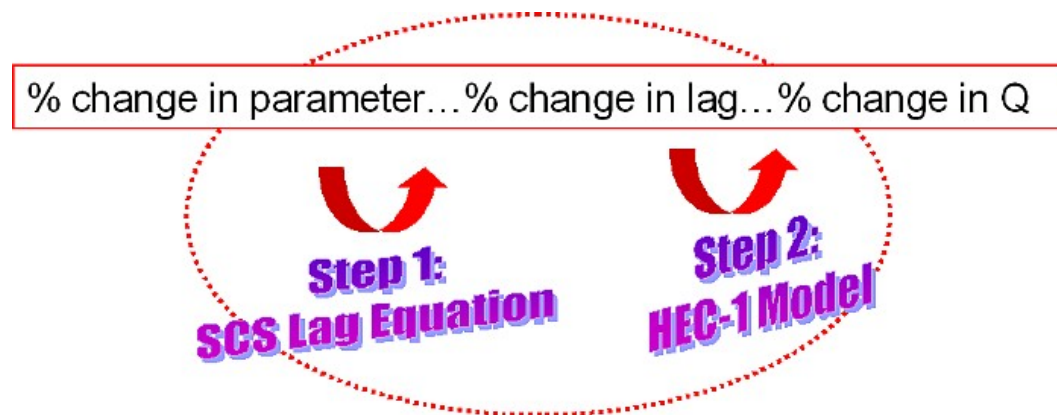


Figure 5.15: Final Discharge Sensitivity Calculation

The effect of each parameter (longest flow path, slope, and curve number) on discharge was evaluated using the elasticity for both discharge (due to

variations in lag) and lag (due to variations in each parameter). These two elasticity values are multiplied together. Figure 5.16 outlines the results from the elasticity study.

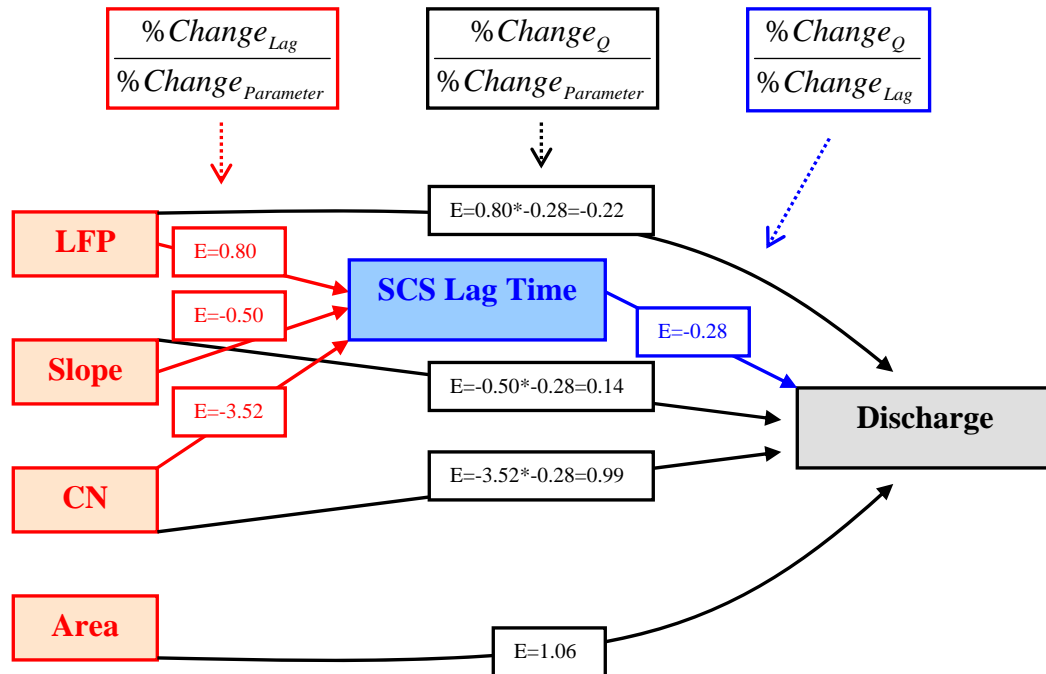


Figure 5.16: Elasticity Diagram

The following relationships can be drawn from Figure 5.16:

- A 1% increase in longest flow path length decreases peak discharge by 0.22%;
- A 1% increase in slope increases peak discharge by 0.14%;
- A 1% increase in curve number increases flow by 1%;
- A 1% increase in drainage area increases flow by 1%.

Both curve number and drainage area have a direct effect on discharge, while longest flow path length and slope have minimal influence on discharge. Figure 5.17 shows the relative discharge elasticities of longest flow path, slope, curve number, and drainage area.

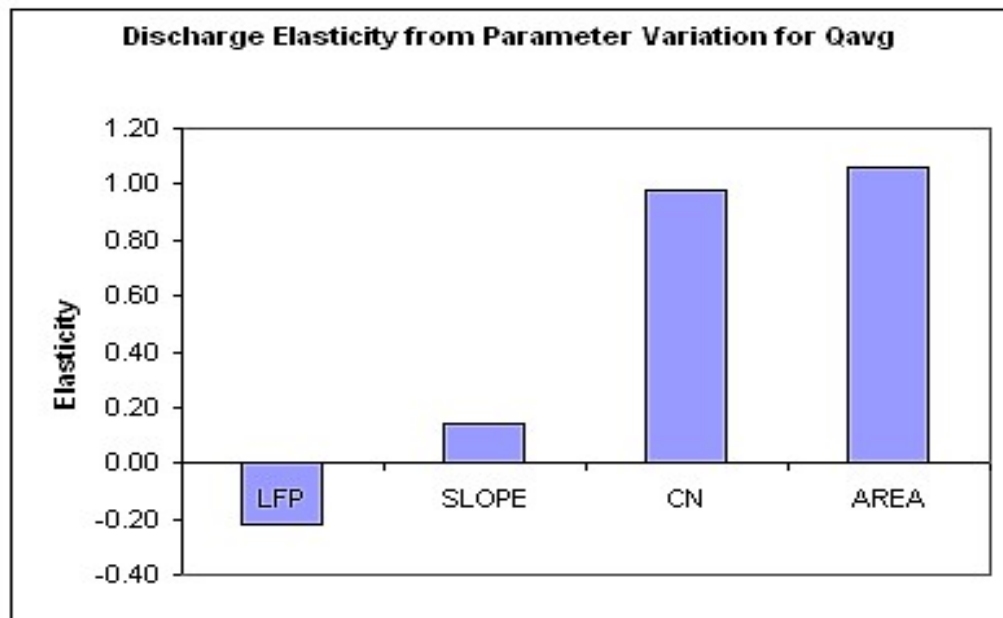


Figure 5.17: Elasticity Results

An analysis of coefficient of variation (CV) values in Table 5.19, as derived for each parameter in Table 5.1, Table 5.2, and Table 5.3, shows that the error associated with determining drainage area is small compared to the error associated with determining longest flow path, slope, and curve number.

Table 5.19: Parameter Coefficients of Variation (CV)

| Study Area | CV (%) Area | CV (%) LFP | CV (%) Slope | CV (%) CN |
|-------------------|--------------------|-------------------|---------------------|------------------|
| Area 1 | 2.07 | 8.42 | 3.65 | 3.01 |
| Area 2 | 0.81 | 3.90 | 2.97 | 3.08 |
| Area 3 | 1.52 | 3.22 | 1.80 | 3.11 |

Drainage area CV values are the smallest of the parameter CV values for Area 1, Area 2, and Area 3. Although the relationship between area and discharge is elastic, the error associated with determining drainage area is small. On the other hand, there is a larger error associated with determining longest flow path and slope. However, since longest flow path and slope are inelastic parameters, large errors in determining these values will cause minimal percent changes in discharge.

Table 5.20 shows the percent discharge variations resulting from parameter variations for Area 1, Area 2, and Area 3.

Table 5.20: Discharge Variations for Area 3

| Parameter | Discharge CV% (Area 1) | Discharge CV% (Area 2) | Discharge CV% (Area 3) |
|------------------|-----------------------------------|-----------------------------------|-----------------------------------|
| Area | $2.07 \times 1.06 = 2.19\%$ | $0.81 \times 1.06 = 0.86\%$ | $1.52 \times 1.06 = 1.61\%$ |
| LFP | $8.42 \times -0.22 = -1.85\%$ | $3.90 \times -0.22 = -0.86\%$ | $3.22 \times -0.22 = -0.71\%$ |
| Slope | $3.65 \times 0.14 = 0.51\%$ | $2.97 \times 0.14 = 0.42\%$ | $1.80 \times 0.14 = 0.25\%$ |
| CN | $3.01 \times 0.99 = 3.00\%$ | $3.08 \times 0.99 = 3.05\%$ | $3.11 \times 0.99 = 3.08\%$ |

The CV for discharge is calculated by multiplying the CV for each parameter by the discharge elasticity with respect to that parameter. Table 5.20 shows that curve number will most influence discharge after taking into consideration the error that occurs as a result of variations in extracting hydrologic parameters.

Chapter 6: Conclusions and Recommendations

This implementation project was conducted to provide guidance to TxDOT regarding parameter sensitivity in hydrologic modeling. The principal factors affecting flood magnitudes in a watershed include runoff, and watershed area information such as slope, flow path length, area, land use, and soil type. These parameters are all important in determining the peak discharge at a watershed outlet such as a culvert or bridge crossing. Currently TxDOT predominantly uses traditional methods of hand delineation to extract hydrologic parameters, although TxDOT is moving towards using more automated methods for this process.

The use of GIS in water resources engineering has proved to be a quick and relatively simple means of computing hydrologic data. In 2000, however, Anderson (2000) conducted a digital floodplain analysis for TxDOT which led to doubts about the automated process. Anderson's watershed lag time values were significantly greater than values found in an earlier analysis conducted by TxDOT. In an effort to determine possible causes of this error, four case studies were developed to analyze three areas of different size: (1) measurement from paper maps; (2) on-screen extraction from raster maps; (3) using GIS and two different resolutions of grid-based digital elevation models (DEMs); and (4) using a triangulated irregular network (TIN). This section of the report discusses conclusions and recommendations as drawn from the implementation study.

6.1 ERROR SOURCES AMONG PARAMETER EXTRACTION METHODS

This study examines parameter extraction methods in three drainage areas of different size in Austin, Texas. Area 1, the smallest area, is approximately 0.5 mi². Area 2, the medium-sized area, is approximately 1.7 m²; and Area 3, the largest area, is approximately 8.8 mi². Errors associated with each of the four levels of parameter extraction, in addition to the influence of drainage area size on parameter extraction method, are evaluated.

6.1.1 Parameter Extraction using Paper Maps

Traditional hydrologic modeling involves calculating watershed parameters from paper maps. Calculation of terrain-based hydrologic data involves delineating the watershed by hand using map contours as guidelines. Once the perimeter of the watershed has been established, a planimeter is used to measure its area. Perimeter and length of the longest flow path are measured using a map wheel. Slope is calculated by taking the difference in elevation between map contours.

Variations in traditional, paper map-based methods were most apparent in Area 3. This drainage area, the largest area under investigation, yielded hand measurements for area and longest flow path, 0.29 mi² and 0.39 miles below the mean, respectively. These area and longest flow path values were smaller than any of the other area or longest flow path measurements for Area 3. The length of perimeter, although not normally used as a hydrologic parameter, was 3.57 miles

below the mean using traditional methods of parameter extraction. For Area 1 and Area 2 the differences between paper map methods and digital automated methods were not as apparent.

The reason for the large deviation from the mean using traditional methods in area, longest flow path, and perimeter measurements is most likely due to the error associated with 1) taping two topographic maps together to make a map large enough to cover the whole drainage area, 2) difficulty in determining flow path and drainage divides from the map contours and 3) the accuracy of manual measurement techniques using a map wheel and a planimeter.

6.1.2 On-Screen Digitizing of Raster Graphic Maps

The process of on-screen digitizing of raster graphic maps closely resembles paper map methods. The methodology is analogous, except that the process of on-screen digitizing of raster graphic maps involves using a computer-aided mouse and a scanned topographic map to draw in watershed boundaries and flow paths. Once the watershed boundaries and flow paths have been determined, a GIS (or similar system) computes drainage area, longest flow path length, and perimeter. Slope is calculated by taking the difference in elevation between map contours, as done with paper maps.

On-screen digitizing eliminates the error of taping maps together, and interpreting lengths and areas from hand-held instruments. As with paper maps, determining flow paths and drainage divides is a very time-consuming and subjective process. On-screen digitizing also has the advantage over paper

map-based methods in that map features can be “zoomed-in” or magnified to better understand flow paths. In this study each area was digitized two ways: by attempting to incorporate the effect of urban infrastructure such as major highways, and by disregarding this infrastructure. The on-screen digitizing results show that area and longest flow path measurements for Area 3 closely resemble results derived from automated processes using DEMs, more so than results derived using paper map-based methods. This result indicates that errors associated with physically measuring parameters with a map wheel and planimeter largely contribute to the variation in area and longest flow path values for Area 3. For on-screen digitizing of larger areas, the measurement error due to the subjective nature of the delineation process is small when compared to the error due to hand-held measurement techniques applied to paper maps.

6.1.3 Parameter Extraction Using Automated Methods

DEM analysis in WMS (Watershed Modeling System) and CRWR-PrePro presents errors associated with data resolution and accuracy in describing the physical characteristics of a surface. DEM resolution affects the channel length, area, slope, and perimeter measurements. If the DEM resolution is too low, small changes in terrain are not observed and small areas may not accurately be described. If the resolution of the DEM is very high, channel lengths become larger due to more tortuous flow paths. This study showed that flow paths for the 10 meter DEM were longer than flow paths for the 30 meter DEM for all three areas as determined in both WMS and CRWR-PrePro. For Area 1 there was a 4%

increase in longest flow path using CRWR-PrePro, and a 12% increase using WMS. For the large area, Area 3, there was a 3% increase in longest flow path using CRWR-PrePro and a 2% increase using WMS. Regardless, the longest flow path standard deviation for Area 1 is 0.13 miles (with a mean of 1.58 miles), and the longest flow path standard deviation for Area 3 is 0.22 miles (with a mean of 6.67 miles). Variations are small, and results show that these variations do not significantly influence lag time and discharge calculations. Distributed properties such as slope and longest flow path require a method or model to reduce the distributed information into a representative value for the entire subcatchment. Variations in subcatchment slope and longest flow path values between WMS and CRWR-PrePro may be attributed to differences in underlying models used for extracting data.

6.1.4 Parameter Extraction Using TINs

TINs, triangulated irregular networks, consist of a set of vertex points connected by triangles, that represent scattered X, Y, and Z locations. TINs have many advantages over DEMs, in that TINs can describe a surface precisely and are adaptive to different types of terrain. The major disadvantage found working with TINs in this project is the large amount of time that is required to create, edit, and condition the TIN. For this reason, TIN development was not conducted for Area 3. Parameter values for area, perimeter, and longest flow path did not vary significantly for the TIN when compared to the DEM methods and on-screen digitizing. Slope measurement using a TIN, however, produced a greater value

than any of the other methods implemented. Probably this is the most accurate slope value since the DEM methods tend to smooth out slopes.

6.2 ERRORS AMONG EXTRACTED HYDROLOGIC PARAMETERS

The parameter variation associated with each of the four levels of parameter extraction is evaluated based on a simple statistical analysis using standard deviation and coefficient of variation (CV). The coefficient of variation (CV) is defined as the standard deviation divided by the mean for a group of measurements.

6.2.1 Drainage Area

The results for drainage area showed little variation among the different methods of parameter extraction. Results show that drainage area can be approximated within $\pm 0.01 \text{ mi}^2$ for areas less than approximately 1.6 mi^2 , and within $\pm 0.13 \text{ mi}^2$ for areas approximately 8.8 mi^2 . Area measurement, whether obtained by using automated or traditional methods, will most likely not result in a large error. This study shows that the maximum coefficient of variation (CV) for area, determined by Area 1, is 2.07%.

6.2.2 Slope

Slope, similar to area, produced fairly consistent measurements for all three study areas. For the largest area, Area 3, slope could be approximated within ± 0.01 as percent slope (a CV of 1.80%). For the small area, Area 1, slope

could be approximated within ± 0.05 as percent slope (a CV of 3.65%). The mean slope for Area 3 was 0.77%, while the mean slope for Area 1 was 1.30%.

6.2.3 Longest Flow Path

Longest flow path results produced errors greater than slope or area errors for all three study areas. However, this error decreased from 8.42% to 3.22% as the study area size increased from Area 1 to Area 3. For the largest area, longest flow path was calculated within ± 0.22 miles, with a mean value of 6.67 miles. For the smallest area, longest flow path was calculated within ± 0.13 miles, with a mean value of 1.58 miles.

6.2.4 Perimeter

Watershed perimeter length, although not a hydrologic parameter, was examined to evaluate trends in line variation among methods. Automated methods using DEMs produced greater values for perimeter than traditional methods for all three study areas. This resulted in consistently high CV values for perimeter. For Area 1, the CV value was 10.28%, and for Area 3, the CV value was 14.99%.

6.2.5 Curve Number

The SCS runoff curve number obtained by combining land use and soil types in GIS for Area 2 was 91.7, while the curve number determined by an independent TxDOT study was 85.8. A range of curve number values, using the

curve number developed by automated methods as an approximate upper limit, and the curve number developed by TxDOT as an approximate lower limit, gave a coefficient of variation of 3.08%, and a mean value of 89. This number is used to reflect a reasonable error one might encounter in determining SCS curve number.

6.3 SIGNIFICANCE OF ERRORS

Following hydrologic parameter extraction, ranging from traditional methods using paper maps to advanced methods using TINs, a sensitivity analysis based on the concept of elasticity was conducted for Area 2.

Quantifying discharge elasticity with respect to parameter variation is a two-step process. The first step involves determining the variation in SCS lag time with slope, longest flow path, and curve number. Variations in parameter values using the four levels of parameter extraction were plotted against resulting SCS lag time values. The range in parameter values, divided by the mean parameter value, was used to describe the parameter variation. The range of resulting SCS lag times, divided by the mean SCS lag time, was used to quantify the lag time variation. The lag time variation, divided by the parameter variation, describes the lag time elasticity with respect to the parameter. In other words, this describes the percent increase that will occur in lag time by a 1% increase in the parameter. If this number is less than 1, then lag time is “inelastic” with respect to the parameter. If this number is greater than 1, then lag time is “elastic” with respect to the parameter. An elastic parameter will cause larger variations in lag time.

The second step in quantifying the discharge elasticity with respect to parameter variation involves determining the variation in discharge with variation in SCS lag time. This step requires running a HEC-1 model developed by TxDOT. For each return period, the HEC-1 model was run seven times. The lag times were changed in each sub-basin by an equal percentage (5%, 10%, 20%, -5%, -10%, and -20%) for each run. The resulting linear equations were used to determine discharge elasticity, or the percent variation in discharge caused by fluctuations in SCS lag time. Dividing the percent variation in discharge by the percent variation in SCS lag time gives discharge elasticity with respect to SCS lag time for each return period. This describes the percent change in discharge resulting from a 1% change in SCS lag time.

Table 6.1 shows the overall discharge elasticity with respect to each parameter. Results from the first step (sensitivity of lag time to parameter variations) and the second step (sensitivity of discharge with respect to lag time variations) are multiplied to produce discharge elasticity with respect to each parameter.

Table 6.1: Elasticity Analysis

| Parameter | Elasticity Lag-Parameter | Elasticity Q_{avg}-Lag | Elasticity Q_{avg}-Parameter |
|------------------|-------------------------------------|---|---|
| LFP | 0.80 | -0.28 | -0.22 |
| Slope | -0.50 | -0.28 | 0.14 |
| CN | -3.52 | -0.28 | 0.99 |
| Area | --- | --- | 1.06 |

Results show that although errors associated with parameter extraction methods may cause significant changes in lag time values, the errors become less significant once entered into a model to calculate discharge. Table 6.1 shows that lag time is inelastic with respect to longest flow path (LFP), as the elasticity of lag time with respect to this parameter is 0.8. Discharge is also inelastic with respect to longest flow path, with an elasticity of -0.22 . This last number, discharge elasticity with respect to longest flow path, was determined by multiplying the lag time elasticity with respect to longest flow path by the discharge elasticity with respect to lag time (-0.28). The discharge elasticity with respect to slope, calculated using the same method as with longest flow path, is also inelastic at a value of 0.14.

Flow path and slope values were originally thought to be large contributors to lag time variations. This analysis shows that this is not necessarily the case. Table 6.1 shows that SCS lag time acts inelastically with respect to both slope and longest flow path (-0.50% and 0.80% respectively). Once entered into a hydrologic model, variations in these parameters have minimal effect on discharge, with discharge elasticities of 0.14% and -0.22% respectively. Thus, a 1% variation in slope will cause a minimal 0.14% increase in discharge, and a 1% variation in longest flow path will cause a 0.22% decrease in discharge.

Table 6.1 shows that curve number, unlike slope and longest flow path, has an elastic effect on lag time. The lag time elasticity with respect to curve number is -3.52 . Discharge is also elastic with respect to curve number (at an

elasticity of 0.99) when lag times, based on curve number variations, are entered into a hydrologic model.

The discharge elasticity with respect to drainage area, calculated to be 1.06, is also elastic. Although discharge is more sensitive to drainage area than to curve number, errors associated with determining area are small. For instance, Area 3 has a CV for area of 1.52%. A 1% increase in area will result in a 1.61% increase in discharge. If curve number has a CV of 3%, the resulting discharge for a 1% increase in curve number will be 3%.

6.4 ADDITIONAL SOURCES OF ERROR

This analysis of parameter sensitivity in hydrologic modeling is general and meant to serve as a guide for TxDOT engineers. Several important elements were not considered in this report when calculating discharge.

First of all, the elasticity analysis does not account for curve number effects on excess rainfall. For each change in lag time within the HEC-1 model, curve numbers used to calculate excess rainfall were held constant.

In highly developed areas, parameter extraction methods used in this report may not apply. Without a thorough knowledge of the storm sewers and other urban structures it is difficult to judge flow paths. Including buildings and structures into the model does not account for the runoff flowing below the ground surface or under a bridge. Storm sewers may enter and leave watersheds, and water may flow along roads and enter into one watershed from another area.

The effects of using traditional methods as opposed to automated methods were not fully evaluated for flat areas. In order to evaluate if the use of automated methods still proves viable in areas of low slope, a more thorough investigation using several study areas of the same shape and area, but different slopes, would have to be implemented.

6.5 RECOMMENDATIONS

Automated methods, requiring the use of a computer to extract hydrologic parameters, produce very consistent results for hydrologic parameters. Paper map-based methods of parameter extraction tend to vary more than do automated methods, especially for large areas.

As with traditional paper map-based methods, on-screen digitization from raster graphic maps is a highly subjective process. However, measurements for the large study area closely resemble results derived from automated processes using DEMs, more so than results derived using paper maps. This result implies that differences are most likely attributed to errors associated with physically measuring parameters with a map wheel and a planimeter, rather than the subjective nature of the application.

As paper map-based methods are more tedious than automated methods (with the exception of the TIN), and more time consuming, moving to automated methods would accelerate the design process. Parameters extracted using WMS, CRWR-PrePro, different resolution DEMs, and on-screen digitization from raster graphic maps do not vary significantly from one another, and any error associated

with parameter extraction using automated methods will not significantly influence discharge calculations. The recommendation, therefore, is to move towards any of the automated methods of hydrologic parameter extraction. On-screen digitization of raster graphic maps for small and medium areas eliminates the need to work with DEMs. For large areas, however, DEMs are recommended for efficiency and precision.

The second observation is that discharge is most sensitive to curve number, and less sensitive to slope or longest flow path. Discharge is also sensitive to drainage area. However, this study shows that the error associated in calculating drainage area is small compared to the error associated with calculating curve number. Determining an accurate curve number will reduce lag time and discharge calculation errors. The recommendation that results from this study is to carefully evaluate soil type, vegetative cover, and land use in a given area to obtain as accurate a curve number as possible.

Appendix A: Online Internet Resources

| Data Type | Source |
|----------------------|--|
| USGS DRG | http://mcmcweb.er.usgs.gov/drg/ |
| 30 Meter DEM | http://edcnts12.cr.usgs.gov/ned/ http://www.tnris.org/DigitalData/DEMs/dem-a.htm |
| STATSGO (USDA-NRCS) | http://www.ftw.nrcs.usda.gov/stat_data.html |
| Land Use/ Land Cover | http://edc.usgs.gov/doc/edchome/ndcdb/ndcdb.html |
| CRWR-PrePro webpage | http://www.ce.utexas.edu/prof/olivera/prepro/prepro.htm |
| WMS Webpage | http://www.ems-i.com/netpagz/wms.htm |
| TOPAZ Webpage | http://duke.usask.ca/~martzl/topaz/ |

Appendix B: Unmodified HEC-1 Model

```

ID      LITTLE WALNUT CREEK HEC-1 MODEL; CONVERSION FROM TR-20
ID      ORIG. DEV'D MURPHEE ENG. 1992; L&M CONVERSION 5/97;  FILE: LW100EX.H1
ID      THIS FILE IS BASED ON ORIGINAL MTEST4.N INPUT.
ID      THIS FILE DIFFERS FROM EXIST.IN IN
ID
ID      *** EXIST2.IN *** TXDOT MICRO MODEL (3 HR DIMENSIONLESS)
*DIAGRAM
*      INITIALIZATION
IT      2      300
IO      5
*      2 YR      5 YR      10YR      25YR      50YR      100YR      3 HR DEPTHS
JR  PREC      2.61      3.48      3.98      4.72      5.34      6.03
*      BEGIN WITH LITTLE WALNUT (LW14)
KK TB711      * UPPER END OF BASIN
BA 0.444
PB 1.00
IN 6      0      0
PC0.0000      0.0077      0.0153      0.0230      0.0345      0.0460      0.0613      0.0766      0.0920      0.1111
PC0.1341      0.1571      0.1916      0.2375      0.3218      0.5824      0.7165      0.7816      0.8238      0.8544
PC0.8774      0.8966      0.9119      0.9272      0.9425      0.9540      0.9655      0.9770      0.9847      0.9923
PC1.0000
UD 0.255
LS      89
KKROUT43      * ROUTE TB711
RS 1      STOR      0
SV 0.00      0.59      1.19      1.93      2.54      3.31      4.07      4.57      5.59
SQ 0      180      450      900      1350      2000      2700      3200      4200
SE 643.0      645.2      646.2      647.2      647.9      648.8      649.6      650.1      650.8
KK TB710      * ORIGINAL MAP LABEL
BA 0.285
UD 0.298
LS      88
KKCOMB01      * COMBINE ROUTE43 + TB710
HC 2
KKROUT44      * ROUTE COMB01
RS 1      STOR      0
SV 0.00      2.93      5.97      9.63      12.70      16.56      20.36      22.87      27.96
SQ 0      180      450      900      1350      2000      2700      3200      4200
SE 643.0      645.2      646.2      647.2      647.9      648.8      649.6      650.1      650.8
KK TB709      * ORIGINAL MAP LABEL
BA 0.052
UD 0.129
LS      80
KKCOMB02      * COMBINE ROUTE44 + TB709
HC 2
KK TB708      * ORIGINAL MAP LABEL
BA 0.241
UD 0.262
LS      86
KKCOMB03      * COMBINE COMB02 + TB708
HC 2
KKROUT45      * ROUTE COMB03
RS 1      STOR      0
SV 0.00      2.90      6.51      11.81      16.32      23.25      30.62      35.87      45.79
SQ 0      180      450      900      1350      2000      2700      3200      4200

```

| | | | | | | | | | |
|----------|---|-------|-------|-------|-------|-------|-------|-------|-------|
| SE 603.0 | 605.5 | 606.8 | 608.1 | 608.9 | 609.9 | 610.8 | 611.3 | 612.1 | |
| KK TB707 | * ORIGINAL MAP LABEL | | | | | | | | |
| BA 0.042 | | | | | | | | | |
| UD 0.156 | | | | | | | | | |
| LS | 87 | | | | | | | | |
| KKCOMB04 | * COMBINE ROUTE45 + TB707 | | | | | | | | |
| HC 2 | | | | | | | | | |
| KK TB706 | * ORIGINAL MAP LABEL | | | | | | | | |
| BA 0.121 | | | | | | | | | |
| UD 0.267 | | | | | | | | | |
| LS | 84 | | | | | | | | |
| KKCOMB05 | * COMBINE COMB04 + TB706 | | | | | | | | |
| HC 2 | | | | | | | | | |
| KKTb1003 | * NORWOOD | | | | | | | | |
| BA 0.150 | | | | | | | | | |
| UD 0.111 | | | | | | | | | |
| LS | 77 | | | | | | | | |
| KK STR80 | * FLOW OF TB1003 THROUGH STR80 | | | | | | | | |
| KM | CHANNEL STORAGE ROUTING FOR RESERVOIR 80 | | | | | | | | |
| RS 1 | ELEV | 628.5 | | | | | | | |
| SV 0.00 | 0.50 | 0.78 | 2.34 | 4.81 | 8.05 | 9.99 | 11.92 | 12.89 | 14.12 |
| SV 16.31 | 21.09 | 25.86 | | | | | | | |
| SQ 0 | 0 | 5 | 30 | 110 | 250 | 289 | 325 | 340 | 470 |
| SQ 900 | 1575 | 2400 | | | | | | | |
| SE 628.5 | 629.5 | 630.0 | 632.0 | 634.0 | 636.0 | 637.0 | 638.0 | 638.4 | 639.0 |
| SE 640.0 | 641.0 | 642.0 | | | | | | | |
| KKROUT46 | * ROUTE STR80 | | | | | | | | |
| RS 1 | STOR | 0 | | | | | | | |
| SV 0.00 | 0.21 | 0.43 | 0.74 | 0.99 | 1.57 | 2.91 | 3.83 | 5.50 | |
| SQ 0 | 35 | 85 | 170 | 240 | 375 | 500 | 600 | 800 | |
| SE 606.0 | 606.9 | 607.3 | 607.7 | 607.9 | 608.4 | 609.4 | 610.0 | 610.9 | |
| KKTb1001 | * FIRST MODIFIED AREA - IMPERVIOUS FROM 183 | | | | | | | | |
| BA 0.025 | | | | | | | | | |
| UD 0.185 | | | | | | | | | |
| LS | 85 | | | | | | | | |
| KK183I01 | * TB1001 AREA CONVERTED TO IMPERVIOUS | | | | | | | | |
| BA 0.011 | | | | | | | | | |
| UI 213.0 | 0 | | | | | | | | |
| KKCOMB06 | * COMBINE ROUTE46 + TB1001 + 183I01 | | | | | | | | |
| HC 3 | | | | | | | | | |
| KKCOMB07 | * COMBINE COMB06 + COMB05 | | | | | | | | |
| HC 2 | | | | | | | | | |
| KKROUT47 | * ROUTE COMB07 | | | | | | | | |
| RS 1 | STOR | 0 | | | | | | | |
| SV 0.00 | 1.16 | 2.39 | 4.15 | 5.66 | 8.74 | 17.13 | 20.26 | 28.33 | |
| SQ 0 | 180 | 450 | 900 | 1350 | 2000 | 2700 | 3200 | 5100 | |
| SE 587.8 | 590.8 | 592.1 | 593.4 | 594.4 | 595.8 | 598.5 | 599.3 | 601.0 | |
| KM | | | | | | | | | |
| KK TB705 | * ORIGINAL MAP LABEL | | | | | | | | |
| BA 0.102 | | | | | | | | | |
| UD 0.205 | | | | | | | | | |
| LS | 83 | | | | | | | | |
| KM | | | | | | | | | |
| KK183I03 | * TB705 AREA CONVERTED TO IMPERVIOUS | | | | | | | | |
| BA 0.004 | | | | | | | | | |
| UI 77.4 | 0 | | | | | | | | |
| KKCOMB10 | * COMBINE tb705 + 183i03 | | | | | | | | |
| HC 2 | | | | | | | | | |
| KKCOMB08 | * COMBINE ROUT47+ comb10 | | | | | | | | |
| HC 2 | | | | | | | | | |
| KK TB704 | * ORIGINAL MAP LABEL | | | | | | | | |
| BA 0.046 | | | | | | | | | |

```

UD 0.129
LS
KKCOMB11 * COMBINE TB704 + COMB08
HC 2
KKROUT48 * ROUT COMB11
RS 1 STOR 0
SV 0.00 1.13 2.37 4.06 5.62 7.50 9.34 10.60 13.01 25.00
SQ 0 180 450 900 1350 2000 2700 3200 4200 8200
SE 570.0 572.8 574.1 575.4 576.3 577.4 578.3 578.9 580.0 585.0
KK TB702 * ORIGINAL MAP LABEL
BA 0.097
UD 0.162
LS
KKCOMB12 * COMBINE ROUT48 + tb702
HC 2
KK TB703 * ORIGINAL MAP LABEL
BA 0.052
UD 0.137
LS
KK183I04 * TB703 AREA CONVERTED TO IMPERVIOUS COVER
BA 0.004
UI 77.4 0
KKCOMB13 * COMBINE COMB12 + tb703 + 183I04
HC 3
KKROUT49 * ROUTE COMB71
RS 1 STOR 0
SV 0.00 3.01 5.67 8.99 11.77 15.22 18.50 20.73 25.72 35.00
SQ 0 180 450 900 1350 2000 2700 3200 4200 7000
SE 548.0 551.4 552.8 554.2 555.3 556.5 557.6 558.3 559.6 562.6
KK TB701 * ORIGINAL MAP LABEL
BA 0.088
UD 0.140
LS
KKCOMB14 * COMBINE ROUT49 + TB701
HC 2
KK183I05 * TB701 AREA CONVERTED TO IMPERVIOUS COVER
BA 0.001
UI 19.4 0
KKCOMB15 * COMBINE COM14 + 183I05
HC 2
KKLW14 * ORIGINAL MAP LABEL
BA 0.127
UD 0.125
LS
KKCOMB16 * COMBINE COMB15 + LW14
HC 2
KK183I06 * LW14 AREA CONVERTED TO IMPERVIOUS
BA 0.006
UI 116.2 0
KKCOMB17 * COMBINE 183I06 + COMB16
HC 2
ZZ

```

Appendix C: Modified HEC-1 Model in HEC-HMS

```
Basin: Exist2mod.in
    Description: LITTLE WALNUT CREEK HEC-1 MODEL; CONVERSION FROM TR-20 ORIG.
DEV'D MURPHEE ENG. 1992; L&M CONVERSION 5/97; FILE: LW100EX.H1 THIS FILE IS BASED
ON ORIGINAL MTEST4.N INPUT. THIS FILE DIFFERS FROM EXIST.IN IN *** EXIST2.IN ***
TXDOT MICRO MODEL (3 HR DIMENSIONLESS)
    Last Modified Date: 18 February 2002
    Last Modified Time: 10:29
    Version: 2.1.2
    Default DSS File Name: D:\hmsproj\Exist.in_feb17\Exist.in_feb17.dss
    Unit System: English
End:

Subbasin: TB711
    Canvas X: -386.946
    Canvas Y: 1940.607
    Label X: 16
    Label Y: 0
    Area: 0.444
    Downstream: ROUT43

    LossRate: SCS
    Percent Impervious Area: 0.0
    Curve Number: 89

    Transform: SCS
    Lag: 15.300
    Show lag in hours: Yes

    Baseflow: None
End:

Reservoir: ROUT43
    Canvas X: -116.602
    Canvas Y: 1794.804
    Label X: 16
    Label Y: 0
    Downstream: COMB01

    Route: Modified Puls
    Routing Curve: Storage-Elevation-Outflow
    Initial Storage: 0
    Routing Table in DSS: Yes
End:

Subbasin: TB710
    Canvas X: 86.915
    Canvas Y: 1974.021
    Label X: 16
    Label Y: 0
    Area: 0.285
    Downstream: COMB01

    LossRate: SCS
    Percent Impervious Area: 0.0
    Curve Number: 88

    Transform: SCS
```

```

    Lag: 17.880
    Show lag in hours: Yes

    Baseflow: None
End:

Junction: COMB01
    Canvas X: 32.239
    Canvas Y: 1752.278
    Label X: 8
    Label Y: 5
    Downstream: ROUT44
End:

Reservoir: ROUT44
    Canvas X: 44.389
    Canvas Y: 1636.850
    Label X: 16
    Label Y: 0
    Downstream: COMB02

    Route: Modified Puls
    Routing Curve: Storage-Elevation-Outflow
    Initial Storage: 0
    Routing Table in DSS: Yes
End:

Subbasin: TB709
    Canvas X: 354.221
    Canvas Y: 1652.038
    Label X: 16
    Label Y: 0
    Area: 0.052
    Downstream: COMB02

    LossRate: SCS
    Percent Impervious Area: 0.0
    Curve Number: 80

    Transform: SCS
    Lag: 7.740
    Show lag in hours: Yes

    Baseflow: None
End:

Junction: COMB02
    Canvas X: 44.389
    Canvas Y: 1536.611
    Label X: 16
    Label Y: 0
    Downstream: COMB03
End:

Subbasin: TB708
    Canvas X: -356.570
    Canvas Y: 1527.498
    Label X: 16
    Label Y: 0
    Area: 0.241
    Downstream: COMB03

```



```

        LossRate: SCS
        Percent Impervious Area: 0.0
        Curve Number: 86

        Transform: SCS
        Lag: 15.720
        Show lag in hours: Yes

        Baseflow: None
End:

Junction: COMB03
    Canvas X: 59.577
    Canvas Y: 1451.559
    Label X: 16
    Label Y: 0
    Downstream: ROUT45
End:

Reservoir: ROUT45
    Canvas X: 68.690
    Canvas Y: 1384.732
    Label X: 16
    Label Y: 0
    Downstream: COMB04

    Route: Modified Puls
    Routing Curve: Storage-Elevation-Outflow
    Initial Storage: 0
    Routing Table in DSS: Yes
End:

Subbasin: TB707
    Canvas X: 354.221
    Canvas Y: 1424.220
    Label X: 16
    Label Y: 0
    Area: 0.042
    Downstream: COMB04

    LossRate: SCS
    Percent Impervious Area: 0.0
    Curve Number: 87

    Transform: SCS
    Lag: 9.360
    Show lag in hours: Yes

    Baseflow: None
End:

Junction: COMB04
    Canvas X: 71.727
    Canvas Y: 1302.718
    Label X: 16
    Label Y: 0
    Downstream: COMB05
End:

Subbasin: TB706
    Canvas X: -222.917
    Canvas Y: 1223.741

```

```

Label X: 16
Label Y: 0
Area: 0.121
Downstream: COMB05

LossRate: SCS
Percent Impervious Area: 0.0
Curve Number: 84

Transform: SCS
Lag: 16.020
Show lag in hours: Yes

Baseflow: None
End:

Junction: COMB05
Canvas X: 32.239
Canvas Y: 1211.591
Label X: 16
Label Y: 0
Downstream: COMB07
End:

Subbasin: TB1003
Canvas X: 335.996
Canvas Y: 1278.417
Label X: 16
Label Y: 0
Area: 0.150
Downstream: STR80

LossRate: SCS
Percent Impervious Area: 0.0
Curve Number: 77

Transform: SCS
Lag: 6.660
Show lag in hours: Yes

Baseflow: None
End:

Reservoir: STR80
Description: CHANNEL STORAGE ROUTING FOR RESERVOIR 80
Canvas X: 348.146
Canvas Y: 1090.088
Label X: 16
Label Y: 0
Downstream: ROUT46

Route: Modified Puls
Routing Curve: Storage-Elevation-Outflow
Initial Elevation: 628.5
Routing Table in DSS: Yes
End:

Reservoir: ROUT46
Canvas X: 384.597
Canvas Y: 1014.149
Label X: -23
Label Y: -21

```

```

Downstream: COMB06

Route: Modified Puls
Routing Curve: Storage-Elevation-Outflow
Initial Storage: 0
Routing Table in DSS: Yes
End:

Subbasin: TB1001
Canvas X: 162.854
Canvas Y: 935.172
Label X: 16
Label Y: 0
Area: 0.025
Downstream: COMB06

LossRate: SCS
Percent Impervious Area: 0.0
Curve Number: 85

Transform: SCS
Lag: 11.100
Show lag in hours: Yes

Baseflow: None
End:

Subbasin: 183I01
Canvas X: 238.794
Canvas Y: 1187.290
Label X: 16
Label Y: 0
Area: 0.011
Downstream: COMB06

LossRate: SCS
Percent Impervious Area: 0.0
Curve Number: 85

Transform: User-Specified UH
Unit Hydrograph Name: 183I01

Baseflow: None
End:

Junction: COMB06
Canvas X: 135.516
Canvas Y: 1068.825
Label X: 16
Label Y: 0
Downstream: COMB07
End:

Junction: COMB07
Canvas X: 32.239
Canvas Y: 1084.013
Label X: -66
Label Y: -8
Downstream: ROUT47
End:

Reservoir: ROUT47

```

```

Canvas X: 83.877
Canvas Y: 810.631
Label X: 16
Label Y: 0
Downstream: COMB08

Route: Modified Puls
Routing Curve: Storage-Elevation-Outflow
Initial Storage: 0
Routing Table in DSS: Yes
End:

Subbasin: TB705
Canvas X: -125.715
Canvas Y: 841.007
Label X: 16
Label Y: 0
Area: 0.102
Downstream: COMB10

LossRate: SCS
Percent Impervious Area: 0.0
Curve Number: 83

Transform: SCS
Lag: 12.300
Show lag in hours: Yes

Baseflow: None
End:

Subbasin: 183I03
Canvas X: -92.302
Canvas Y: 698.241
Label X: 16
Label Y: 0
Area: 0.004
Downstream: COMB10

LossRate: SCS
Percent Impervious Area: 0.0
Curve Number: 83

Transform: User-Specified UH
Unit Hydrograph Name: 183I03

Baseflow: None
End:

Junction: COMB10
Canvas X: 190.192
Canvas Y: 755.955
Label X: 16
Label Y: 0
Downstream: COMB08
End:

Junction: COMB08
Canvas X: 193.230
Canvas Y: 591.926
Label X: 21
Label Y: -1

```

```

        Downstream: COMB11
End:

Subbasin: TB704
    Canvas X: 354.221
    Canvas Y: 546.363
    Label X: 16
    Label Y: 0
    Area: 0.046
    Downstream: COMB11

    LossRate: SCS
    Percent Impervious Area: 0.0
    Curve Number: 87

    Transform: SCS
    Lag: 7.740
    Show lag in hours: Yes

    Baseflow: None
End:

Junction: COMB11
    Canvas X: 211.455
    Canvas Y: 519.025
    Label X: -10
    Label Y: 37
    Downstream: ROUT48
End:

Reservoir: ROUT48
    Canvas X: 214.493
    Canvas Y: 440.048
    Label X: 15
    Label Y: 2
    Downstream: COMB12

    Route: Modified Puls
    Routing Curve: Storage-Elevation-Outflow
    Initial Storage: 0
    Routing Table in DSS: Yes
End:

Subbasin: TB702
    Canvas X: -235.067
    Canvas Y: 637.490
    Label X: 16
    Label Y: 0
    Area: 0.097
    Downstream: COMB12

    LossRate: SCS
    Percent Impervious Area: 0.0
    Curve Number: 86

    Transform: SCS
    Lag: 9.720
    Show lag in hours: Yes

    Baseflow: None
End:

```

```

Junction: COMB12
  Canvas X: 223.606
  Canvas Y: 364.109
  Label X: 23
  Label Y: -49
  Downstream: COMB13
End:

Subbasin: TB703
  Canvas X: 10.699
  Canvas Y: 356.652
  Label X: 16
  Label Y: 0
  Area: 0.052
  Downstream: COMB13

  LossRate: SCS
  Percent Impervious Area: 0.0
  Curve Number: 85

  Transform: SCS
  Lag: 8.220
  Show lag in hours: Yes

  Baseflow: None
End:

Subbasin: 183I04
  Canvas X: 351.184
  Canvas Y: 382.334
  Label X: 16
  Label Y: 0
  Area: 0.004
  Downstream: COMB13

  LossRate: SCS
  Percent Impervious Area: 0.0
  Curve Number: 85

  Transform: User-Specified UH
  Unit Hydrograph Name: 183I04

  Baseflow: None
End:

Junction: COMB13
  Canvas X: 257.019
  Canvas Y: 248.681
  Label X: -10
  Label Y: 29
  Downstream: ROUT49
End:

Reservoir: ROUT49
  Canvas X: 260.056
  Canvas Y: 166.667
  Label X: 16
  Label Y: 0
  Downstream: COMB14

  Route: Modified Puls
  Routing Curve: Storage-Elevation-Outflow

```

```

        Initial Storage: 0
        Routing Table in DSS: Yes
End:

Subbasin: TB701
    Canvas X: 123.366
    Canvas Y: 187.930
    Label X: 16
    Label Y: 0
    Area: 0.088
    Downstream: COMB14

    LossRate: SCS
    Percent Impervious Area: 0.0
    Curve Number: 86

    Transform: SCS
    Lag: 8.400
    Show lag in hours: Yes

    Baseflow: None
End:

Junction: COMB14
    Canvas X: 275.244
    Canvas Y: 90.728
    Label X: 16
    Label Y: 0
End:

Default Attributes:
    Default Basin Unit System: English
    Default Meteorology Unit System: SI
    Default Loss Rate: Initial+Constant
    Default Transform: Modified Clark
    Default Baseflow: Recession
    Default Route: Muskingum
    Enable Flow Ratio: No
    Enable Evapotranspiration: No
    Compute Local Flow At Junctions: No
    Warning On Delete Component: Yes
    Warning On Change Method: Yes
End:

```

Bibliography

- Anderson, David James. 2000. CRWR Online Report 00-11: *GIS-Based Hydrologic and Hydraulic Modeling for Floodplain Delineation at Highway River Crossings*. Center for Research in Water Resources, The University of Texas at Austin, Austin, Texas.
- Barrett, Michael. 2000. *LCRA/Marble Falls Regional Drainage Feasibility Study*. Center for Research in Water Resources, Bureau of Engineering Research, Austin, Texas.
- Chow, V. T., D. R. Maidment, and L. W. Mays. 1988. *Applied Hydrology*. McGraw-Hill, New York, New York.
- Djokic, D., Z. Ye, and A. Miller. 1997. *Efficient Watershed Delineation Using ArcView and Spatial Analyst*. Proceedings, 17th Annual ESRI User's Conference, San Diego, California.
- Garbrecht, J. and L. W. Martz. 1994. *Grid Size Dependency of Parameters Extracted from Digital Elevation Models*. Computers and Geosciences, 20(1): 85-87.
- Garbrecht, J. and L. W. Martz., 1999a. *Digital Elevation Model Issues in Water Resources Modeling*. In Hydrologic and Hydraulic Modeling Support, ed. by D. R. Maidment and D. Djokic, Environmental Systems Research Institute, Redlands, California. 1-27. Internet website: <http://grl/ars/usda.gov/topaz/esri/paperH.htm>.
- Garbrecht, J., L. W. Martz, K. H. Syed, and D. Goodrich. 1999b. *Determination of Representative Catchment Properties from Digital Elevation Models*. 1999 International Water Resources Engineering Conference, American Society of Civil Engineers, Session HY-3, Geographic Information Systems (GIS) Applications in Hydrologic Engineering, Seattle, Washington. Published on CD-ROM. Internet Website: <http://grl.ars.usda.gov/topaz/ASCE99/ASCE99.HTM>
- Hellweger, F. and D. R. Maidment. 1997. *HEC-PREPRO: A GIS Preprocessor for Lumped Parameter Hydrologic Modeling Programs*. CRWR Online Report 97-8. Center for Research in Water Resources, The University of Texas at Austin, Austin, Texas.

- Jennings et. al., 1993. *National Summary of U.S. Geological Survey Regional Regression Equations for Estimating Magnitude and Frequency of Floods for Ungauged Sites*. Water Resources Investigations Report 94-4002.
- Jones, N. L., S.G., Write, and D.R, Maidment. 1990. *Watershed Delineation with Triangle-Based Terrain Models*. Journal of Hydrologic Engineering, ASCE, 116(10), 1232-1251.
- Knill, Oliver. 2000. *The Planimeter and the Theorem of Green*. Internet Website: <http://www.math.harvard.edu/~knill/math21a2000/planimeter/>
- Kunkle, Paul. 2002. *Kunkel's Mathematics Lessons: The Planimeter*. Internet Website: <http://www.nas.com/~kunkel/planimeter/planimeter.htm>
- Lee, D. T., and B. J. Schacter. 1980. *Two Algorithms of Constructing a Delauney Triangulation*. International Journal of Computer and Information Sciences, ASCE, 9(3): 219-242.
- Miller, Scott N., D. Phillip Guertin, Kamram H. Syed, and David C. Goodrich., 1999. *Using High Resolution Synthetic Aperture Radar for Terrain Mapping: Influences on Hydrologic and Geomorphic Investigation*. 1999 Annual Summer Specialty Conference Proceedings, Science Into Policy: Water in the Public Realm/ Wildland Hydrology. Internet Website: <http://www.awra.org/proceedings/Montana99/Miller1/>
- Moglen, Glen. and Ginger L. Hartman. 2001. *Resolution Effects on Hydrologic Modeling Parameters and Peak Discharge*. Journal of Hydrologic Engineering. 6 (6): .
- Nelson, James E.and Norman L. Jones. 1996. *Utilizing the ArcInfo Data Model to Build Conceptual Models for Environmental/Hydraulic/Hydrologic Simulations*. ESRI User's Conference.
- Nelson, James E., Norman L. Jones and Christopher M. Smemoe. 1997. *From a Grid or Coverage to a Hydrograph: Unlocking Your GIS Data for Hydrologic Applications*. ESRI User's Conference, July 1997. Published on CD ROM. Internet Website: <http://www.esri.com/library/userconf/proc97/proc97/to200/pap198/p198.htm>.
- Nelson, James E., Norman L. Jones, and Russell J. Barrett. 1999a. *Adaptive Tessellation Method for Creating TINs from GIS Data*. ASCE Journal of Hydrologic Engineering, 4(1)

- Nelson, James E., Christopher M. Smemoe, and Bing Zhao. 1999b. *A GIS Approach to Watershed Modeling in Maricopa County, Arizona*, American Society of Civil Engineers, Water Resources Planning and Management Conference, June 6-10, 1999, Tempe, AZ. Published on CD ROM. <http://emrl.byu/chris/documents/asceconf.pdf>
- Olivera, F. and D. R. Maidment. 1999. *GIS-Based System of Hydrologic and Hydraulic Applications for Highway Engineering*. Research Report 1738-6. Center for Transportation Research, The University of Texas at Austin, Austin, Texas.
- Stolpa, David. 2001-2002. Personal Interviews.
- Tarboton, D. G. 1997. *A New Method for the Determination of Flow Directions and Upslope Areas in Grid Digital Elevation Models*. Water Resources Research, 33(2): 309-319.
- Tarboton, D. G., R. L. Bras, and I. Rodriguez-Itube. 1991. *On the Extraction of Channel Networks from Digital Elevation Data*. Water Resources Research, 5(1): 81-100.
- Texas Department of Transportation (TxDOT). 2001 Hydraulic Design Manual.
- USACOE – HEC. 2000. *HEC-HMS Hydrologic Modeling System: User's Manual. Version 2.0*. Hydrologic Engineering Center, Davis, California.
- United States Geological Survey (USGS). Digital Raster Graphics (DRG). 1999. Internet Webpage: <http://mcmcweb.er.usgs.gov/drg/>
- Watershed Modeling System (WMS) Reference Manual, Version 6.0*. 1999. Environmental Modeling Research Lab., Brigham Young University.

